Surface hydrophilicity: a key factor in developing bone tissue engineering constructs

Mohammed Ahmed Alamin Yousif Yassin

Thesis for the degree of philosophiae doctor (PhD)
at the University of Bergen

2017

Date of defence: 16.02.2017

Year: 2017

Title: *Surface hydrophilicity: a key factor in developing bone tissue engineering constructs*

Author: *Mohammed Ahmed Alamin Yousif Yassin*

Print: AiT Bjerch AS / University of Bergen

"Happiness lies in the joy of achievement and the thrill of creative effort"

Franklin D. Roosevelt

Table of Contents

1. Scientific Environment

All the experiments in this series of studies were undertaken at the Faculty of Medicine and Dentistry, University of Bergen, Bergen, Norway.

Laboratory experiments

were carried out at Department of Clinical Dentistry.

Animal experiments

were conducted at the Animal Laboratory Facility, Department of Clinical Medicine.

3D porous scaffolds

were fabricated in collaboration with Department of Fibre and Polymer Technology, Royal Institute of Technology (KTH), Stockholm, Sweden.

Modified scaffolds

Tween 80 modifications were carried out at Department of Fibre and Polymer Technology, Royal Institute of Technology (KTH), Stockholm, Sweden.

Nanodiamonds particle modification was done at University of Wurzburg, Germany and Diacoating, Austria.

The principal supervisor of this project was Professor ***Knut N. Leknes***. The co-supervisors were Professor ***Kamal Mustafa*** and Dr. ***Zhe Xing***. External supervisor was Associate Professor ***Anna Finne-Wistrand***.

2. Abstract

Poly(L-lactide-co-ε-caprolactone) (poly(LLA-co-CL)) meets many of the requirements of a scaffolding material for bone tissue engineering, such as adequate biocompatibility, degradability, and tunable properties. However, poly(LLA-co-CL) scaffolding tends to be hydrophobic and does not favor cellular attachment and differentiation. The overall purpose of this research project was to improve the physical and chemical properties of poly(LLA-co-CL) scaffolds to enhance biological responses. The modifying effects were evaluated and characterized *in vitro* and *in vivo*.

The aim of **Paper I** was to compare the influence on bone regeneration of low (1×10^6 cells/scaffold) and high (2×10^6 cells/scaffold) seeding densities of bone marrow stromal stem cells (BMSCs) onto poly(LLA-co-CL) scaffolds. The influence of osteogenic supplements was also assessed. Scaffolds seeded at high cell density exhibited higher mRNA expressions of osteogenic markers than those with low seeding density. Osteogenic supplements significantly increased cell proliferation; more bone was formed in response to high seeding density with osteogenic medium. The results show that cell seeding density and osteogenic supplements may have a synergistic effect on the induction of new bone.

After optimizing the culture conditions for BMSCs, the hydrophilicity of the surfaces of poly(LLA-co-CL) scaffolding was increased, either by blending with Tween 80 (**Paper II**), or coating with nanodiamond particles (nDPs) (**Paper III**).

Compared with pristine scaffolds, the modified poly(LLA-co-CL) scaffolds exhibited reduced albumin adsorption and significantly increased the seeding efficiency of BMSCs.

In **Paper II**, poly(LLA-co-CL)/3% Tween 80 scaffolds implanted subcutaneously in rats exhibited significantly increased mRNA expression of Runx2 and *de novo* bone formation. In **Paper III**, BMSCs-seeded into poly(LLA-co-CL)/nDPs scaffolds were implanted into rat calvarial defects and live imaging at 12 weeks disclosed significantly increased osteogenic metabolic activity. Micro-computed tomography, confirmed by histological data, revealed a substantial increase in bone volume.

These results show that increasing the density of cell seeding onto poly(LLA-co-Cl) scaffolds promotes BMSCs differentiation and bone formation. Modifying the surface of poly(LLA-co-CL) scaffolds to improve hydrophilicity promotes osteoconductivity and bone regeneration.

3. List of Publications

This thesis is based on the following papers:

Paper I

Mohammed Ahmed Yassin, Knut N. Leknes, Torbjørn Østvik Pedersen, Zhe Xing, Yang Sun, Stein Atle Lie, Anna Finne-Wistrand, Kamal Mustafa. **Cell seeding density is a critical determinant for copolymer scaffolds-induced bone regeneration**. Journal of Biomedical Materials Research Part A 2015;103(11):3649-3658.

Paper II

Mohammed Ahmed Yassin, Knut N. Leknes, Yang Sun, Stein Atle Lie, Anna Finne-Wistrand, Kamal Mustafa. **Surfactant tuning of hydrophilicity of porous degradable copolymer scaffolds promotes cellular proliferation and enhances bone formation**. Journal of Biomedical Materials Research Part A 2016;104(8):2049-2059.

Paper III

Mohammed Ahmed Yassin, Kamal Mustafa, Zhe Xing, Yang Sun, Kristine Eldevik Fasmer, Thilo Waag, Anke Krueger, Doris Steinmüller-Nethl, Anna Finne-Wistrand, and Knut N. Leknes. **Polymer scaffolds functionalized with nanodiamond particles enhances osteogenic metabolic activity and bone regeneration**. *Accepted in* Macromolecular Bioscience.

The Author contributed to the following papers during the PhD period (Not part of the current thesis)

Yang Sun, Anna Finne-Wistrand, Thilo Waag, Zhe Xing, ***Mohammed Ahmed Yassin***, Akihito Yamamoto, Kamal Mustafa, Doris Steinmüller-Nethl, Anke Krueger, Ann-Christine Albertsson. **Reinforced Degradable Biocomposite by Homogenously Distributed Functionalized Nanodiamond Particles**. Macromolecular Materials and Engineering 2015;300(4):436-447.

Papadakou Panagiota, Athanasia Bletsa, ***Mohammed Ahmed Yassin,*** Tine Veronica Karlsen, Helge Wiig, Ellen Berggreen. **Hyperplasia of gingival lymphatics does not protect against periodontal inflammation in VEGFC overexpressing mice**. *Submitted manuscript*

Cecilie Gjerde, Sølve Hellem, ***Mohammed Ahmed Yassin,*** Bjørn Tore Gjertsen, Aymen B Ahmed, Siren Skaale, Trond Berge, Annika Rosén, Harald Gjengedal, Marcus Rojewski, Hubert Schrezenmeier , Pierre Layrolle, Kamal Mustafa. **Stem cells in bone regeneration, a systematic approach and an observational first-in-human trial**. *Manuscript.*

4. Definitions

Allogenic: “From individuals of the same species”

Allograft: “Graft harvested from an individual other than the one receiving the graft”

Autograft: “Graft obtained from the same individual receiving the graft”

Autologous: “Originating from the recipient rather than from a donor”

Biodegradation: “Capable of being decomposed by bacteria or other biological means”

Blend: “A uniform combination of two or more materials”

Coating: “A thin layer or covering of something”

Composite: “A combination of two or more distinctly different materials where each component contributes positively to the properties of the final product”

De novo: “A Latin expression meaning "from the beginning,"”

Extracellular matrix: “Collection molecules secreted by cells that provide structural and biochemical support to the surrounding cells”

Ex vivo: “Experimentation or measurements done in or on tissue from an organism in an external environment”

Hydrophilic: “Having a tendency to mix with, dissolve in, or be wetted by water”

Hydrophobic: “Tending to repel or fail to mix with water”

In vitro: “Taking place in a culture dish, or elsewhere outside a living organism”

In vivo: “Taking place in a living organism”

In situ: “In the natural, original, or appropriate position”

Osteoblast: “Bone forming cell”

Osteoclast: “A large multinucleate bone cell which absorbs bone tissue during growth and healing”

Osteoconductive: “Supports bone growth and encourages the ingrowth of surrounding bone”

Osteocyte: “A bone cell that is formed when an osteoblast becomes embedded in the material it has secreted”

Osteogenesis: “When vital osteoblasts originating from the bone graft material contribute to new bone growth”

Osteoid: “Unmineralized and/or collagenous organic component of bone”

Osteoinductive: Capable of promoting the differentiation of progenitor cells down an osteoblastic lineage

Osteointegration: “Integrates into surrounding bone Strength Ability of a material to withstand an applied load without failure”

Polymer: “A substance which has a molecular structure built up from a large number of similar units bonded together”

Scaffold: “In general means a structure providing support”

5. Abbreviations

μ-CT	Micro–computed tomography
α-MEM	Alpha-minimum essential medium
3D	Three-dimensional
3DF	Three-dimensional fiber deposition
18F-NaF	18F-Sodium Fluoride
ALP	Alkaline phosphatase
BMP	Bone morphogenetic proteins
BMSCs	Bone marrow stromal cells
BSP	Bone sialoprotein
BTE	Bone tissue engineering
CD	Cluster of differentiation
Col1	Collagen 1
DNA	Deoxyribonucleic acid
Đ	Molar-mass dispersity
ECM	Extracellular bone matrix
FBS	Fetal bovine serum
FDM	Fused deposition modeling
HA	Hydroxyapatite
H NMR	Nuclear magnetic resonance
LLA	L-lactide
Mn	Number averaged molecular weight
MSC	Mesenchymal stem cell
MTT	Methylthiazol tetrazolium

mRNA	Messenger ribonucleic acid
nDPs	Nano-diamond particles
OC	Osteocalcin
PBS	Phosphate buffered saline
PCL	Poly(ε-caprolactone)
PET/CT	Positron emission tomography–computed tomography
PLA	Poly(L-lactide)
Poly(LLA-co-CL)	Poly(L-lactide-co-ε-caprolactone)
ROP	Ring opening polymerization
qRT-PCR	Quantitative real time transcriptase polymerase chain reaction
Runx2	Runt-related transcription factor 2
SD	Standard deviation
SDS	Sodium dodecyl sulphate
SE	Standard error
SEC	Size exclusion chromatography
SEM	Scanning electron microscopy
$Sn(Oct)_2$	Stannous octoate

6. Figures and Tables

7. Introduction

7.1 Bone Tissue Engineering

"Look deep into nature, and then you will understand everything better"
Albert Einstein

Bone has a wide array of functions and responds to a variety of metabolic, physical, and endocrine stimuli. It is the basis of locomotion, stores biological elements required for hematopoiesis, provides the load-bearing skeleton, and protects the internal organs [1]. The adult human skeleton comprises more than 200 bones, consisting of two components: cortical (compact) and trabecular (cancellous) bone. Cortical bone, which comprises 80% of all bone tissue, is arranged in a compact solid pattern, with less than 10% porosity and is generally present in long, short, and flat bones [1]. Trabecular bone, about 20% of all bone tissue, is structured in sponge-like pattern with porosity up to 50–90%. It can be found in the bone marrow and is essentially present in the metaphysis of long bones, the iliac crest, and the vertebral bodies.

Bone has the ability to regenerate without forming scar tissue. In addition, it is a highly dynamic tissue and constantly changes in response to mechanical and hormonal signals. The dynamic state of homeostasis is mediated by bone cells such as osteoblasts, osteoclasts, and osteocytes [1]. Osteoblasts are derived from mesenchymal stem cells (MSCs) and secrete osteoid. The osteocyte is a mature osteoblast, surrounded by osteoid. Osteoclasts, derived from hematopoietic cells of the marrow, secrete acids and proteolytic enzymes which dissolve mineral salts and digest the organic matrix of bone [1]. Bone can be considered as a truly composite material with bone matrix components, a mineral part (hydroxyapatite (HA)) which comprises 65–70% of the matrix and an organic part (collagen, glycoproteins, proteoglycans, and sialoproteins) which comprises the remaining 25–30% of the total matrix [2]. However, the regenerative capacity of bone might be compromised when the defect size is beyond the normal potential for self-healing [3].

One of the challenges confronted by clinicians is the repair and restoration of bone defects resulting from congenital anomalies, resection of a neoplasm or trauma.

To date, the autologous bone graft has served as the gold standard because of histocompatiblity and other essential properties of a bone grafting material [4], necessary to achieve osteogenesis, osteoinduction, and osteoconduction [5]. However, in many cases, only a limited amount of bone is available and the procedure may be complicated by donor site morbidity and post-operative pain [6]. These limitations can be overcome by the use of allografts [6]. There are however, documented cases of infection transmission associated with allografts and the risks of bacterial contamination and immune rejection of the graft must be considered [6].

Bone tissue engineering is a promising alternative approach to bone regeneration, circumventing such issues as insufficient donor tissue for transplanting and the potential risk of adverse tissue responses [7]. This dynamic process comprises a number of steps: recruitment of osteoprogenitor cells followed by their proliferation and differentiation, and matrix deposition and remodeling of the bone [8]. The classical concept of bone tissue engineering involves seeding of cells into a supporting structural framework called a scaffold: the cells are allowed to deposit a matrix before implantation of the seeded scaffold into the defect (**Figure 1**) [9]. Several studies of tissue engineering and regenerative medicine have shown that cells are important for stimulating bone regeneration [10-13]. This can be enhanced by exposure to certain signaling molecules or other growth factors which can be loaded into the scaffold [14]. In another approach, the scaffolding material may be implanted without cells and regeneration then relies on the recruitment of host native cells into the scaffolds and the subsequent deposition of an extracellular matrix (ECM) [15].

Regardless of the approach being used, the scaffold is a fundamental component in bone tissue engineering.

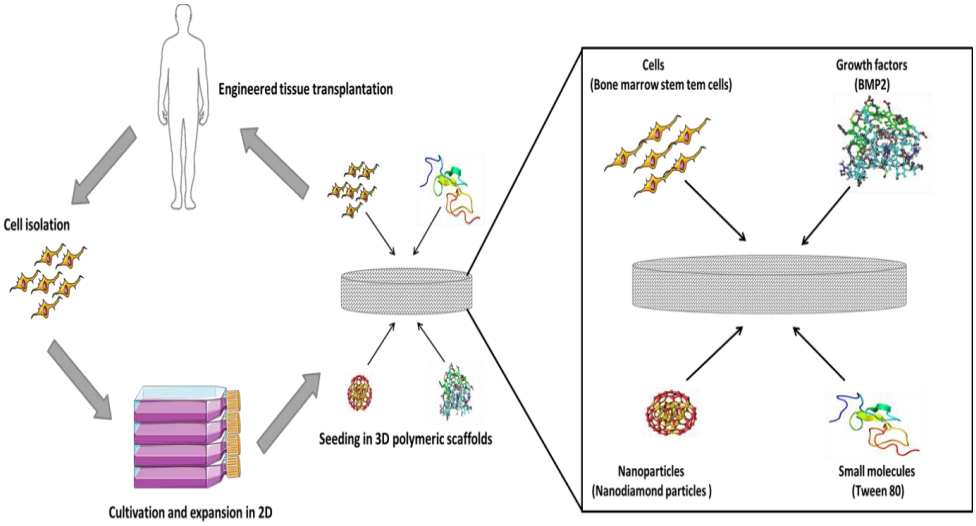

Figure 1. Bone tissue engineering construct in which cells are seeded into 3D porous biomaterial scaffolds. Cells are isolated from the patient, cultured, and expanded *in vitro* on 2D surfaces. The cells are then seeded into porous scaffolds, with or without growth factors, small molecules, and micro- and/or nanoparticles.
The scaffolds act as a temporary extracellular matrix and provide high mass transfer and waste removal. Once functioning tissue has been successfully engineered, the construct is transplanted into the defect to restore function (Figure modified from [16])

7.1.1 Scaffolds for bone regeneration

The scaffold functions as a template or ECM for cells or growth factors in regeneration of damaged tissues or organs [17]. Before implantation into the site of the defect, the construct is engineered by seeding cells into the 3D scaffold *in vitro*, and synthesizing tissues by dynamic cell culture [18]. After implantation, the engineered construct may influence the host by releasing osteogenic growth factors, or by housing cells that release growth factors [5]. This leads to accelerated cell homing and enhances regeneration of the defect site.

7.1.1.1 Benchmarks of scaffolds

Because the scaffolds abut against such a sensitive and complex biological tissue as bone, there are stringent requirements for scaffold materials and scaffold design for application in bone tissue engineering. Biomimetic bone scaffolds are usually made of porous degradable materials which provide mechanical support during the regeneration process [9]. These scaffolds require specific physical and mechanical properties appropriate to the site of application.

In order to simulate the characteristic features of native bone, composite scaffolds have been developed [17]. Scaffolding materials must be *osteoinductive*, *i.e.* capable of promoting differentiation of progenitor cells along an osteoblastic lineage; *osteoconductive*, *i.e.* allow the bone cells to adhere, proliferate, and form ECM on its surface, and capable of *osseointegration i.e.* integrate into the surrounding tissues [19].

A successful biomimetic scaffold should meet the following requirements:

i. Biocompatibility

Biocompatibility refers to the ability to support normal cellular activity including molecular signaling systems, without any local or systemic toxic effects on the host tissue [20]. *In vivo*, the immune reaction to the implanted construct must be negligible, in order to prevent a severe inflammatory response which might impair healing or cause failure of the engineered constructs [20].

ii. Degradability

According to the concept of regenerative therapy, the implanted scaffolds should degrade and eventually be replaced by the newly formed tissues. Thus, scaffolds are not intended as permanent implants and should be biodegradable, with an appropriate degradation time *in vivo*, enhancing tissue ingrowth and subsequent formation of new bone [21, 22]. More specifically, the scaffold degradation rate should mirror the rate of bone formation. Another important requirement is that the by-products of the degradation process must be non-toxic and able to exit the body in some natural manner, without interfering with the regenerative process. Further, an inflammatory

response, combined with controlled infusion of cells such as macrophages, is required in order to allow degradation to occur in tandem with tissue formation [23].

iii. Scaffold architecture and topography

The physical features of the scaffold, defined by the micro-architecture (pore geometry, porosity, and interconnectivity) and the surface properties (surface topography), are known to have a profound influence on cell function [24]. In order to ensure cellular penetration, adequate diffusion of nutrients to cells within the construct and diffusion of waste products out of the scaffold, scaffolds should have interconnected pores and high porosity [17]. Under *in vivo* conditions, the success of the engineered construct depends on survival of growing cells and tissues within the scaffold through angiogenesis [25]. The interconnected pores facilitate rapid blood vessel formation in or around the implanted scaffolds to actively support nutrient, oxygen, and waste transport [17]. Pore sizes in the range of 100 – 500 μm have been found to be appropriate for bone tissue ingrowth [26].

Cells interact with scaffolds *via* chemical groups (ligands) on the material surface [17]. The density of ligands is influenced by the specific surface area, *i.e.* the available surface within a pore to which cells can adhere [17]. Thus, a large surface area favors cell attachment and growth [27].

iv. Mechanical properties

An essential function of bone tissue engineering scaffolds is to provide temporary mechanical integrity at the defect site until the bone tissue is regenerated and normal biomechanical function is restored [19]. For compact bone, Young's modulus is between 15 and 20 GPa and for trabecular bone between 0.1 and 2 GPa. The compressive strength of compact bone ranges from 100 to 200 MPa; the range for trabecular bone is from 2 to 20 MPa [8]. The implanted scaffold must have sufficient mechanical integrity to function from the time of implantation to completion of the remodeling process [28].

Scaffold mechanical strength affects the mechano-transduction of the adherent osteoblast or progenitor cells on the scaffold, which is critical to the bone regeneration and remodeling processes [29]. In mechano-transduction, the cells respond to stress by

producing more bone cells, *i.e.* a mechanical stimulus is converted into chemical activity [29]. Both high and low mechanical properties of a scaffold may affect the growth and integration of new tissue [30]. Moreover, increasing the porosity of the scaffolding material detracts from the mechanical properties and complicates the manufacture of reproducible scaffolding [8]. An appropriate construct for bone tissue engineering might be tailored by reinforcement of porous scaffolds with polymers, ceramics, composites, and metals.

7.1.1.2 Candidate materials for scaffolds

The market for materials for biomedical application is expanding rapidly. As the biomaterial matrix is a fundamental component of the temporary synthetic bone substitute, the choice of an appropriate biomaterial is the crucial step in the scaffold design process. It is essential to select biomaterials that fulfill scaffold criteria, with surface properties appropriate to the requirements of the clinical site. Scaffold materials can be organic or inorganic, natural or synthetic, degradable or non-degradable, depending on the intended use [31].

Porous metallic scaffolds, predominantly made of magnesium (Mg), titanium (Ti), and tantalum (Ta), have been studied as materials in bone replacement [32-34]. Metals have high compressive strengths and excellent fatigue resistance, but cannot be integrated and are not biodegradable. Moreover, there are concerns about the release of metal ions into the surrounding tissues [35].

Ceramics have high biocompatibility and are similar to the mineral phase of bone [19]. The calcium phosphate (CaP), group consisting of HA and tricalcium phosphate, is the most commonly used in bone tissue engineering [19]. However, the potential clinical application is limited because ceramics are brittle, with a tendency to fracture and have poor biodegradability [36].

Polymers are the most commonly studied biomaterials for tissue engineering, followed by ceramics [37]. The polymeric biomaterials vary widely, depending on the source, composition, and structure. In addition, the polymers can often be reinforced with other materials and used as composites [36]. A number of natural polymers has

been developed and identified as biomaterials, differing in terms of chemical structure and composition such as protein, polysaccharide, and polyhydroxyalkanoate content. Collagen, chitosan, and hyaluronic acid are attractive scaffold materials and were the first biodegradable biomaterials tested for clinical application [38]. Owing to their bioactive properties, natural polymers have better interactions with the cells, thus enhancing the cellular events in biological systems [38]. They are also used as coating or blending materials to improve cell-material interactions on synthetic polymeric devices [21]. However, this inherent bioactivity has some disadvantages: complications and difficulties associated with their purification, strong immunogenic responses, and the potential for transmission of disease. In addition, the mechanical properties and batch to batch variations of natural polymers limit their application [19].

Synthetic biomaterials on the other hand, have been widely studied and offer a versatile alternative. Their properties (*e.g.* degradation time, porosity, and mechanical features) can be tailored for specific applications. Some of synthetic polymers have physico-chemical and mechanical properties comparable with natural tissues and represent the largest group of biodegradable polymers [39]. Aliphatic polyesters are notable for their great diversity and synthetic adaptability. Polyesters can be developed from different monomers via *e.g.* ring opening and condensation polymerization routes depending on the monomeric units [40]. The aliphatic polyesters include poly(glycolide) (PGA), poly(lactide) (PLA), and poly(caprolactone) (PCL). These are the most widely used biomaterials. They are synthesized using different polymerization methods such as ring-opening polymerization of the respective cyclic monomers; catalysts and initiators must be used. However, aliphatic polyesters generally lack mechanical strength and load bearing applications may be contraindicated [39]. Moreover, the degradation rates are either too fast or too slow [41].

Various monomers have been co-polymerized [39]. Poly(lactide-co-glycolide) (PLGA) copolymers have been widely investigated, because they exhibit important properties such as adjustability of degradation rates and excellent processability [42]. PLGA have been approved by the US Food and Drug Administration (FDA) for clinical use, such as bioresorbable sutures [43]. However, despite biocompatibility and

controllable degradation, clinical application of pure PLGA for bone regeneration is limited because of poor osteoconductivity and mechanical properties which are inadequate to withstand load-bearing applications [42]. In order to render PLGA more biomimetic and able to enhance regeneration of bone, PLGA is therefore often functionalized or combined with other materials, such as ceramics [39, 42].

Degradable PLA, PCL, and their co-polymers have received FDA approval for application in drug delivery and a number of medical devices [44]. They are also very promising for scaffold production [22]. Copolymers can be produced with different ratios of monomers: the chemical and physical properties of the resultant copolymer depend on the monomer ratio within the copolymer. It has been shown that poly(L-lactide-co-ε-caprolactone) (poly(LLA-co-CL)) with 25 mol% ε-CL provides suitable properties as scaffolding for bone tissue engineering [22]. The degradation mechanism of poly(LLA-co-CL) starts with random hydrolysis ester cleavage and ends with weight loss through the diffusion of degraded compounds, which are usually oligomers [22]. It can be degraded by several mechanisms (by microorganisms, by bulk hydrolysis, and by enzymatic surface erosion), making it suitable for biomedical applications [22, 45]. The major advantages of poly(LLA-co-CL) as scaffolding material are better osteoinductive potential, and good mechanical properties [22, 46-48]. However, poly(LLA-co-CL) is hydrophobic, which might not favor stem cell attachment and differentiation [49]. Moreover, the inadequate mechanical properties (depending on scaffold design) may limit load-bearing applications [27].

7.1.1.3 Degradation of polymer scaffolds

Polymer degradation is defined as "the chemical changes in a polymeric material resulting in a cleavage of main-chain ester bonds producing shorter oligomers, monomers, and/or other low molecular weight degradation products" [50]. The degradation rate of polymer scaffolds depends on several factors including surface hydrophilicity, chemical composition, molar mass, degree of crystallinity, and the geometry of the scaffolds [51]. In addition, the degradation mechanism influences polymer structure and the environment it is subjected to *e.g.* oxygen, the presence of

moisture, microorganisms, pH, enzymes, and temperature [52]. The effects of pore size and porosity have been investigated, but the reported results are inconsistent [53, 54].

Among synthetic polymers, aliphatic polyesters are degraded by cleaving the ester bond, either by passive hydrolysis, or actively, by enzymatic reaction which can proceed *via* surface or bulk-degradation pathways [50, 55]. The degradation of polyester scaffolds occurs in three stages. In the first stage the measured mechanical properties and structural integrity remain constant, while the relative number average molecular weights start to decrease. The second stage begins when the Young's modulus of the scaffold decreases, but weight loss and structural changes are not yet significant. The third stage begins with the first significant weight loss and lasts until complete dissolution of the material [41]. It has been shown that the time required for the degradation of the copolymer is related to the ratio of monomers used in its production [41]. For instance, the higher the content of PGA in PLGA, the shorter the degradation time [41].

The degradation rates of polymeric scaffolds can be tailored by additives, which promote degradation for example, poly(d,l-lactide) (PDLA) scaffolds can be blended with PLGA, poly(lactide-b-ethylene glycol-b-lactide), and a lactide [56]. A weight loss of 65% was recorded in the blended material, which is much greater than pure PDLA. The degradation rate of a polymer may also be influenced by adjusting the hydrophobicity. In a previous report, grafting high amounts of nano-HA onto PLA resulted in a degradation rate longer than that of pure PLA [57]. This has been attributed to reduced hydrophobicity as well as an increase in the surface area. In another study, PCL scaffolds modified with β-Tri-calcium phosphate exhibited an accelerated the degradation rate compared with PCL scaffolds, due to increased water diffusion: PCL/TCP scaffolds were more hydrophilic than PCL scaffolds [58]. Instead of adding a promoter to enhance the degradation rate of polyesters, it has been shown that adding nano-HA can also slow the degradation rate [59]. It is hypothesized that the presence of nHA neutralizes the acidic degradation products, which might reduce auto-hydrolysis and therefore the degradation.

7.1.1.4 Polymer scaffold fabrication techniques

In addition to biomaterial chemistry, the maximum functional properties of scaffolds and their interactions with the seeded cells depend on the processing technique [60]. In the body, cells and tissues are organized into 3D architecture. Thus, to engineer functional tissues successfully, the scaffolds have to be designed to facilitate cell distribution and guide regeneration of tissue three dimensionally. Scaffold design and fabrication techniques influence morphology, pore size, and interconnectivity. These scaffolding characteristics strongly affect cellular events and must therefore be taken into account in bone regeneration techniques [60]. The rapid growth in the field of tissue engineering has resulted in a plethora of technologies for tailoring various porous synthetic scaffolds.

Conventional techniques to produce scaffolds have focused mainly on the introduction of open and interconnected pores within biodegradable scaffolds, in order to increase the viability of the seeded cells. In particular, the salt leaching technique has been widely used because it is cost-effective, simple, and easy to scale up [61]. Numerous scaffolds prepared from this technique might result in successful clinical outcomes [62]. However, the technique can produce only thin scaffolds or membranes up to 3 mm thick and it is very difficult to reproduce scaffolds with accurate pore interconnectivity [63].

As an alternative, electrospinning allows nanoscaled fibrous design of scaffolds that mimic functional collagen structures [64]. These nanofibers are characterized by a complex interconnective fibrous structure, which may make it possible to fabricate highly structured scaffolds for inducing cellular events [65]. During the last decade, rapid prototyping (RP) techniques have been introduced including selective shape deposition manufacturing, laser sintering, fused deposition modeling, 3D bio-plotting, and stereolithography. The scaffolds fabricated by these techniques are precise and reproducible, controlling the internal pore size, pore interconnectivity, porosity, and mechanical performance [65]. In addition, they are considered to be effective methods for fabricating custom-made scaffolds [65, 66].

7.1.2. Cell-based strategies in bone tissue engineering

The potential of the cell-based strategy has been demonstrated in several *in vitro* and *in vivo* preclinical studies [10-13]. However, to date there has been no extensive translation of these results to clinical bone regenerative applications [67]. Despite promising data, several factors have contributed to the fact that bone tissue engineering has not yet become an established clinical procedure [5].

Multipotent stromal cells or mesenchymal stem cells (MSCs) are the most extensively investigated and applied [68]. These cells are non-hematopoietic and of mesodermal derivation, capable of self-renewal and multilineage differentiation *e.g.* into osteoblasts, adipocytes, and chondrocytes [67]. MSCs are found throughout the body and numerous extraction protocols have been established for different tissues *e.g.* umbilical cord [69], adipose tissue [70], skeletal muscle [71], deciduous teeth [72], and other tissues. For more than 40 years, bone marrow-derived stem cells (BMSCs) have been the most frequent sources for cell therapy [73]. These cells can be isolated from bone marrow and from bone chips (cortical or trabecular bone).

A series of reports on preclinical studies has confirmed that BMSCs can induce formation of new bone [10, 11] due to their proliferation and differentiation capacities [10-13]. There are also a limited number of clinical trials demonstrating the stimulatory osteogenic effect of BMSCs [12, 13]. However, it has been shown that the proliferative capacity and differentiation potential of BMSCs are inversely correlated with donor age [74]. BMSCs have been found to be positive for STRO-1, SH3, CD29, CD44, CD71, CD90, CD105, CD106, CD120a and CD124 and negative for negative CD14, CD34, and CD45 [75].

Autologous BMSCs are the most commonly used in regenerative medicine [76]. However, a major disadvantage is the difficulty in harvesting a sufficient number of cells, particular in elderly patients [74]. Tissue regeneration requires a minimum number of cells for each application: thus *ex vivo* expansion and multiplication of the harvested cells may be necessary. This expansion procedure requires a clean cell processing environment to avoid any kind of contamination. In addition, it is a time consuming

procedure and there is a risk of viral infection from serum supplementation in the culture medium [77].

7.1.2.1 Cell expansion

After isolation of BMSCs, *ex vivo* expansion is a vital step. The goal is to achieve a sufficient number of undifferentiated stem cells capable of efficiently differentiating into osteoblast-like cells. For reproducible expansion of BMSCs, essential culture parameters need to be considered, such as the type of culture medium, cell passaging density, and doubling numbers. It is often, necessary to grow millions of BMSCs *in vitro*, thus, significant cell proliferation is required. It has been reported that rapid proliferation of BMSCs could result in an expansion of a thousand-fold in 14 to 21 days [78]. One major challenge in cell-based engineering and regenerative medicine is to achieve large scale expansion of harvested cells without loss of multipotency. Prolonged expansion and extensive subculture has been shown to impair cellular function, leading to cellular senescence, which is associated with proliferation, arrest and apoptosis [79, 80].

Although the standard protocol for maintaining BMSCs on feeder cells *i.e.* serum, is successful and widely adopted, such a serum-based culture protocol is labor intensive, prone to contamination from feeder cells, and difficult for high-throughput automation [81]. Thus, to facilitate the transition of a cell-based strategy tissue engineering approach, from basic studies to clinical application, the need has arisen to review the reagents used to expand stem cells [82]. One of the most important achievements in this area is the transition to xenogeneic-free medium.

7.1.2.2 Cell seeding and cell seeding density

Generation of engineered constructs starts with the attachment of isolated cells onto 3D scaffolds. This is an essential procedure before *in vivo* implantation and plays a decisive role in the development of the engineered tissue [18]. Successful cell seeding depends on many factors, including uniform spatial distribution of cells throughout the scaffold volume and high cell survival rate [83]. Uniform cell distribution is important for uniform ECM protein and therefore well-organized tissue ingrowth [84]. For

instance, non-homogeneous seeding distribution results in increased tissue growth at the periphery of the scaffold with gradients in nutrient and metabolite concentrations throughout the scaffold [85, 86].

Cell seeding efficiency can be increased either by optimizing cell seeding methods or by selecting scaffolds with suitable chemical and physical properties [18]. For the former, to date, a diversity of seeding techniques has been employed: static and dynamic methods and combinations of the two. For instance, dynamic cell seeding (*e.g.* using a perfusion bioreactor) has been shown to yield higher cell seeding efficiencies and more homogenous cell distribution than static cell seeding [87]. For the latter, the criteria and scaffold design are explored in tandem with properties such as biodegradability, porosity, interconnectivity, and mechanical integrity. It has been shown that various scaffold properties affect seeding efficiency. For example, more cells were predicted in the isotropic than in the gradient scaffold although both had a similar overall porosity and surface area [18, 88].

Scaffold surfaces can also be modified to enhance surface biological recognition sites for cells. For example, surface treatments of polymer scaffolds by alkaline hydrolysis, followed by oxygen plasma treatment, resulted in more cell infiltration than non-modified scaffolds [89]. The permeability of the scaffold in relation to scaffold geometry may be more important than the actual porosity and pore size, since it is more directly related to mass transport and fluid flow distribution throughout the scaffold [90].

One of the key elements related to cell seeding is the seeding density (number of cells per construct unit or volume). It is widely accepted that the cell seeding density of constructs is influenced by seeding efficiency and the spatial distribution [18, 83, 91]. Cell seeding density is dependent on tissue type and culture conditions. A study in cartilage tissues has demonstrated that initial cell seeding density and nutrient accessibility through dynamic cell culture are important parameters in modulating the tissue development of engineered constructs [92]. With respect to regeneration of bone tissue, cell seeding density influences cellular events and tissue formation [69, 84, 91, 93-95]. Compared with low cell seeding densities, high numbers of cells in a scaffold may

enhance cell seeding and spatial uniformity of cell distribution and/or cell morphology and alignment [84, 94, 96, 97]. It has been shown that an increase in cell seeding density from 1×10^6 cells/mL to 10×10^6 cells/mL results in homogenous cell distribution throughout the constructs, which might facilitate tissue development [98]. However, seeding efficiency and cell survival tend to decrease with increased cell seeding density, indicating saturation of the scaffold [87]. On the other hand, low cell seeding densities have been associated with limited cell proliferation and loss of mechanical integrity [99]. This has been attributed to loss of cell-cell contact and inadequate matrix production.

Table I presents the results of published studies of *in vivo* cell seeding density, showing that no definite data about optimal cell seeding density are available, because of the diversity of the scaffold material and properties and the types of cells used in the various studies. One reason for this diversity could be the difficulty in measuring the surface area of scaffolds. However, with recent technological advances, it will be easy to calculate surface area and correlate this with the appropriate cell number. Moreover, with 3D printed scaffolds, the total surface area might be predetermined using computer-aided design (CAD) technologies.

Table 1. *In vivo* preclinical studies involving BMSCs transplantation in bone tissue engineering (adapted and modified from [100])

Cells	Scaffold	Seeding density/ scaffold	*In vivo* implantation period	Experimental animal model	Defect size	Efficacy of bone formation (Fold change, cell seeded/ cell-free)	Reference
BMSCs	Mineralized collagen	20×10^6	24 weeks	Sheep Tibia	3 cm	Bone percentage (%): 18.0/13.0 = 1.4	[101]
BMSCs	Chitosan	1×10^6	8 weeks	Mouse calvarial defect	5 mm	More bone formation in cell-seeded constructs: (No quantitative analysis)	[102]
BMSCs	PCL	3×10^6	12 weeks	Rat femur	8 mm	one volume (mm3): 25.0/10.0 = 2.5	[103]
BMSCs	PCL/β-TCP	1×10^6	3 weeks	Rat femur	8 mm	Bone volume (mm3): 1.0/0.3 = 3.3	[104]
BMSCs	Hyaluronic acid	1×10^6	4 weeks	Rat calvarial defect	5 mm	Bone percentage (%): 61.0/16.0 = 3.8	[105]
BMSCs	PLGA	5×10^5	20 weeks	Rat calvarial defect	5 mm	Bone percentage (%): 54.0/20.0 = 2.7	[106]

7.1.3 Cell-scaffold interactions

Over the past few decades, numerous smart biomaterial platforms have been generated for biomedical applications. The interaction of cells with these biomaterials is critical for achieving functional engineered tissue [107]. Based primarily on its structure, a biomaterial will transmit specific signals to cells capable of decoding these into biochemical signals [108]. Therefore, fundamental to the conduct of studies of optimal biomedical applications is a concise understanding of the cell-biomaterial interaction, cell biology, and cell-extracellular matrix interactions [108].

When a scaffold is exposed to a biological environment (*in vitro* or *in vivo*), non-specific protein adsorption occurs. In this process, cells interact indirectly with the biomaterial surface through the layer of adsorbed proteins [107]. The adsorbed layer of protein is the substrate that recruits monocytes/macrophages and induces a number of reactions at the interface with the biomaterial [109]. These reactions will determine the degree of the biocompatibility of the material [109].

Adverse responses to implantation of biomaterials *in vivo* include injury, cell-biomaterial interactions, acute inflammation, chronic inflammation, granulation tissue development, foreign body reaction, and fibrosis/fibrous capsule development [110]. For instance, after implantation of polymeric constructs, fibrous encapsulation occurs and this may impair tissue regeneration [110]. Thus, the main goal in developing biomaterials suitable for tissue regeneration is to design an intelligent material that is able to integrate and interact with the surrounding tissues by biomolecular recognition [111]. By manipulating the design parameters of the biomaterial, the non-specific protein adsorption might be altered. This may make the biomaterial capable of eliciting specific cellular responses and directing new tissue formation [111].

There are two theories explaining the mechanism of cell adhesion to a scaffold [112]. The first is the physicochemical theory: passive adhesion which includes electric, ionic, and hydrophobic interactions between cells and the protein layer. The second theory is the biological theory of active adhesion, characterized by the ability of cell membrane specific receptors to interact with specific ligands. These ligands may be situated on the ECM and interaction is mediated by integrin [112]. The integrin family comprises at least 24 distinct heterodimers which bind to specific amino acid

sequences such as the arginine–glycine–aspartic acid (RGD) recognition motif, present in many ECM proteins, including fibronectin and vitronectin [113, 114]. Alternatively, the ligands may be located on the membranes of neighboring cells, mediated by cadherin [112].

While cellular recognition of a biomaterial "the bio-recognition process" is essentially based on integrin-mediated interactions, it also depends in particular on the chemical and physical properties of biomaterials [115]. For example, nanostructure materials are recognized as favorable biomaterials, not only because they increase the surface area of the material but also because they modify the surface topology without chemical alteration [116]. Therefore, cell-surface interactions through the adsorbed protein layer and its structure and nature determine the subsequent cellular events [117].

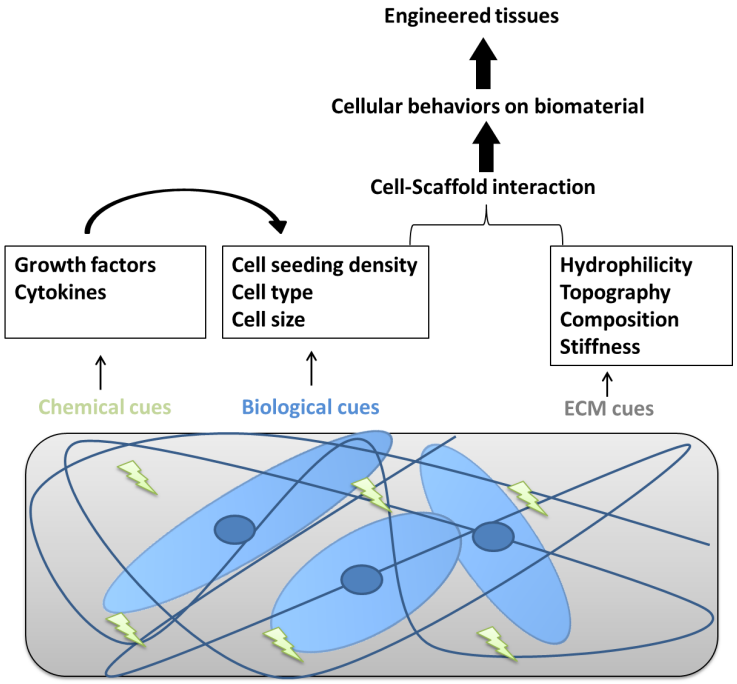

Figure 2. 3D microenvironment with three categories of cues that regulate cell-scaffold interaction and the engineered constructs (Modified and adapted from [118])

Based on the understanding of cell-material interactions (**Figure 2**), different approaches can be used to achieve biomolecular recognition of materials, such as by introducing defined molecular recognition elements into biomaterials (*e.g.* integrin). A successful means of providing sites for integrin attachment in scaffolds is to include purified ECM proteins [119]. Another approach is to modulate the chemical composition and physical properties of the material surface, which has been shown to have a pronounced influence on cellular characteristics and activities (*e.g.* morphology, motility, and migration) [119]. The latter approach is the focus of the current thesis.

7.1.4 Preparation of hydrophilic polymer scaffolds

The selection of polymer materials for bone tissue engineering applications includes assessment of chemical stability, logistics issues, compatibility with sterilization techniques, mechanical performance, and the surface properties of the material [17, 22]. However, this does not necessarily ensure that the final surface properties of the 3D scaffold are optimal for cell-material interaction. Accordingly, it is often necessary to modify the surface properties of scaffold materials, without adversely changing the bulk properties.

The 'hydrophobic character' and lack of natural recognition sites of polyester surfaces has restricted their application as scaffolding materials. In the absence of bioactive peptides RGD, cells interact with scaffolds by means of adsorbed protein, which depends on the physical and chemical properties of the surface [119]. The initial factor affecting protein adsorption may be hydrophilicity/hydrophobicity related to surface chemistry. Hydrophobic surfaces favor the adsorption of proteins from aqueous solutions thermodynamically [120]. However, this might induce irreversible adsorption and denature the protein's native conformation and bioactivity [120]. Although it is recognized that surface wettability influences protein adsorption, its effect on cellular events is quite controversial [121-123]. It has been shown that compared with hydrophilic surfaces, hydrophobic surfaces might have a positive effect on cell attachment [121, 122]. On the other hand, improving surface hydrophilicity is necessary if hydrophobic materials are to support cell adherence, and particularly tissue ingrowth [123].

Hydrophilizing 3D porous scaffolds can improve not only cell-biomaterial interactions, but also the diffusion of cell culture medium and nutrient transfer into the scaffold, and therefore tissue ingrowth. Techniques to modify the polymer surface may be chemically and/or physically-based [124]. Chemically-based surface modifications are employed to change the surface chemistry of synthetic polymers by introducing new functional groups onto the scaffold polymer surfaces, or by coating the polymer with a thin layer of another polymer, or other chemical species, such as material derived from HA [124, 125]. On the other hand, because of the importance of surface topography on cell behavior, a wide range of physical methods has been applied to modify the surface topography of scaffolds [126].

Numerous techniques have been developed to improve the hydrophilicity of synthetic polymer scaffolds:

a) *Pre-wetting technique*

This is considered a simple procedure to achieve dense, uniform cell seeding into a hydrophobic polymer scaffold [127]. In brief, the hydrophobic porous polymer scaffold is pre-wet in alcohol (*i.e.* ethanol). The ethanol is then replaced with culture medium. This is in turn later replaced with cell-containing culture. This method was also used to sterilize scaffolds using 70% ethanol [21]. However, this is used as a temporary measure to achieve uniform cell seeding during initial cell culture: the inherent hydrophobic character of polymer surfaces is not changed [49].

b) Bulk blending technique

This technique is considered to be an easy way of improving the hydrophilicity of synthetic polymers. It involves mixing hydrophobic synthetic polymers, which provide the mechanical and construction properties of the scaffolds, with hydrophilic natural /synthetic polymers, which provide cell recognition sites [123, 128, 129]. The optimal hydrophilic polymer content in the scaffold is determined by balancing the cell affinity of the surface and the mechanical properties of the bulk scaffold [130]. Several hydrophilic natural/synthetic polymers and surfactants have been utilized to fabricate hydrophilized blended scaffolds, including collagen [131], dextran [130], silk fibroin [132], and poly(vinyl alcohol) [123]. However, this technique has some shortcomings,

including phase separation between hydrophilic and hydrophobic polymers and leaching out of hydrophilic polymers from the blend in an aqueous state [49].

To overcome these drawbacks, copolymers have been blended with Tween 80 as a simple means of adjusting the hydrophilicity of the polymers [128]. The interaction between the hydrophobic chain of Tween 80 and the main chain hydrophobic copolymer may prevent excessive extraction in aqueous conditions [129]. Tween 80 contains a long hydrophobic chain (hydrophobic tail) and a water-soluble region comprising three hydrophilic polyethylene glycol (PEG) chains (hydrophilic head) with a total of 20 ethylene oxide units (**Figure 3**). This surfactant is widely used in parenteral and topical pharmaceutical formulations and is generally regarded as nontoxic and nonirritant [133]. It has been shown that Tween 80 may enhance the solubility of compounds, improving the absorption of drugs [134, 135]. Moreover, when compared with five different surfactants tested on human fibroblast cells, Tween 80 showed the lowest cytotoxicity [136]. It functions as an antibacterial agent at concentrations demonstrated to be safe in humans [137].

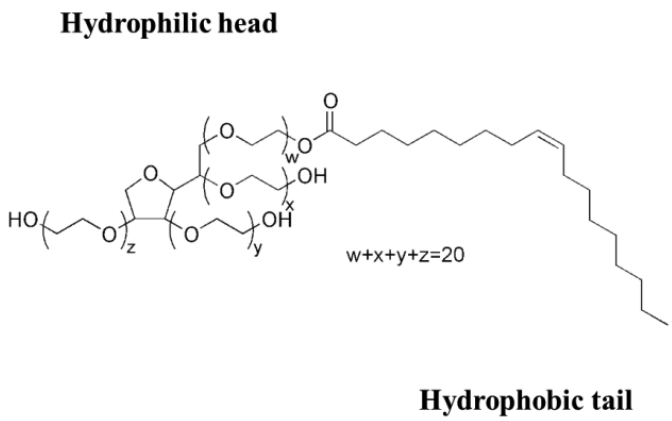

Figure 3. Chemical composition of **Tween 80**

c) Surface coating technique

This physical adsorption technique aims to improve surface properties by coating hydrophilic components (*e.g.* polymer) onto surfaces of 3D porous synthetic biodegradable scaffolds. This technique is applicable to different scaffolds and implants and depends on surface properties (such as surface energy and surface charge), solvent interaction, and scaffold structure [124]. However, the instability of the interactions between the scaffold matrix and the applied hydrophilic polymer may be a drawback [138].

Several methods are used to produce different types of coatings to functionalize the surface of the scaffolds. According to surface chemistry, these coatings can be categorized as inorganic, *e.g.* calcium phosphate [139, 140], organic, *e.g.* ECM-derived coatings [141] or alginate [142], or hybrid.

It has been shown that nanoscale topography has a pronounced influence on biocompatibility and protein adsorption [143]. Recently, it was shown that nanocomposite materials offer favorable solutions as biomaterials, not only by increasing the surface area of the material but also by modifying the surface topology [116]. Of particular interest for biomedical applications is surface coating with nano-diamond particles (nDPs) [144]. nDPs produced by detonation are one of the most promising materials for use in multifunctional nanocomposites to improve surface characteristics of biomaterials (*e.g.* polymers) [145-148]. The purified nDPs are composed of particles with an average diameter of ~ 5 nm. They contain an inert diamond core, covered by a layer of oxygen-containing functional groups such as hydroxyl (– OH), carboxylic acid (– COOH), *etc* (**Figure 4**). These are useful for tailoring the surface properties of polymer scaffolds, for instance hydrophilicity [149, 150] and surface functionalization with signal molecules (*i.e.* BMP2) [148].

nDPs need to be dispersed as single particles to serve as nanofillers in polymeric scaffolds. The surface area of the nanoparticles accessible for interaction with the polymer matrix depends on the quality of filler dispersion. When adequately dispersed, nDPs increase the physical and mechanical properties of the nanocomposites [151]. Moreover, unpublished data from our laboratory show

enhancement of Teflon surface hydrophilicity in response to nDPs (reduction of contact angle from 119° in pristine Teflon to 10° when modified with nDPs).

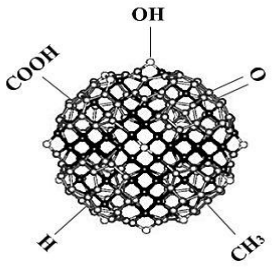

Figure 4. Schematic model illustrating the structure of a single ~5-nm **nanodiamond particle** following oxidative purification. The diamond core is covered by a layer of surface functional groups (Figure adapted from [146])

d) Surface hydrolysis technique

Hydrolysis of a polymer surface using strong acid (hydrochloric acid) or strong alkali such as sodium hydroxide or potassium hydroxide can be used to create –COOH and –OH groups on the surface, resulting in increased hydrophilicity [152]. It has been shown that treating a polymer surface with sodium hydroxide may improve hydrophilicity and increase cell seeding density [153]. This has been explained by hydrolysis of the ester group of polymer to –COOH and –OH groups. However, surface hydrolysis may alter the surface topography and bulk mechanical properties [154].

e) Plasma treatment technique

Polymer surface modification using plasma treatment has been commonly employed to adjust surface adhesion and wetting properties by changing the chemical composition of the surface. The plasma is composed of highly excited atomic, molecular, ionic and radical species and is typically achieved when gases are excited into energetic states by radio frequency, microwave, or electrons from a hot filament discharge [155]. The aim is to introduce polarized groups (–COOH, –OH, $–SO_2$, and $–NH_2$) on polymer

surfaces using gaseous, metallic and laser-based plasma sources [155, 156]. However, some critical issues need to be addressed, such as the limited depth of penetration of plasma into the pores of 3D scaffold: this can lead to heterogeneous modification throughout the entire structure of the scaffolds and loss of surface modification over time (hydrophobic recovery) [157]. Thus, this method can be only used for 2D films or very thin 3D constructs.

8. Rationale for the Project

In a cell-based approach to bone tissue engineering, the scaffold is central to success of the construct. Several studies have described implantation of a scaffold seeded with cultured osteogenic cells in treatment of human bone defects [12, 13, 158]. However, because the bone tissues comprise a complex biological system, the requirements of scaffold materials are very diverse [159]. Thus, many researchers from different scientific backgrounds have studied specific hypotheses related to bone tissue engineering, with special reference to such aspects as cells, biomaterials, design and fabrication of scaffolds, dynamic culture conditions, and cell-scaffolds interactions.

Several *in vitro* and *in vivo* studies have demonstrated excellent biocompatibility and new bone formation using poly(LLA-co-CL) scaffolds [46, 48, 149]. In the studies on which this thesis is based, poly(LLA-co-CL) was used as the scaffold material and was synthesized by random ring-opening polymerization [160]. Before seeding the scaffolds with BMSCs, it is important to ensure that the *in vitro* cell culture environment is carefully controlled with respect to the osteoblast-like cells. Several factors have been shown to influence cellular behavior and subsequent tissue regeneration, such as the addition of soluble factors to directly promote osteogenic differentiation, cell seeding related factors, the use of dynamic culture, and chemical and physical properties of the scaffold surface. Among these factors, cell seeding density may play a vital role in the fate of the seeded cells and must be optimized for specific scaffolding materials [91]. Moreover, the inconclusive and contradictory results using osteogenic supplements for BMSCs indicate the need for further investigation.

After optimizing culture conditions, biocompatibility in terms of surface properties of these copolymer scaffolds should meet the requirements of a biomimetic bone scaffold. Unfortunately, one of the disadvantages of most synthetic degradable polymers is low biocompatibility due to inherent high surface hydrophobicity [161]. Thus, for the present series of studies, it was decided to modify the hydrophilicity of the poly(LLA-co-CL) scaffold surface by blending with Tween 80 and coating with nDPs. A previous study investigated the impact of modifying the hydrophilicity of poly(LLA-co-CL) with Tween 80 on the mechanical properties of the scaffolding and

the cellular response of human osteoblast-like cells [128]. The results demonstrated that a high concentration of Tween 80 increased the surface hydrophilicity but had a toxic effect on the cells and an adverse effect on the material properties of the scaffolds. Thus, further studies are indicated to determine the optimal concentration of Tween 80 and then to test the biological responses both *in vitro* and *in vivo*.

In addition to surface hydrophilicity, the influence of surface topography on BMSCs needs to be addressed. nDPs-BMSCs interactions have been studied under *in vitro* conditions, with specific reference to their application in bone regeneration [149]. An *in vivo* investigation is now required. There is very limited published data on this topic. Collectively, the research project on which this thesis is based was undertaken in order to evaluate cellular and tissue responses to modified copolymer scaffolds.

9. General Aim

"If I have seen further than other, it is by standing upon shoulders of giants"
Sir Isaac Newton

A tissue engineering approach to repair of bone defects comprises the use of a biocompatible scaffolding material, seeded with cells capable of osteogenic activity to stimulate bone regeneration. Current research focuses on improvement, modification, and enhancement of biomaterials synthesized by increasing the hydrophilicity and osteoconductivity of the material. In the present project, a new generation of biodegradable biomaterials is being designed, to elicit specific cellular responses at the molecular level as well as at tissue level. This is based on molecular modifications of degradable polymer surfaces, which stimulate specific interactions with cells and thereby direct osteogenic cell differentiation. The overall purpose of this research project was to improve the physical and chemical properties of poly(LLA-co-CL) scaffolds to enhance biological responses.

9.1 Specific aims:

- To assess the influence of cell seeding density and the effect of osteogenic supplements on BMSC proliferation and differentiation. (**Paper I**)
- To evaluate the effect of cell seeding density with osteogenic supplements on bone regeneration. (**Paper I**)
- To investigate whether enhancing the hydrophilicity of copolymer scaffolds affects albumin adsorption and seeding efficiency of BMSCs (**Paper II** and **Paper III**)
- To evaluate ectopic bone formation by poly(LLA-co-CL) scaffolds seeded with BMSCs and blended with 3% Tween 80. (**Paper II**)
- To assess osteogenic activity and bone regeneration of poly(LLA-co-CL) scaffolds modified with nDPs as a carrier for BMSCs using a rat calvarial defects model. (**Paper III**)

10. Materials and Methods

10.1 Materials

The materials, reagents, and their suppliers used in this project are presented in Table 1

Table 2. The materials and **reagents** used in all studies

Material/Reagent	Supplier	Paper
ε-Caprolactone	CL, Sigma-Aldrich, Germany	I - III
L-Lactide	LLA, Boehringer Ingelheim, Germany	I - III
Ethylene glycol	Sigma-Aldrich, Germany	I - III
Stannous octoate $Sn(Oct)_2$	Sigma-Aldrich, Germany	I - III
Sodium choloride (NaCl)	Fluka Chemika, Germany	I - III
Minimum essential medium	αMEM, Invitrogen™, Carlsbad, California, USA	I - III
Fetal Bovine Serum	HyClone™ , South Logan, Utah, USA	I - III
Antibiotic/Antimycotic	HyClone™ South Logan, Utah, USA	I - III
Dexamethasone	Sigma-Aldrich, Germany	I - III
β-Glycerophosphate	Sigma-Aldrich, Germany	I - III
Ascorbic acid	Sigma-Aldrich, Germany	I - III
Sevoflurane	SevoFlo , Abbott Laboratories, UK	I - III
Tween 80	Polysorbate 80 HX2™, Ultra-Pure grade, Japan	II
MTT reagent	Sigma, St Louis, MO, USA	II
Detonation diamond particles	Gansu Lingyun Corp. Lanzhou, China	III
BCA Protein Assay	Pierce™ protein assay, Thermo Fisher.	III

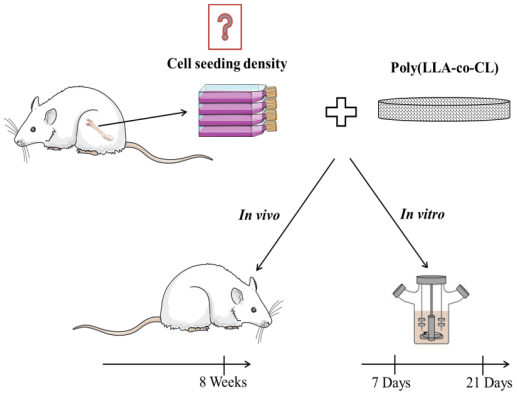

Paper I

- SEM
- DNA quantification
- PCR
- Calvarial bone defect
- μ-CT
- Histology

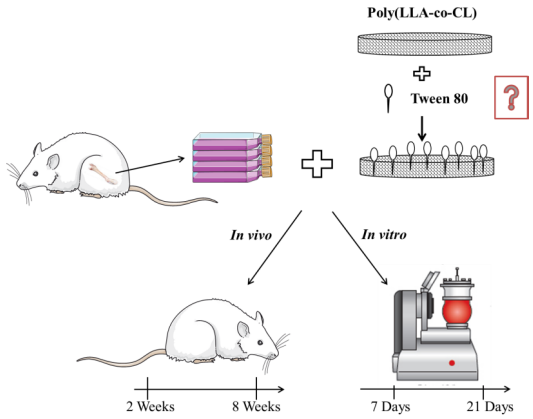

Paper II

- SEM
- SEC and ^{1}H NMR
- Protein adsorption
- Seeding efficiency
- MTT
- Subcutaneous implantation
- PCR
- μ-CT
- Histology

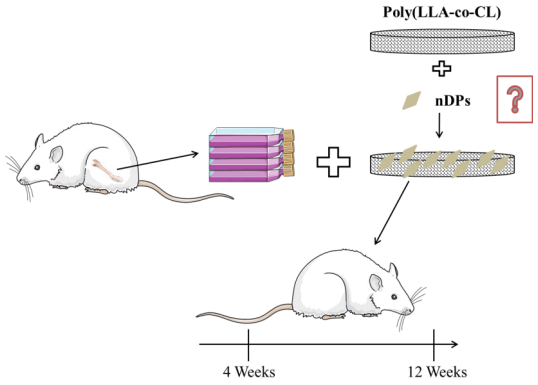

Paper III

- SEM
- Protein adsorption
- Seeding efficiency
- Calvarial bone defect
- PET/CT
- μ-CT
- Histology

Figure 5. Summary of **study design** and **methods** used in the research project.

10.2 Methods

10.2.1 Polymerization (Papers I - III)

Poly(LLA-co-CL) was synthesized by ring-opening polymerization (ROP) at 110°C for 72 h [160]. ε-Caprolactone was dried and purified. L-Lactide was recrystallized and dried before use. In the polymerization reaction, ethylene glycol was used as an initiator and stannous octoate ($Sn(Oct)_2$) as the catalyst. The monomer to catalyst molar ratio was set to 10,000:1 to ensure low amounts of residual tin. The copolymer product was precipitated in cold hexane and methanol three times.

10.2.2 Scaffold fabrication (Papers I - III)

3D poly(LLA-co-CL) porous scaffolds were fabricated by a salt leaching technique as previously described [46]. Polymers were dissolved in chloroform. Sodium chloride to serve as the porogen was sieved; the ratio of polymer to porogen was set at 1:10. After the solvent had evaporated, scaffold samples were shaped to 10 mm (Ø) × 1.3 mm (δ) cylinders (for *in vitro* experiments) and 5 mm (Ø) × 1.3 mm (δ) (for *in vivo* experiments).

10.2.3 Scaffold modification

10.2.3.1 Poly(LLA-co-CL)/Tween 80 (Paper II)

Synthesized poly(LLA-co-CL) was blended with Tween 80 at ratios of 0.5%, 1%, and 3% (*w/w*). Tween 80 was dissolved in chloroform, mixed with copolymer solutions and stirred overnight. To prepare 3D porous scaffolds, polymer blends with Tween 80/NaCl (1:10 w/w) solutions were poured into Petri dishes [128].

10.2.3.2 Nano-composite poly(LLA-co-CL) (Paper III)

Acid purified detonation diamond particles were subjected to attrition milling as previously described [162] to achieve a narrow size distribution at ~ 5 nm particle diameter with low agglomeration of the nanodiamond particles. Poly(LLA-co-CL) scaffolds were modified with the nDPs (4% (w/v), i.e. 40 mg/ml) by a vacuum technique as previously described [148]. In brief, 0.5 ml nDPs solution and one scaffold were put into a glass beaker and perfused in vacuum. The vacuum chamber was

evacuated down to the pressure at which the nDP-water-solution changes into the vapour phase and the nDP burst into the scaffold surface. This cycle was repeated 10 times. The nDPs modified poly(LLA-co-CL) scaffolds were rinsed in distilled water and vacuum dried.

10.2.4 Characterization of scaffolds

10.2.4.1 Nuclear magnetic resonance (^{1}H NMR) (Papers I - III)

^{1}H NMR was used to analyze the monomer conversion. A Bruker Avance 400 NMR instrument (Bruker, Switzerland) was used [22]. The analysis was carried out at room temperature and samples were dissolved in deuteron-chloroform ($CDCl_3$).

10.2.4.2 Size exclusion chromatography (SEC) (Papers I - III)

The molecular weights of all polymers were determined by the SEC system [22]. The molecular weights of the polymers used in the 3D porous scaffold samples were measured using the Verotech PL-GPC 50 (Polymer Laboratories, Varian Inc., MA, US) equipped with a refractive index detector and two Polar-Gel-M Organic GPC Columns (300 × 7.5 mm) from Varian Inc. Chloroform was used as the mobile phase. Narrow linear polystyrene standards were used for universal calibrations.

10.2.4.3 Scanning electron microscopy (SEM) (Papers II and III)

A SEM (Jeol JSM 7400F, Tokyo, Japan) was used to characterize the microstructure of the scaffolds. All scaffolds were coated with gold (Cressington Sputter Coater). The analysis was performed at an accelerating voltage of 10 kV and magnifications up to 40000 X.

10.2.4.4 Micro-computed tomography (μ-CT) (Papers II and III)

μ-CT was carried out in SkyScan model 1172 (Kontich, Belgium). μ-CT was used to determine the pore structure of the scaffolds (porosity, pore size, surface area, and pore size distribution). No filters were used.

10.2.4.5 Water contact angle (Paper II)

Static contact angle measurements were made in CAM 200 contact angle system (KSV Instruments Ltd., Helsinki, Finland). A drop of 5 µL Milli-Q water was placed onto the surface of film samples and contact angles were recorded by analyzing frames captured using an optical camera. Recorded frames were evaluated by CAM 2008 software (version 4.0, KSV) to calculate contact angles. Average values were calculated from five independent measurements [128].

10.2.4.6 The protein adsorption measurement (Papers II and III)

The protein adsorption of pristine and modified poly(LLA-co-CL) scaffolds was assessed as previously described [163]. Samples were incubated in PBS for 4 h, and then incubated in 10 mg/mL BSA at 37 ° C for 2 h. The samples were rinsed twice with PBS. The samples were then treated overnight with 1% sodium dodecyl sulfate (SDS), to remove protein adsorbed to the surface. The amounts of adsorbed protein were quantified using a Pierce™ BCA protein assay kit.

10.2.5 Cell culture

10.2.5.1 Cell isolation (Papers I - III)

BMSCs were isolated from the femurs of donor Lewis male rats [164]. In brief, the rats were housed under uniform conditions, and euthanized by carbon dioxide (CO_2) inhalation. The metaphyseal ends of the femurs were cut off, and the marrow cavity was flushed with minimum essential medium (αMEM) supplemented with 1% antibiotic/antimycotic (AB) and 15 % fetal bovine serum (FBS) into a sterile falcon tube. The cells were centrifuged and cultured in fresh α-MEM medium containing 15% FBS and plated in culture flasks (NUNC A/S, Roskilde, Denmark). The medium was changed the next day, with fresh αMEM medium containing 1% PS and 10% FBS. Cells were cultured until they reached 80% confluence, after which they were passaged.

10.2.5.2 Expansion (Papers I - III)

The cells were cultured in αMEM only, supplemented with 1% AB and 10 % FBS (**Paper I**). Osteogenic supplements were added to the culture medium (0.05 mM ascorbic acid, 10 mMb-glycerophosphate, and100 nM dexamethasone (dex)) [69, 165] 7 days before the experiments (**Papers I - III**).

10.2.6 Sterilization (Papers I - III)

The 3D scaffolds used in these studies were sterilized by irradiation with electron beam radiation (25 kGy dose), created by a pulsed electron accelerator (Mikrotron, Acceleratorteknik, Stockholm, Sweden) at 6.5 MeV [22].

10.2.7 Seeding efficiency (Papers II and III)

In order to determine seeding efficiency [166], pristine and modified scaffolds were placed into 96-well plates and soaked with the culture medium overnight. Thereafter, the cells were seeded directly onto the scaffolds, at a concentration of 5×10^5 cells/scaffold, and incubated for 3h, to allow adequate time for seeding. The scaffolds were then removed and the cells remaining in the wells were counted using automated cell counters (Countess™, Invitrogen, Life Technologies, USA). The seeding efficiency was calculated using the following equation:

$$\text{Seeding efficiency (\%)} = \frac{(\text{Cells seeded into scaffold} - \text{Cells in wells})}{\text{Cells seeded into scaffold}} \times 100$$

10.2.8 Graft preparation (Papers I - III)

3D porous scaffolds were pre-wet with the culture medium in an incubator at 37 °C and 5% CO_2 overnight. The BMSCs were then seeded into the various scaffolds, placed at the bottom of wells in 96-well plates, at a density of 1×10^6 cells/scaffold (**Paper I**) and 2×10^6 cells/scaffold (**Papers I-III**). An orbital shaker (EppendorfVR, Hamburg, Germany) was used for 5 minutes at 1000 rpm to facilitate cell distribution within each scaffold [167].

10.2.9 Bioreactors

To improve *in vitro* culture conditions, bioreactor systems have been widely used for tissue engineering applications. Compared with static cultures, dynamic cell cultures increase medium perfusion: this might enhance nutrient delivery as well as mechanical stimulation of cells [168]. Spinner flasks, rotating wall bioreactors, and perfusion systems have all been tested. Each system has been shown to be effective [169].

10.2.9.1 Spinner flask bioreactors (Paper I)

In a simple bioreactor, scaffolds were suspended from the lid of a flask, and a stir bar was used to induce a convection current in the medium surrounding the scaffolds (**Figure 6**) [169]. The dynamic culture system was constructed using four modified spinner flasks (purchased from Belleco Glass; Figure 6) inside a 37 °C incubator with a humidified 5 % CO_2 atmosphere. This system was used to incubate BMSCs for up to 21 days. The original driver paddle in the flasks was replaced by a metal component with holders for scaffold fixation and equipped with a magnetic stir bar to control the rotation speed [165].

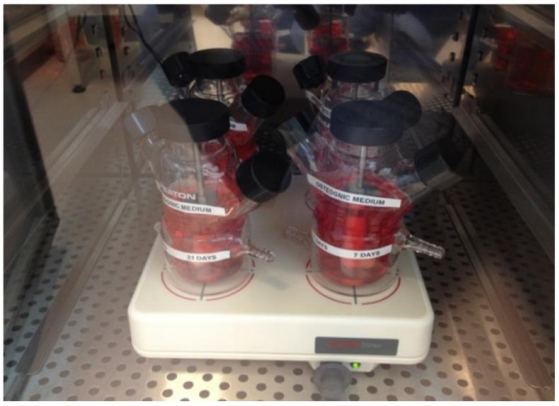

Figure 6. Spinner flask bioreactor. Scaffolds are suspended in the medium and the medium is stirred with a magnetic stirrer, to improve nutrient delivery to the scaffold

10.2.9.2 Biaxial rotating bioreactor (BXR) (Paper II)

The BXR bioreactor consists of a spherical culture chamber, where the cellular scaffolds are anchored to the cap of the bioreactor with pins, a medium reservoir and a perfusion system, which connects the culture chamber and the medium reservoir, as previously described [170]. The spherical culture chamber is designed to rotate on two perpendicular axes (Y and Z). The bioreactor systems were placed in an incubator during the culture period (**Figure 7**).

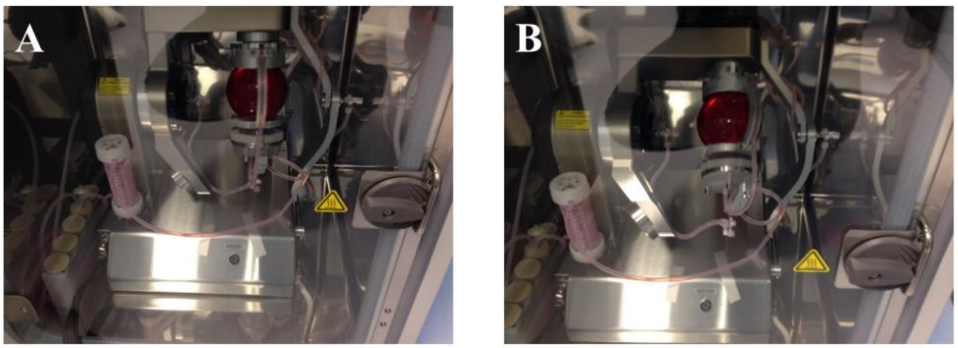

Figure 7. Biaxial rotating bioreactor (BXR): The bioreactor system consisted of a spherical culture vessel (volume 500 ml) connected to the medium reservoir through tubing in which a perfusion flow is generated. The spherical vessel sits on an articulator which allows rotation in two perpendicular axes, as shown in A and B (X and Z).

10.2.10 *In vitro* experiments

10.2.10.1 SEM (Paper I)

Samples were placed in 2.5% glutaraldehyde α-MEM without serum and fixed for 30 min at room temperature. The samples were then fixed in 2.5% glutaraldehyde in 0.1M Na-cacodylate pH 7.2 with 0.1M sucrose for 30 minutes at room temperature. The samples were then treated with 1% osmium tetroxide in distilled water for 1 h, followed by dehydration through a graded series of ethanol solutions, critical point dried and sputter coated with a 10 nm conducting layer of gold platinum. Finally, the specimens were examined by SEM (Jeol JSM 7400F, Tokyo, Japan), using a voltage of 10 kV. Cell adhesion and spreading on the scaffolds were documented.

10.2.10.2. DNA quantification of cell proliferation (Paper I)

DNA quantification was conducted using reagents from the MasterPure™ Complete DNA and RNA Purification Kit (Epicentre® Biotechnologies, Madison, Wisconsin, USA) [171]. The amount and purity of DNA per scaffold were measured by optical densitometry at 260 and 280 nm, using a Nanodrop ND 1000 spectrophotometer (NanoDrop Technologies, Wilmington, Delaware, USA).

10.2.10.3 Cell proliferation assay (Paper II)

Methyl Thiazlol Tetrazolium (MTT) assay, measuring mitochondrial metabolic activity was used to assess cell proliferation [48]. This colorimetric assay is based on the ability of living cells to reduce the yellow reagent MTT to a purple formazan product. Briefly, scaffolds were transferred into 96-well plates and washed with PBS. MTT reagents were added to each sample and incubated for 4 hours in the dark at 37°C, under a CO_2 (5%) atmosphere. The MTT was aspirated and the formazan product was solubilized in 0.2 mL DMSO containing 6.25% (v/v) 0.1M NaOH. The resultant absorbance was measured at 570 nm, using a microplate reader (BMG LABTECH, GmbH, Germany).

10.2.10.4 Real-time reverse transcription-polymerase chain reaction analysis (RT-PCR) (Papers I and II)

RNA isolation and RT- PCR were carried out as described previously [165]. Briefly, total RNA was collected from cells grown onto the scaffolds using an isolation kit (E.Z.N.A^{VR}, Omega Bio-Tek, Norcross, Georgia, USA) according to the manufacturer's protocol. RNA purity and quantification were determined by spectrophotometry (NanoDrop Spectrophotometer, NanoDrop Technologies). Real-time reverse transcription-polymerase chain reaction (RT-PCR) was conducted under standard enzyme and cycling conditions on a StepOne^{TM} real-time PCR system, using TaqMan^{VR} gene expression assays (Applied Biosystems^{TM}, Carlsbad, California, USA). The data were analyzed using a comparative Ct method by StepOne. Expression levels of the genes were normalized to the Housekeeper index with GAPDH serving as the endogenous control.

10.2.10.5 Chemical analysis of hydrophilic scaffolds (Paper II)

^{1}H NMR was used to analyze Tween 80 composition remaining in the scaffolds up to 21 days. A Bruker Avance 400 NMR instrument (Bruker, Switzerland) was used. The analysis was carried out at room temperature and samples were dissolved in deuteron-chloroform ($CDCl_3$). Change in scaffold *Mn* was determined using the SEC system, up to 21 days.

10.2.11 Animal models

The development of bioengineered bone scaffolds is a stepwise process which starts with a crucial *in vitro* optimization step, comprising assessment of scaffold parameters, such as scaffold material and design, cellular events on the biomaterial surface, and osteoconductivity and osteoinductivity. The next step is conducted in an *in vivo* environment, usually in an animal model, before eventually proceeding to human clinical trials.

10.2.11.1 Scaffold-related criteria for appropriate choice of animal model in bone tissue engineering

In bone tissue engineering, animal models are used to evaluate the bone regeneration process and the bone–biomaterial interactions. Physiological or pathological evidence of modulation of the ossification pathway can also be assessed [172]. The size, nature (*e.g.* granular or injectable), hardness, and chemical composition of the scaffolds are the parameters which have to be considered when selecting the appropriate the animal species (small *vs.* large animals), the anatomical site (endochondral *vs* intramembranous bone) and site (load-bearing *vs.* non-load-bearing). Depending on proximity to the autologous bone tissue, *in vivo* models can be classified into heterotopic or ectopic (bone is formed at an abnormal anatomical site, usually in soft tissue) or orthotopic (bone is formed at its normal anatomical site).

10.2.11.2 Assessment of biofunctionality of pristine and modified poly(LLA-co-CL) scaffolds

10.2.11.2.1 Orthotopic bone formation (Papers I and III)

The rat calvarial model is the gold standard for orthotopic implantation studies (**Figure 8**). The orthotopic implantation method allows assessments of osteoconductivity and osteointegration of the pristine and modified poly(LLA-co-CL) scaffolds [173]. Because calvaria have poor blood supply and relatively little bone marrow, achieving bone regeneration is a challenge.

Using a custom-made mask, the rats were anesthetized with isofluorane (Isoba vet^{VR}, Schering Plough, Kenilworth, NJ, USA) in combination with O_2. A full-thickness defect (5 mm in diameter) was created in the central area of each parietal bone. The dura mater was left undisturbed. The skin was repositioned and stabilized with sutures (Vicryl Plus 4-0). All animals were given an intramuscular dose of Buprenorphine (Temgesic® 0.3 mg\kg) as an analgesic and allowed to recover. The status of the surgical wound, signs of infection, food intake, and activity were monitored daily.

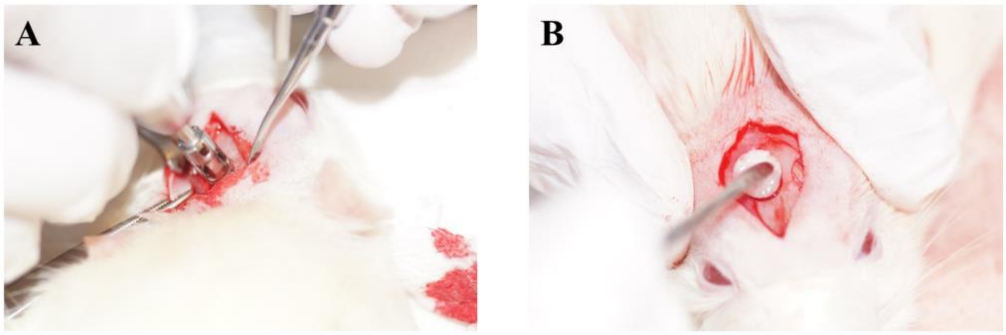

Figure 8. Lewis rat calvarial defect. (A) The bone was exposed and the defect created by incision and retraction of the skin and periosteum. (B) Poly(LLA-c-oCL) scaffolds, pristine or modified, were insterted into the defects.

10.2.11.2.2 Ectopic bone formation (Paper II)

Heterotopic implantation is the gold standard for testing both the biocompatibility and the osteoconductive potential of constructs *in vivo*. Poly(LLA-co-CL) scaffolds modified with Tween 80 were implanted subcutaneously into Lewis male rats to evaluate the biocompatibility of the modified material (**Figure 9**).

The rats were anesthetized with isofluorane (Isoba vet^{VR}, Schering Plough, Kenilworth, NJ, USA) in combination with O_2. Using blunt dissection, a pocket was created on both sides of an incision and one cell/scaffold construct was inserted into each pocket. All animals were given an intramuscular dose of Buprenorphine (Temgesic® 0.3 mg\kg) as an analgesic and allowed to recover. The status of the surgical wound, signs of infection, food intake, and activity were monitored daily.

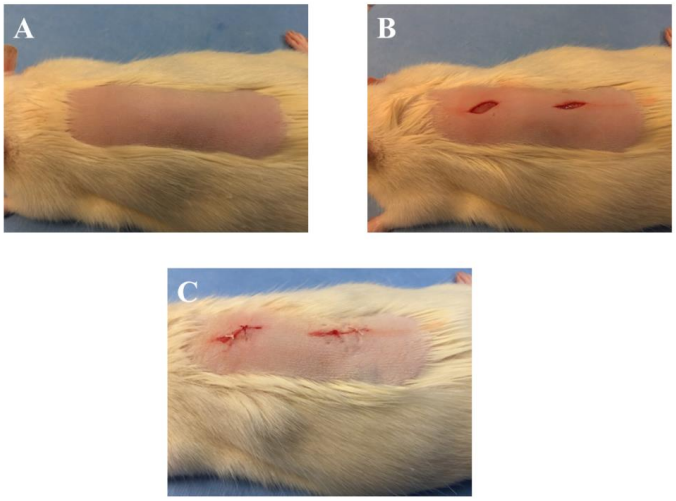

Figure 9. Subcutaneous implantation of scaffolds in to Lewis rats, (A) shaving, (B) skin incision on the dorsal aspect, and (C) closure of the incision.

10.2.12 *In vivo* evaluation

10.2.12.1 Positron emission tomography/computed tomography PET/CT (Paper III)

PET/CT scanning with ^{18}F-Sodium Fluoride (^{18}F-NaF) provides information on bone formation. Fluoride is metabolised into the bone mineral by exchanging with hydroxyl groups on hydroxyapatite to form fluoroapatite, which can be used to produce quantitative images which correlate with new bone formation [174]. The development of a rat imaging system integrating PET with x-ray computed tomography allowed simultaneous anatomic and molecular imaging *in vivo*, for precise measurements of bone-forming activity [175]. Clinical application of bone scanning with [18]F-NaF was first described in 1993 [176]. It provides highly sensitive, 3D tomographic images, and hybrid PET/CT imaging of the skeleton, with , high spatial resolution, and attenuation correction [175].

For PET/CT scanning (**Figure 10**), the rats were anesthetized with sevoflurane (Sevoflo®, Abbott, Illinois, USA). ^{18}F-NaF data were acquired from a PET/CT scanner (Mediso Medical Imaging System, Budapest, Hungary). PET emission scans were acquired for 10 min just after injection of ^{18}F-NaF, followed by CT acquisitions for anatomic correlation. Nucline software (Mediso Medical Imaging System, Budapest, Hungary) was used for PET data reconstruction, with correction for attenuation based on CT data. Inter View Fusion software (Mediso) was used for co-registration of PET and CT data, quantification of standard uptake values in an area of interest, and three dimensional visualization.

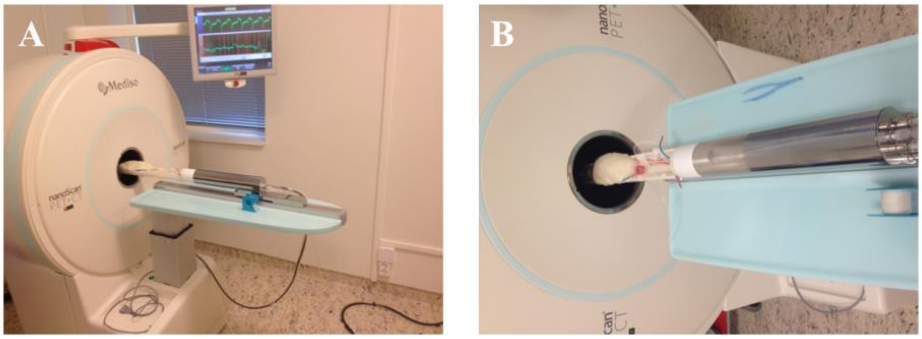

Figure 10. Anaesthetized rat on **PET/CT** scanner bed in supine position after injection of ^{18}F-NaF.

10.2.13 *Ex vivo* evaluation

10.2.13.1 µ-CT (Papers I - III)

For quantitative evaluation of new bone formation in the rat calvarial defects or subcutaneous implants µ-CT scans were taken using the SkyScan1172^{VR} X-ray system (SkyScan^{VR}, Kontich, Belgium) with the CTAn 1.8^{VR} and NRECON RECONSTRUCTIONVR CT software (SkyScan^{VR}), as previously described [177]. A 0.5-mm aluminum filter was used to optimize the images. Source voltage and current were set at 50 kV and 200 µA, respectively. After applying CTAn 1.8^{VR} to each reconstructed BMP file, Bone volume (BV), Tissue volume (TV) and Bone volume/Tissue volume (BV/TV) values were obtained.

10.2.13.2 Histology (Papers I - III)

Specimens for histological examination were fixed with 4% paraformaldehyde (Merck, White House Station, NJ, USA) and decalcified, using 10% ethylenediaminetetraacetic acid (EDTA) in 0.1M Tris buffer and 7.5% polyvinylpyrrolidone (PVP) (Merck). The specimens were then washed in PBS, embedded in paraffin and serially sectioned using a microtome (HM 325, Thermo Scientific). The sections, 4–6 µm thick, were mounted on glass slides, deparaffinized,

hydrated by the application of xylene and alcohol in series and stained with Hematoxylin and eosin (H&E) and Masson's Trichrome (MT) stains.

10.2.14 Statistics

i. ***Paper I***

For accurate data of the hierarchical structure of the outcome variables, a multilevel modelling analysis was applied. For the PCR statistical analyses, reference values were first calculated for all the expression measures. A random effect model with each particular gene as the random factor (to control for the two repeated measures for each gene) was applied. The reference value was defined as the predicted mean from these models. $^{\Delta}$Ct values for each gene were thereafter calculated as the difference between the gene measures and the reference values. The $^{\Delta\Delta}$Ct values for all the expressions were then analyzed in linear models using robust variance estimates to control for the repeated measures for each particular gene. Mean values, standard deviations and 95 % confidence intervals were estimated from these models. The effects were tested hierarchically. First the main effects of seeding density, osteogenic medium and days were tested. Thereafter a model including the first order interaction was applied (densities*medium, medium*days, density*days), followed by a model including the second order interaction (densities*medium*days). The μ-CT observations were measured at only one time point. This analytic approach will correspond with repeated measures analyses of variance. The statistical package StataIC version 13 was used to analyze the data. P-values less than 0.05 were considered statistically significant.

ii. Paper II

Fourteen scaffolds from each group were available for the statistical analysis *in vitro* and 14 rats were included in the *in vivo* analysis. To provide accurate data on the hierarchical structure of the outcome variables, a multilevel modelling analysis was applied. For proliferation assays, fours scaffold replicates were repeated in triplicate for all experiments. One-way analysis of variance (ANOVA) was used to test the effect of the different Tween 80 concentrations on cell proliferation. For PCR, reference values for different gene expressions for each rat were calculated using

mixed effects models. $^{\Delta}$Ct values were calculated as the gene expression minus the calculated reference values. Next, a general linear model, with robust variance estimators adjusted for data clustering within rats, was applied. The results expressed mean differences for the $^{\Delta\Delta}$Ct values and were presented as xFold-values. For quantitative analysis of bone formation (mean ± standard errors), Student t-test was used to compare pristine and modified scaffolds. Stata version 13 (Texas, USA) was applied. P-values less than 0.05 (5 %) were considered statistically significant.

iii. Paper III

A two-tail Student's t-test (assuming equal variances) was applied to determine the statistical significance of the differences in microstructure parameters of scaffolds, protein adsorption, SUV_{mean}, and SUV_{max}. To compare bone volume (BV) and percentages of bone volume and tissue volume (BV/TV) between poly(LLA-co-CL), poly(LLA-co-CL)/nDP with cells, adjusting for the repeated measures for each rat, a linear mixed model was used. The results from the model were reported as mean differences. StataIC version 14 (Tx, USA) was used for the analyses.

10.3 Ethical approval

All animal experiments were approved by the Norwegian Animal Research Authority and conducted according to the European Convention for the Protection of Vertebrates Used for Scientific Purposes (local approval numbers 20124903, 20142029 and 20146866 for **Paper I**, **II**, and **III** respectively).

11. Main Results and Discussion

In tissue engineering, the cell-scaffold interaction is a major determinant of success. The surface properties of the scaffolding influence the growth and function of the seeded cells. A disadvantage of many synthetic degradable polymers for application as scaffolding material is poor bioactivity, due to surface hydrophobicity [178]. Hydrophobic porous scaffolds tend to float in cell culture medium and most of the pores remain empty [49]. This in turn may influence the homogeneous cellularity of the engineered constructs.

The effect of surface wettability on the efficiency, viability, and uniformity of cells attached to scaffolds has been investigated in a number of studies [123, 132, 152], showing good proliferation and differentiation of cells seeded onto hydrophilic surfaces. Surface wettability may also influence the morphological and compositional properties of the engineered constructs. It is defined as the interaction between fluid and solid. The contact angle, measured through water droplet on a surface, is an indicator of surface wettability: the less the angle, the more hydrophilic the surface [179]. The preferred range of surface wettability varies, depending on cell type. For instance, adhesion of osteoblasts is reported to decrease when the contact angle increases from 0° to 106° [180]. Maximum adhesion of fibroblasts occurs at contact angles between 60° and 80° [181].

However, the contact angles of hydrophobic degradable polymers lie outside the preferred range for optimal cellular behavior, hence the need for modification [182]. Despite other positive properties of PCL as a scaffolding material for tissue engineering applications, it is hydrophobic, with a water contact angle of around 123°. Coating with poly(vinyl phosphonic acid-co-acrylic acid) can convert PCL to a hydrophilic material, with a water contact angle of 43° [183]. In this study in which surface hydrophilicity was improved by coating the scaffolds, *in vitro* culture of osteoblasts for up to 14 days resulted in a better defined cytoskeleton, indicating better spreading of cells [183]. In another study, MSCs seeded onto a modified hydrophilic surface (contact angle $\theta = 57°$) exhibited accelerated proliferation and neurogenic differentiation compared with cells seeded onto unmodified surfaces [184].

Thus, the main focus of the present series of studies was to achieve uniform distribution of BMSCs onto poly(LLA-co-CL) scaffolds, by modifying the hydrophilicity of the scaffolding surface. An initial study (**Paper I**) was undertaken to optimize the culture conditions for BMSCs seeded onto poly(LLA-co-CL) scaffolds: the outcomes were evaluated *in vitro* and then *in vivo*, using a rat calvarial defect model. Two techniques for modifying the surface properties of scaffolds were then investigated: in **Paper II**, copolymer was blended with Tween 80 and in **Paper III**, copolymer scaffolds were coated with nDPs. In **Paper II**, the promising *in vitro* results were followed by an *in vivo* experiment using a subcutaneous rat model. Similarly, in **Paper III,** the successful *in vitro* experiment was followed by an *in vivo* experiment, using a critical size rat calvarial defect. Thus, the studies comprised investigation not only of different approaches to modifying the surface properties of the scaffolding material, but also evaluation of the response of the modified scaffolds in *in vivo* models of orthotopic or ectopic bone formation.

11.1 Optimizing culture conditions for BMSCs

BMSCs have an essential role in the maintenance of bone turnover throughout life and can be a source of adult stem cells [185]. These are the cells most widely used in (pre)clinical bone tissue engineering studies [10-13, 186, 187]. Bone marrow contains a very low percentage of mesenchymal stem cells (one per 100,000 mono-nucleated cells), and several studies have shown that in order to form bone tissue, *in vitro* expansion of the stem cells is necessary to ensure an adequate volume for seeding into the scaffolds [188]. In a previous study, BMSCs were first expanded *in vitro* to increase the number of osteoprogenitor cells, then seeded onto scaffolds, and finally implanted into clinically critical defects, to achieve bone regeneration [189].

A bone formative experimental system, using BMSCs derived from rats, was first described by Maniatopuoulas et al [164]. The cells were characterized morphologically, immunohistologically, and biochemically [164]. In the present studies, isolation of BMSCs (**Papers I - III**) was based on the capacity for plastic attachment under standard culture conditions. Colonies of fibroblast-like cells (50 - 60 cells/colony) attached to the plastic were visualized on day 4 (**Figure 11A**) after

seeding. BMSCs exhibited characteristic spindle shapes and polygonal morphology. Moreover, distinct proliferative properties were observed and only a few days after passaging the cells reached about 80 - 90% confluence (**Figure 11B**). Viability was around 90%.

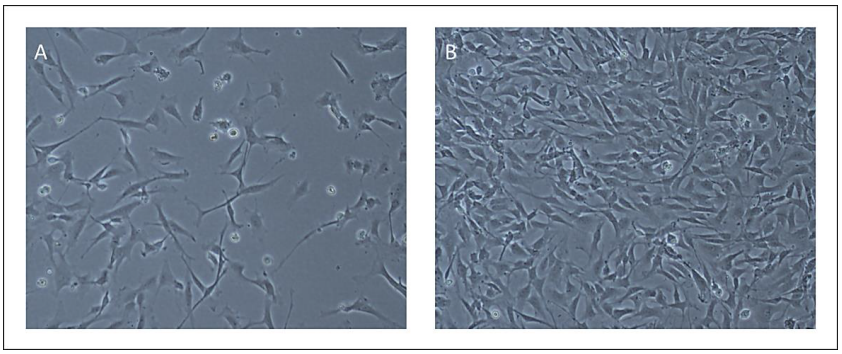

Figure 11. Morphology of BMSCs *in vitro*. Primary cells after culture **(A)** for 4 days and **(B)** after 10 days of culturing, showing 80-90% confluence.

11.1.1 Maturation stages of BMSCs as key determinants in induction of new bone tissue

During culture and passage, the ability of BMSCs to differentiate into osteoblast-like cells is easily disturbed [190]. Thus, it is important that BMSCs are appropriately cultured, expanded, and induced into osteogenic cells [190]. It is somewhat surprising that although numerous studies using BMSCs have been published, there is no established and widely accepted cell expansion (culture/induction) protocol. Thus, an important issue is to establish optimal culture protocols for BMSCs seeded into poly(LLA-co-CL) scaffolding using *in vitro* and *in vivo* models.

Mineral deposition has been observed when BMSCs are cultured and expanded in culture medium supplemented with dexamethasone, L-ascorbic acid, and β-glycerophosphate, denoting that BMSCs are able to differentiate into osteoblasts [191]. At a very early stage of osteoblastic differentiation, BMSCs have a high proliferation rate, allowing them to increase in number following implantation [191]. This concept is supported by the results of **Paper I**, showing a significant overall positive effect on the quantity of DNA in BMSCs treated with osteogenic supplements.

Osteogenic supplements were also associated with significant enhancement of osteogenesis and bone formation in rat cranial defects. Thus, BMSCs were committed to osteoblastic differentiation after exposure to osteogenic medium. Full maturation of these cells might have occurred in the defect site, followed by ECM deposition, which in turn could enhance recruitment of new osteo-progenitor cells from the host. These findings are in accordance with previous studies in which scaffolds, seeded with MSCs pre-cultured with osteogenic supplements, showed an increase in bone formation [191, 192]. On the other hand, it has been reported that when MSCs fully differentiate, pluripotency and immunosuppressibility decrease and this may result in rejection of xenogeneic and allogeneic transplantation, jeopardizing the viability of MSCs and leading to compromised osteogenicity [193]. In a previous study intended to evaluate whether MSCs in cultures retain immunomodulating properties *in vivo* following intravenous or local allotransplantation, MSCs were strongly immunosuppressive *in vitro*, but this immunosuppressive response was reduced *in vivo* because they were recognized and rejected by the host [193]. Therefore, the implanted MSCs should be at a certain stage of maturation.

The effect of osteogenic supplements might be influenced by the tissues from which the stem cells were isolated: cells of different origin may have inherited different degrees of osteogenicity [194-196]. It has been reported that MSCs originating from adipose tissue demonstrate a significant increase in osteogenesis when pre-treated with osteogenic supplements, whereas MSCs from umbilical cord blood undergo a significant decrease in osteogenicity [196]. In another study, in 22 out of 24 donors, BMSC strains propagated with and without osteogenic supplements formed similar amounts of bone *in vivo* [197]. In contrast, it has recently been proposed that an ideal scaffold for bone tissue engineering should be able to trigger and continuously support the MSCs commitment towards osteoblast-like cells, avoiding the need to expose the cells to osteogenic supplements [198]. These contradictory results could be attributable to lack of consistency in the design of the studies, such as variations in concentrations of osteogenic supplements, the duration of treatment, and the timing of supplementation, with negative consequences for osteogenesis [199].

11.1.2 Cell seeding density may promote bone formation

Because of heterogeneity in cell types and scaffold materials, there are no published studies on optimal cell seeding density. However, there is consensus that a certain threshold of cell density is essential to achieve successful *in vivo* bone regeneration [93]. Initial seeding density can alter the proliferation as well as the expression of osteogenic genes by affecting the distance of signals among cells [84]. Thus, in the present studies, it was essential to determine the influence of cell seeding density on cell proliferation and differentiation of BMSCs. In **Paper I**, high and low cell seeding densities were used: 1×10^6 cells/scaffold and 2×10^6 cells/scaffold respectively, in order to investigate the influence of cell seeding density on bone formation.

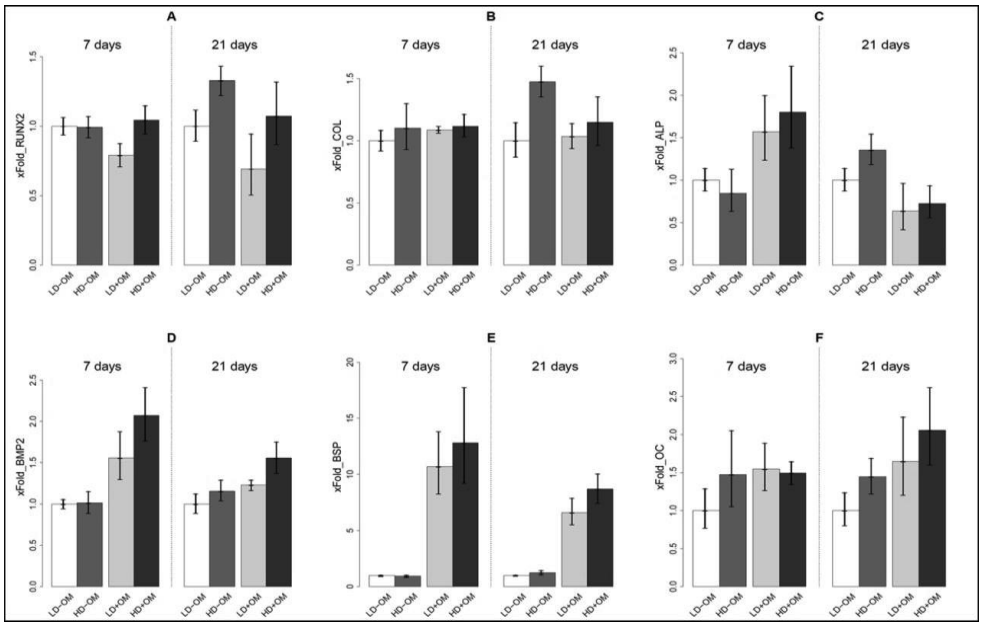

Figure 12. **mRNA expression** of by qRT-PCR, presented as x-fold changes relative to the expression of the mean of the calibrator sample LD-OM. *Figure 11.A.* Runx2 expression is downregulated by osteogenic medium (p=0.005) and upregulated by high cell seeding density (p=0.001). *Figure 11.B.* Col1 expression is upregulated by high cell seeding density (p=0.001). *Figure 11.C.* ALP expression, disclosing a significant relationship between high cell density, osteogenic medium and number of days (p=0.026). *Figure 11.D.* BMP2 expression is upregulated by osteogenic medium (p<0.001) and high cell seeding density (p=0.003). *Figure 11.E.* BSP expression is upregulated by osteogenic medium (p<0.001) and high cell seeding density (p=0.033). *Figure 3F.* OC expression is upregulated by osteogenic medium (p=0.002) and high cell seeding density (p=0.013).

The *in vitro* data generated in **Paper I** confirmed the influence of seeding density of BMSCs on cell proliferation. DNA assay was used to assess proliferation: high cell seeding density significantly stimulated the amount of DNA detected. Cell proliferation is strongly regulated by (1) surface area available for attachment and (2) contact-inhibition between adjacent cells [84, 91]. The porosity of 3D porous scaffolds used in the current series of experiments (**Papers I - III**) exceeds 85%, providing a large surface area for cellular events, conducive to uniform cell distribution [200-202]. The extent of cell-cell interactions may be controlled by the density of seeded cells.

The effect of cell seeding density on the osteogenic differentiation of BMSCs was monitored for up to 21 days. High seeding density led to significantly upregulated

expression of osteogenic markers, suggesting that high seeding density is associated with more efficient differentiation of BMSCs. As shown in **Figure 12**, numerous genes are expressed at high levels during distinct stages of differentiation, *e.g.* alkaline phosphatase (ALP), type-I collagen, bone sialoprotein, and osteocalcin (OC) [203]. ALP, an early marker for osteoblasts [204], was first upregulated at 7 days and then downregulated at 21 days. In contrast, OC a late marker of osteoblast maturation [205], plays a vital role in osteogenesis and was first upregulated at 21 days. This is accordance with a previous report showing that increased cell numbers in the presence of osteogenic supplements, were associated with upregulated osteocalcin expression and maturation of osteoblasts [84]. There may be a correlation between increased extracellular protein secretion and increased number of mature osteoblasts, leading to promotion of bone formation.

The *in vitro* results of **Paper I** indicate that the three distinct stages of osteoblastic phenotype development are sensitive to cell seeding density. According to a previous report [203], the first stage of osteogenic progenitor cell growth is highly proliferative, with formation of extracellular matrix. The second stage shows matrix maturation, with decreased cell proliferation and upregulated ALP expression, a sequence of events also seen in the present study [203]. The final stage comprises mineralization by expression of OC. At all these stages, high cell seeding density had a significant impact: enhanced cellular proliferation, upregulated expression of ALP and OC (early and late osteogenic markers). Our results suggest that cell seeding density promotes osteogenic differentiation in an *in vitro* environment.

There is a need for *in vivo* testing of cell seeding density, in order to confirm consistency between *in vitro* and *in vivo* microenvironments. There is lack of consistency in the results of published studies [84, 94, 96, 97]. One report suggests that low seeding densities can prolong the time needed to achieve a well-populated scaffold, ready for implantation, and may compromise cellular contact and hence influence bone formation [69]. However, high cell seeding densities do not necessarily benefit cell behavior because overloading may result in limited nutrient transport and insufficient waste removal from the internal structures [69].

In the present studies, the *in vitro* and *in vivo* findings were in good agreement: high cell seeding density promoted bone formation in the calvarial defects (**Figure 13**). Doubling the number of cells from 1×10^6 per scaffold to 2×10^6 resulted in a significant increase in bone formation.

In general, a certain threshold (i.e., the optimal cell density) is required to enhance osteogenic marker expression and extracellular matrix production (*i.e.*, mineralization). In a previous study the same seeding density was used to grow the MSCs onto biphasic calcium phosphate granules and was found to promote formation of a mature bone organ [206]. It cannot be assumed that a further increase in cell seeding density would lead to more bone formation: a previous study has shown that doubling cell density did not yield significantly more bone [206].

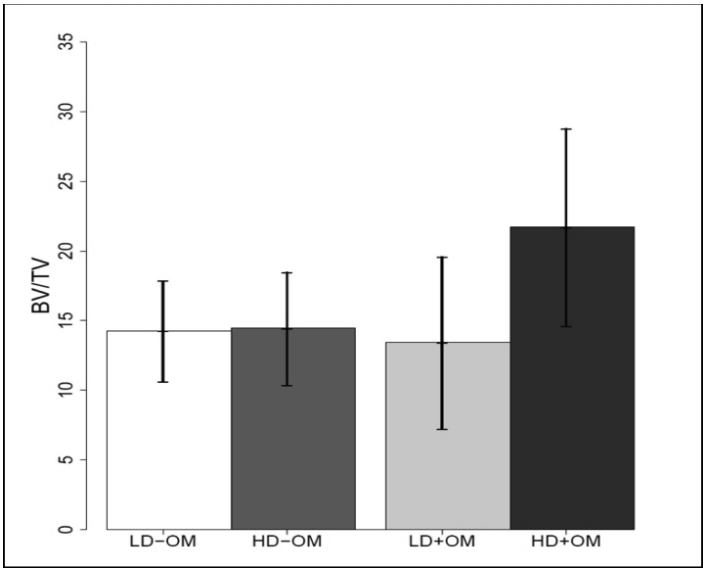

Figure 13. Quantification of percentage of area and volume of bone regeneration in calvarial defects after 8 weeks of healing. Implantation of scaffolds containing cells seeded at high density and cultured with osteogenic medium exhibit a significant percentage of bone volume (p=0.038).

Collectively, the findings of **Paper I** demonstrated a synergistic stimulation of cell seeding density and osteogenic supplements on bone regeneration. The initial seeding density clearly influenced cellular events and the resulting bone formation.

However, the stage of cell maturation and differentiation warrant further in depth investigation.

11.2 Hydrophilic copolymer scaffolding as a carrier for BMSCs

After optimizing culture conditions and seeding density of BMSCs in 3D porous poly(LLA-co-CL) scaffolds, the hydrophilicity of the scaffolds was modified either with Tween 80 (**Paper II**) or nanodiamond particles (**Paper III**).

11.2.1 Enhanced seeding efficiency of BMSCs onto hydrophilic copolymer scaffolds

Cell seeding efficiency is a major determinant of successful engineering and is governed mainly by the surface properties of the scaffold and the architecture of the porous structure [166]. The increase in seeding efficiency in poly(LLA-co-CL) scaffolds modified with 3% Tween 80 was 23% (unpublished complementary data) and 14% in those modified with nDPs (**Paper III**) (**Figure 14**).

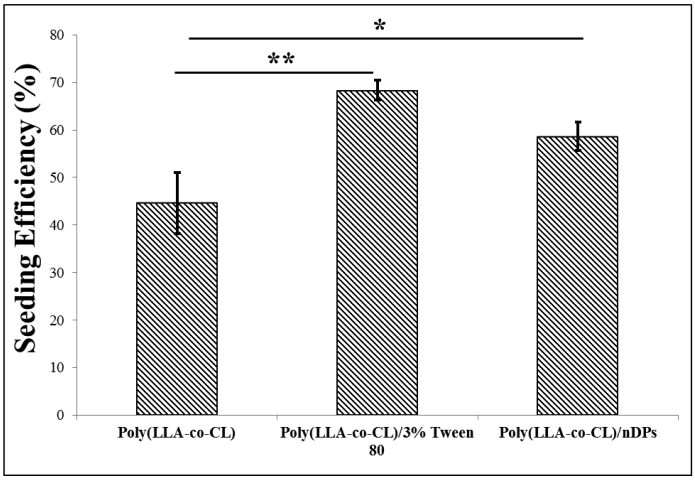

Figure 14. Seeding efficiency for each type of scaffold. There was a significant increase in the seeding efficiency of BMSCs seeded into modified poly(LLA-co-CL). (* $P \leq 0.05$ and ** $P \leq 0.01$)

The hydrophilicity of the copolymer scaffold surface promoted the attachment expressed by seeding efficiency of BMSCs. Hydrophilicity is an important parameter because it relates to the diffusion of nutrients and cellular waste. Moreover, it allows the maintenance of tissue fluid and nutrients which are necessary for cells to attach and proliferate. The result in **Paper II** is consistent with previous findings that modifying hydrophilicity by blending with surfactant significantly improved initial cell attachment onto biodegradable copolymer nanofibrous surfaces [207]. Moreover, the results of **Paper III** are in accordance with another study exhibiting enhanced cell adhesion when human osteoblast-like cells were seeded onto copolymer nanofibrous membranes functionalized with nDPs [208]. Copolymer scaffolds modified with nDPs may provide good support for the adhesion and growth of osteoblasts [149]. Increasing the amount of nDPs in gelatin fibrous scaffolds resulted in an upturn in the number of adherent cells [209]. A suitable surface can be provided by coating the polymer with nDPs, which in turn is beneficial for cell adhesion and growth via providing multiple binding sites for adhesion molecules [149, 210].

Although seeding efficiency has been associated primarily with the surface area available for cell attachment, numerous studies have shown that other factors such as surface chemistry, scaffold architecture, and the pore structure are also important [166, 211]. Thus, the differences in cell seeding efficiency between pristine and modified scaffolds might be attributable to the synergistic effects of multiple contributing factors, such as increased hydrophilicity of the surfaces (Tween 80 and nDPs) and the influence of reactive functional groups (nDPs) on protein attachment/conformation. This is in agreement with the findings of a previous study showing that surface chemistry has a profound effect on cell adhesion, area of spread, and proliferation [212]. The synergistic effects of multiple causal factors, such as surface wettability and surface functional groups, may influence all cellular events [212]. The generated data clearly confirm that modification of surface hydrophilicity has a bearing on the seeding efficiency.

11.2.2 Modifying poly(LLA-co-CL) with 3% Tween 80 enhanced ectopic bone formation

Tween 80 is a hydrophilic nonionic surfactant commonly used in drug delivery systems and for dispersion of substances in medical and food products [213-215]. One advantage of using Tween 80 as a hydrophilic additive in fabricating 3D porous scaffolding is that it does not readily leach out into water or cell culture medium, owing to the hydrophobic interaction between the hydrophobic long alkyl tail of Tween 80 and the polymer main chain [129]. Blending Tween80 with a hydrophobic scaffold polymer has previously been described, producing hydrophilic polymers [128, 129]. However, inconsistent *in vitro* cell culture results indicated that the concentration of Tween 80 needs to be optimized before proceeding to *in vivo* experiments.

In **Paper II**, blending 3% (w/w) Tween 80 with poly(LLA-co-CL) improved the hydrophilicity and after 2 weeks of subcutaneous implantation, significantly upregulated expression of Runx2 was observed. At 8 weeks, there was a significant increase in *de novo* bone formation (**Figure 15**).

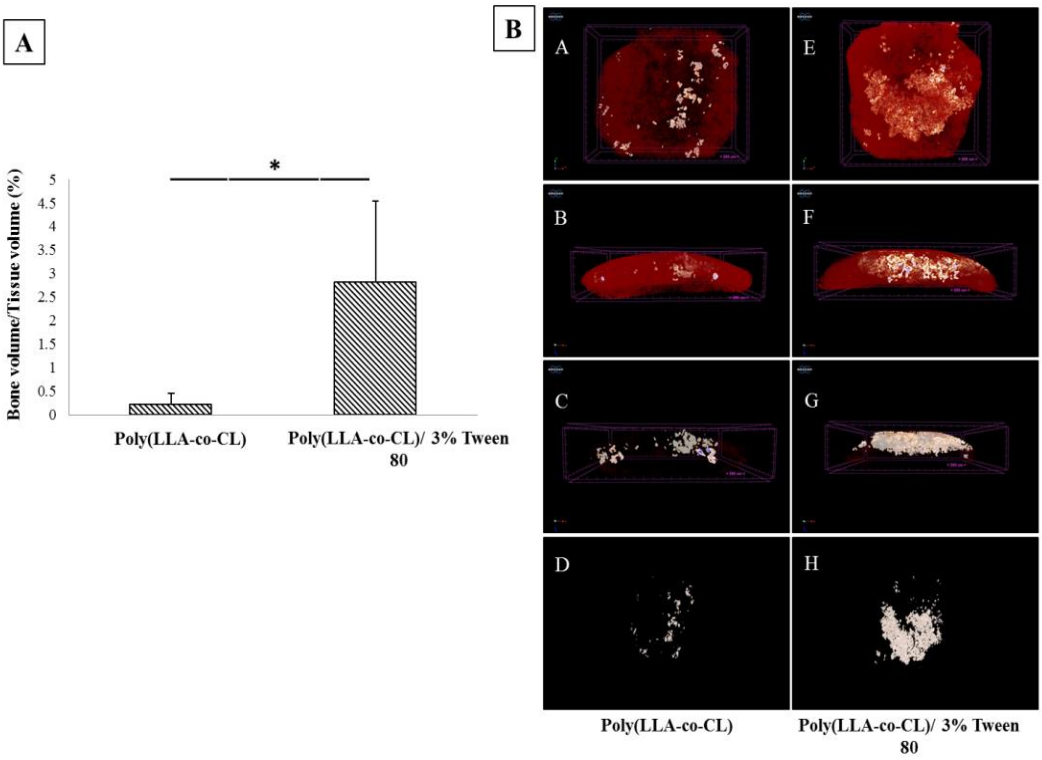

Figure 15. µ-CT of implanted copolymer scaffolds loaded with BMSCs: (A) The histogram shows the statistical difference in bone/tissue formation between pristine poly(LLA-co-CL) and poly(LLA-co-CL)/3% Tween 80 modified scaffolds and (B) corresponding µ-CT images of the scaffolds. (* $P \leq 0.05$)

Runx2 is recognized as a critical regulator of osteogenic development and induces the expression of osteogenic extracellular matrix genes during osteoblast maturation *e.g.* osteocalcin [216, 217]. Culturing osteoblasts on hydrophilic surfaces might lead to increased expression of osteogenic markers [218]. In skeletal development, bone formation from condensing mesenchymal cells involves two distinct pathways: endochondral and intramembraneous ossification [219]. Both processes are dependent on optimal carrier properties and cell seeding density [220]. For example, depending upon the surface properties of the polymer scaffolds, stem cells differentiate towards an osteogenic phenotype and *in vivo* produce bone tissues through two different pathways [221]. In hydrophilic polymer scaffolds [222] ectopic bone formation associated with subcutaneous transplantation of human embryonic stem cells, demonstrated that

modifying the polymeric scaffolds with hydroxyapatite upregulated Runx2 and resulted in bone formation through an intramembranous ossification pathway [221]. This can explain the results of **Paper II,** whereby a large quantity of collagenous and mineralized matrix was deposited on hydrophilic copolymer scaffolds. Moreover, it may be assumed that a hydrophilic surface is advantageous for tissue regeneration and the cascade of events that occurs during osseointegration [223]. Thus, the results of the present series of studies further contribute to the body of evidence that the osteogenic potential of BMSCs is highly dependent on the physical and chemical architecture and surface properties of polymeric scaffolds.

11.2.3 nDPs enhanced the osteoconductive properties of poly(LLA-co-CL) scaffolds

Paper III documented that functionalizing poly(LLA-co-CL) scaffolds with nDPs altered the surface topography. Moreover, in the calvarial defects, poly(LLA-co-CL)/nDPs scaffolds exhibited enhanced osteogenic metabolic activity and showed significantly increased bone formation. Cellular sensing of extracellular nanotopographical cues initiates downstream intracellular mechanotransductive events, resulting in a multitude of nanotopography-sensitive cellular behaviors, including cell adhesion, proliferation, self-renewal, and differentiation [224-226]. Enhanced osteogenic differentiation, measured as upregulated expression of osteogenic markers, was observed when mesenchymal stem cells derived from human bone marrow were seeded onto nanostructured titanium surfaces [227]. In another study, miRNA analysis confirmed that exposure of stem cells to nanoparticles affects the genes responsible for osteogenic differentiation [228]. It has also been shown that functionalization of polymer scaffolds with nDP not only supports the proliferation, but also controls the osteogenic differentiation of BMSCs *in vitro* [149]. Thus, the introduction of nanoscale structures may improve osteoblast differentiation, indicating a potential to improve osseointegration of the engineered construct.

As shown in **Paper III**, the uptake of $^{[18]}$F-NaF is directly proportional to the metabolic activity of living osteogenic cells [229]. The data obtained from

multimodality PET/CT systems (**Figure 16**) suggest an increase in the osteogenic metabolic activities of BMSCs when seeded into poly(LLA-co-CL)/nDPs scaffolds.

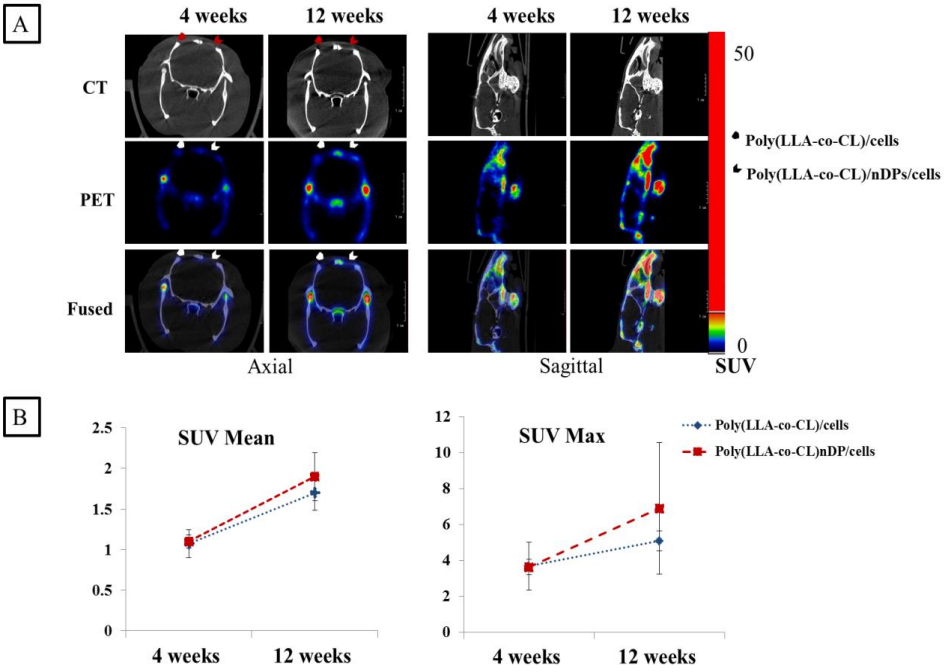

Figure 16. **PET/CT analysis** (A) Images for each animal of experimental groups (pristine poly(LLA-co-CL) or functionalized with nDPs seeded with BMSCs) after 4 (left side) and 12 (right side) weeks. (B) SUVmean and SUVmax values extrapolated from the quantitative analysis of images acquired at 4 and 12 weeks.

Acid treatment of nDPs following oxidative purification selectively increases the number of oxygenated functional groups. These groups may lead to modulation of the adsorbed protein *i.e.* fibronectin (FN) [230], resulting in recruitment of different levels of focal adhesion components, and therefore cell attachment, proliferation, and osteogenic differentiation [231-233]. Further, the surface nanotopography can enhance osteogenic differentiation of stem cells synergistically with a biochemical induction substance [234]. In the *in vivo* experiment in **Paper III**, at twelve weeks, implantation of poly(LLA-co-CL)/nDPs seeded with BMSCs resulted in significant bony bridging of the defect. The increased bone volume within the defect was shown by μ-CT and confirmed histologically. In combination, these data suggest that the local microenvironment, generated by interactions among modified polymer scaffolds,

BMSCs, and native cells may regulate the osteogenic activity induced by the biomaterials and/or stem cells [149]. The osteoconductivity of poly(LLA-co-CL)/nDPs is attributed to surface hydrophilicity as well as to surface charge, which allows osteoblastic differentiation of the seeded cells [235]. Moreover, under *in vivo* conditions copolymer scaffolds functionalized with nDPs might modulate protein adsorption to recruit host osteoprogenitor cells [149]. Thus poly(LLA-co-CL)/nDPs scaffolding may facilitate bone formation, either alone [149], in combination with growth factors [148], or stem cells (**Paper III**).

11.2.4 Reduction of albumin adsorption in hydrophilic copolymer scaffolds

In cell–material interactions, protein adsorption is the first event to occur at the solid/liquid interface when materials are exposed to culture media or body fluid. Cellular attachment, proliferation, and migration then follow [236]. Protein adsorption occurs on the scaffold surface, mediating cell adhesion, and also provides signals to the cell through the cell adhesion receptors, mainly integrin [237]. Thus, protein adsorption plays a vital role in bone tissue regeneration [238]. The effect of different materials and surface properties on the amounts and types of bound proteins, as well as the conformation, orientation or binding strength of the adsorbed protein, is well documented [239, 240]. The influence of surface hydrophilicity on albumin adsorption was assessed as illustrated in **Figure 17**.

Serum albumin is the main protein of human blood plasma and represents around 50–60% of the total plasma protein fraction [241]. Its most important physiological functions are to maintain the osmotic pressure and pH of blood and to transport a wide variety of endogenous and exogenous compounds, including fatty acids, metals, amino acids, steroids, and drugs [241]. In the present series of studies, bovine serum albumin (BSA) was chosen as an experimental protein because of such favorable properties as solubility in water, stability, and availability at high purity [242].

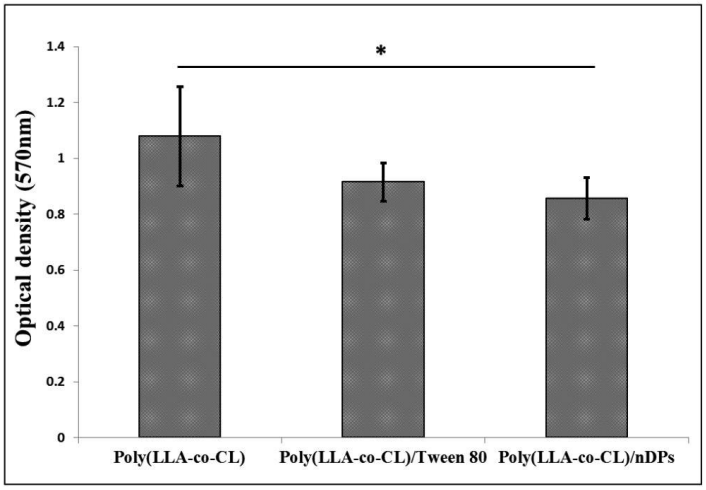

Figure 17. BSA adsorption rate measurements. BSA overall adsorption rate as a function of surface hydrophilicity. (* $P \leq 0.05$)

Compared with the pristine scaffolds, there was a significant reduction in adsorbed albumin on the scaffolds modified with nDPs. Commonly used polymers are mostly hydrophobic and have high affinity to a wide variety of proteins [239, 243]. The proteins tend to adsorb onto the hydrophobic surface by hydrophobic patches of residues present in the protein's amphiphilic structure [240]. The proteins are adsorbed via hydrophobic interactions and tend to assume an altered conformation and to expose hydrophobic domains which become tightly adherent to hydrophobic biomaterial surfaces [244]. Hydrophobic surfaces tend to adsorb more protein than hydrophilic surfaces because a stronger attraction to the protein will result in a denser layer of protein on the surface [245]. Thus modifying the surface hydrophilicity of poly(LLA-co-CL) through blending with Tween 80 [128] or functionalizing with nDPs [149, 246] might result in selective adsorption of proteins due to the hydrated interfacial phase between hydrophilic surfaces and proteins [121]. A previous study has shown suppressed albumin adsorption in hydrophilic polymer scaffolds [163]. In another study, modifying poly(D,L-lactide-co-glycolide) with poly(ethylene oxide) led to transformation of hydrophobic degradable polyesters to hydrophilic fibers, which caused suppression of albumin adsorption on the surface of the fibers [247]. A study focusing on the influence

of nanotopography on protein conformation and adsorption has shown a significant reduction in protein adsorption on the curved nanoscale surface compared with the flat surface [248]. It has been speculated that nano-roughness is significantly smaller than the dimensions of albumin (~10 nm) and this might reduce albumin adsorption [249]. The reduction of albumin adsorption to polymer surfaces is believed to be a vital step for the generation of specific cell adhesion and for triggering the immune system by reducing of fibrous capsule thickness and inhibiting macrophage adhesion to the implant *in vivo* [163]. Therefore, both composition and conformation of an adsorbed protein layer are considered to be critical factors in determining the nature of the cell-scaffolds interaction [117].

11.2.5 Impact of hydrophilicity on biocompatibility and efficacy of poly(LLA-co-CL)

Water is an important determinant of biocompatibility and efficacy of synthetic materials. It has been assumed that high water levels within the surface of materials might help to provide low interfacial free energy with blood and reduce protein adsorption to the polymeric surface [239]. "The biocompatibility of a scaffold or matrix for a tissue engineering product refers to the ability to perform as a substrate that will support the appropriate cellular activity, including the facilitation of molecular and mechanical signaling systems, in order to optimize tissue regeneration, without eliciting any undesirable local or systemic responses in the eventual host" [20]. In accordance with this definition, the results of **Paper II** and **Paper III** show that surface modification of the hydrophilicity of poly(LLA-co-CL) scaffolding improved its cyto-histocompatibility *i.e.* the improved wettability actively promoted the proliferation and differentiation of BMSCs *in vitro* and *in vivo*.

It is generally accepted that a protein-resistant surface (*e.g.* hydrophilic in nature and the presence of hydrogen bond acceptors) can help to tailor material surfaces to control protein adhesion and interactions following adsorption, and may thus improve biocompatibility [239]. In evaluating biocompatibility, assays of cellular events (*e.g.* proliferation and differentiation) are important. In **Paper II**, hydrophilic scaffolds exhibited significant increases in cell proliferation. Moreover, the findings in

Paper III indicated improved osteogenic metabolic activity in the calvarial defects treated with modified scaffolds. Overall, this suggests that the modified scaffold provides better conditions for efficient transport of cell culture medium into the scaffold and therefore improved oxygen and nutrient transport to the seeded cells and the host cells [49]. Further, it has been reported that a hydrophilic polymer surface triggers the immune system by inhibiting adhesion of inflammatory cells [247, 250]. Several studies have reported that surface functionality/hydrophilicity may alter biomaterial-mediated acute inflammatory responses and minimally influence chronic fibrotic responses *in vivo* [251, 252]. Further investigations into inflammatory responses could provide more information about the biocompatibility and efficacy of the modified scaffolds.

The results of this series of studies confirm that under both *in vitro* and *in vivo* conditions, hydrophilic modification of poly(LLA-co-CL) influences protein adsorption and induces positive cellular responses, including proliferation and differentiation of osteogenic phenotypes, resulting in new bone formation.

12. Conclusions

The following conclusions can be drawn from the included studies:

- The appropriate number of cells to be loaded onto a specific scaffold is a critical factor in promoting ECM synthesis and bone formation.
- The maturation stage of mesenchymal stem cells is a key factor in inducing new bone tissue formation.
- Modifying scaffold surfaces by increasing hydrophilicity improves the seeding efficiency of BMSCs and suppresses albumin adsorption.
- Modification of porous degradable scaffolds with 3% Tween 80 increases BMSCs proliferation, promotes osteogenic differentiation of BMSCs and *de novo* bone formation.
- nDPs influence the surface properties of copolymer scaffolds resulting in enhanced osteoconductive potential and promoting bone regeneration.

13. Future Perspectives

"The best thing about the future....is that it comes one day at a time"
Abraham Lincoln

In field of tissue engineering, polymeric materials show great promise as scaffolds materials. The parameters of biomimetic scaffolds, including mechanical properties, bioactive agent release profile, architecture, and interactions with cells, are all highly dependent on fabrication technologies. The next generation scaffolding technique (3DF) may customize bio-inspired artificial extracellular matrices, incorporating optimal physical and chemical surface properties to improve stem cell support. Stem cells delivered by designed scaffolds can then guide and stimulate reconstruction of functional tissues *in vivo*. Furthermore, rapid advances in stem cell biology have led to increased availability of a variety of cell types which may also be employed with spatial control, *e.g.* in the form of printed 3D cells/organs, to generate complex tissues *ex vivo*, with tissue hierarchy.

With reference to Tween 80 and nDPs modifications, further studies are needed to understand the immunogenic responses, because implantation of a biomaterial always initiates an inflammatory foreign body reaction. Moreover, there is a need for models focusing on treatment of long bone defects, in order to establish the relationships between surface hydrophilicity, stem cell function, and bone regeneration.

14. Acknowledgements

(الحمد لله حمدا كثيرا طيبا مباركا فيه)

I gratefully acknowledge Department of Clinical Dentistry and Center for International Health for providing me with the opportunity to undertake my doctoral studies there. I would like to acknowledge to the source of funding: the Norwegian State Educational Loan Fund (Quota program), the FP7 EU (VascuBone) for supporting my attendance to International Conferences and all the support in achieving my PhD plan.

During my PhD journey, several people have contributed decisively to this important step in my life, and to whom I wish to express my gratitude.

First and foremost, I would like to thank ***Knut N. Leknes*** for the opportunity of performing my PhD under his supervision. Leknes has been an inspiration as a mentor and as a supervisor, from whom I learnt that high goals are accessible with the right dose of motivation, resilience, and effort. Thank you for believing in my abilities. This journey has been a unique and inspiring experience both personally and professionally. Leknes encouraged me to leave my comfort zone, to question and test my limits. This exercise made me stronger and more open to forthcoming scientific challenges.

I also wish to express my gratitude to my co-supervisor ***Kamal Mustafa***. Thank you for the opportunity of undertaking my PhD in the Tissue Engineering Group. I want to thank you for your support, guidance, and dedication to your students. Your amazing strength and determination in pursuing all of your goals is inspirational, and has encouraged me every step of the way. Throughout this journey, I became a better and more confident scientist (to some extent ☺), mostly because you believed in me and made me aware of my potential. I also appreciate the opportunity of participating in parallel projects and scientific meetings which sometimes seemed like overwhelming assignments.

Zhe Xing, my co-supervisor, thank you for teaching me "How to be Independent" and "How to google it".

Special thanks to ***Anna Finne-Wistrand*** and ***Yang Sun*** for introducing me to Polymer World, and for interesting discussions and warm hospitality during my stay in your department at KTH.

I also wish to express my gratitude to ***Cecilie Gudveig Gjerde***, for the opportunity to participate in your wonderful research ☺ and for being so supportive.

I thank all my co-authors ***Stein A. Lie***, ***Torbjørn O. Pedersen***, ***Anke Krueger***, ***Doris Steinmüller-Nethl***, ***Kristine Eldevik Fasmer***, and ***Thilo Waag*** for their contributions to my research and for sharing their expertise with me.

Siren Hammer Østvold, thank you for sharing with me that cozy feelings of companionship, when mentoring and friendship come together. Because of that I can only remember good things, even in the most stressful moments, as you were always there for 4th floor people. ***Rita Griener-Simonsen***, thank you for introducing me to cell

culture laboratory techniques. Thank you ***Randi Sundfjord*** for sharing with me your expertise in the processing of calcified bone samples and with the histological analysis.

I could never forget, of course, ***Asgeir Bårdsen***, ***Annika Rosén***, ***Nils R. Gjerdet***, ***Sølve Hellem***, ***Rune Nilsen***, ***Bente Elisabeth M***, ***Harald Gjengedal***, ***Jørgen Barth***, ***Endre Hellem***, ***Mihaela Roxana Cimpan***, ***Marit Øilo***, ***Anne-Isine Bolstad***, ***Inge Fristad***, ***Sivakami Rethnam***, ***Ellen Berggreen***, ***Athanasia Bletsa***, ***Anne N. Åstrøm***, ***Lars Björkman, Gunvor Lygre***, ***Merete Allertsen***, ***Johanna Svahn***, for your generosity to me.

Mona Isakson, ***Randi Bente Hansen***, ***Marit Stubdal***, ***June-Vibecke Knudtsen***, ***Borgny L***, ***Linda Forshaw***, ***Kaia Berstad*** among others – Thanks for helping me during my study period.

All my colleagues, ***Shaza B***, ***Manal M, Sarah Y***, ***Hasaan***, ***Salwa***, ***Heba B***, ***Ferda***, ***Dagmar***, ***Niyaz***, ***Amin***, ***Sushma***, ***Sunita***, ***Samih***, ***Mohamed I***, ***Ahmad***, ***Nancy***, ***Maryam***, ***Kemal***, ***Hager***, ***Penny***, ***Kenji Hara***, ***Masahito***, ***Kathrin B***, ***Alexander S***, ***Christian***, ***Melanie O***, ***Victoria***, ***Bettina H***, ***Zrinka***, ***Trine-Lisa***, ***Mohammed Ali***, ***Ying***, ***Eivind***, ***Julie***, ***Siddharth***, ***Espen***, ***Siri***, ***Catherine K***, ***Everest***, ***Pritam***, ***Åse***, ***Jeanette***, ***Rafal***, ***Valentina***, I am grateful to all of you who have helped me in my PhD research when I was in need of help and support.

Salah Ibrahim, ***Hisham***, ***Alwalid***, ***Nada***, ***Hassan***, ***Alsheikh***, ***Sheihab***, ***Mohammed Salih***, ***Tarig***, ***Omnia***, ***Mona***, ***Aymen***, ***Sally***, ***Nuha***, ***Fatima***, ***Ragadah***, ***Salma***, ***Ahmed S***, ***Dalia***, ***Alfatih***, ***Ahmed Almokashfi***, ***Amani***, ***Israa***, ***Nazar***, ***Marwan***, ***Mohammed Babiker***, ***Houwaida***, among others, you deserve a warm thank for creating such a nice family atmosphere in Bergen.

My friends ***Ahmed Babiker***, ***Mohamed Alshaygi***, ***Osman Hamid***, ***Osama Mukhtar***, thank you for support and encouragement through all the along the twists and turns on this journey.

Last but not least, to my parents (***Ahmed Alamin Yousif*** and ***Nadia Algaali***), siblings, and extended family all over the world ☺, I dedicate this PhD thesis to you. Your unconditional love and heartfelt support gave me strength and comfort throughout my PhD journey.

Mohammed Ahmed Yassin

October 2016

Bergen

15. Bibliography

[1] J. A. Buckwalter, M. J. Glimcher, R. R. Cooper, R. Recker, *The journal of bone & joint surgery* **1995**, *77*, 1256.
[2] D. Sommerfeldt, C. Rubin, *European spine journal* **2001**, *10*, S86.
[3] R. Dimitriou, E. Jones, D. McGonagle, P. V. Giannoudis, *BMC medicine* **2011**, *9*, 66.
[4] C. G. Finkemeier, *The journal of bone & joint surgery* **2002**, *84*, 454.
[5] A. R. Amini, C. T. Laurencin, S. P. Nukavarapu, *Critical reviews in biomedical engineering* **2012**, *40*, 363.
[6] G. Zimmermann, A. Moghaddam, *Injury* **2011**, *42, Supplement 2*, S16.
[7] R. Langer, *Molecular therapy* **2000**, *1*, 12.
[8] S. Bose, M. Roy, A. Bandyopadhyay, *Trends in biotechnology* **2012**, *30*, 546.
[9] D. Howard, L. D. Buttery, K. M. Shakesheff, S. J. Roberts, *Journal of anatomy* **2008**, *213*, 66.
[10] M. H. Mankani, S. A. Kuznetsov, B. Shannon, R. K. Nalla, R. O. Ritchie, Y. Qin, P. G. Robey, *The american journal of pathology* **2006**, *168*, 542.
[11] M. H. Mankani, S. A. Kuznetsov, R. M. Wolfe, G. W. Marshall, P. G. Robey, *Stem cells* **2006**, *24*, 2140.
[12] H. Kitoh, T. Kitakoji, H. Tsuchiya, M. Katoh, N. Ishiguro, *Bone* **2007**, *40*, 522.
[13] M. Marcacci, E. Kon, V. Moukhachev, A. Lavroukov, S. Kutepov, R. Quarto, M. Mastrogiacomo, R. Cancedda, *Tissue engineering* **2007**, *13*, 947.
[14] S. J. Stephan, S. S. Tholpady, B. Gross, C. E. Petrie-Aronin, E. A. Botchway, L. S. Nair, R. C. Ogle, S. S. Park, *Laryngoscope* **2010**, *120*, 895.
[15] E. S. Place, J. H. George, C. K. Williams, M. M. Stevens, *Chemical society reviews* **2009**, *38*, 1139.
[16] T. Dvir, B. P. Timko, D. S. Kohane, R. Langer, *Nature nanotechnology* **2011**, *6*, 13.
[17] F. J. O'Brien, *Materials today* **2011**, *14*, 88.
[18] Y. Chen, V. Bloemen, S. Impens, M. Moesen, F. P. Luyten, J. Schrooten, *Tissue engineering part c methods* **2011**, *17*, 1211.
[19] M. M. Stevens, *Materials today* **2008**, *11*, 18.
[20] D. F. Williams, *Biomaterials* **2008**, *29*, 2941.
[21] S. J. Lee, G. J. Lim, J.-W. Lee, A. Atala, J. J. Yoo, *Biomaterials* **2006**, *27*, 3466.
[22] S. Danmark, A. Finne-Wistrand, K. Schander, M. Hakkarainen, K. Arvidson, K. Mustafa, A. C. Albertsson, *Acta biomaterialia* **2011**, *7*, 2035.
[23] B. N. Brown, J. E. Valentin, A. M. Stewart-Akers, G. P. McCabe, S. F. Badylak, *Biomaterials* **2009**, *30*, 1482.
[24] J. J. Norman, J. M. Collins, S. Sharma, B. Russell, T. A. Desai, *Tissue engineering part a* **2008**, *14*, 379.
[25] R. K. Jain, P. Au, J. Tam, D. G. Duda, D. Fukumura, *Nature biotechnology* **2005**, *23*, 821.
[26] V. Karageorgiou, D. Kaplan, *Biomaterials* **2005**, *26*, 5474.
[27] S. Yang, L. Kah-Fai, Z. Du, C. Chee-Kai, *Tissue engineering* **2001**, *7*, 679.
[28] D. W. Hutmacher, *Biomaterials* **2000**, *21*, 2529.
[29] C. V. B. d. Gusmão, W. D. Belangero, *Revista brasileira de ortopedia* **2009**, *44*, 299.
[30] K. A. Hing, *Philosophical transactions. a, mathematical, physical, and engineering sciences* **2004**, *362*, 2821.
[31] S. Ramakrishna, J. Mayer, E. Wintermantel, K. W. Leong, *Composites science and technology* **2001**, *61*, 1189.
[32] V. K. Balla, S. Bodhak, S. Bose, A. Bandyopadhyay, *Acta biomaterialia* **2010**, *6*, 3349.
[33] B. Dabrowski, W. Swieszkowski, D. Godlinski, K. J. Kurzydlowski, *Journal of biomedical materials research part b: applied biomaterials* **2010**, *95B*, 53.
[34] F. Witte, H. Ulrich, C. Palm, E. Willbold, *Journal of biomedical materials research part a* **2007**, *81A*, 757.
[35] V. Sansone, D. Pagani, M. Melato, *Clinical cases in mineral and bone metabolism* **2013**, *10*, 34.
[36] A. Yeo, W. J. Wong, H. H. Khoo, S. H. Teoh, *Journal of biomedical materials research part a* **2010**, *92A*, 311.

[37] Y. Liu, J. Lim, S.-H. Teoh, *Biotechnology advances* **2013**, *31*, 688.
[38] J. F. Mano, G. A. Silva, H. S. Azevedo, P. B. Malafaya, R. A. Sousa, S. S. Silva, L. F. Boesel, J. M. Oliveira, T. C. Santos, A. P. Marques, N. M. Neves, R. L. Reis, *Journal of the royal society interface* **2007**, *4*, 999.
[39] L. S. Nair, C. T. Laurencin, *Progress in polymer science* **2007**, *32*, 762.
[40] M. Okada, *Progress in polymer science* **2002**, *27*, 87.
[41] D. Eglin, D. Mortisen, M. Alini, *Soft matter* **2009**, *5*, 938.
[42] P. Gentile, V. Chiono, I. Carmagnola, P. V. Hatton, *International journal of molecular sciences* **2014**, *15*, 3640.
[43] F. Haghighat, S. A. H. Ravandi, *Fibers and polymers* **2014**, *15*, 71.
[44] B. D. Ulery, L. S. Nair, C. T. Laurencin, *Journal of polymer science. part b, polymer physics* **2011**, *49*, 832.
[45] A. Göpferich, *Biomaterials* **1996**, *17*, 103.
[46] S. Dånmark, A. Finne-Wistrand, M. Wendel, K. Arvidson, A.-C. Albertsson, K. Mustafa, *Journal of bioactive and compatible polymers* **2010**, *25*, 207.
[47] S. B. Idris, K. Arvidson, P. Plikk, S. Ibrahim, A. Finne-Wistrand, A. C. Albertsson, A. I. Bolstad, K. Mustafa, *Journal of biomedical materials research part a* **2010**, *94*, 631.
[48] S. B. Idris, S. Dånmark, A. F.-. Wistrand, K. Arvidson, A.-C. Albertsson, A. I. Bolstad, K. Mustafa, *Journal of bioactive and compatible polymers* **2010**.
[49] S. H. Oh, J. H. Lee, *Biomedical materials (Bristol, England)* **2013**, *8*, 014101.
[50] A. Gleadall, J. Pan, M.-A. Kruft, M. Kellomäki, *Acta biomaterialia* **2014**, *10*, 2223.
[51] N. Kamaly, B. Yameen, J. Wu, O. C. Farokhzad, *Chemical reviews* **2016**, *116*, 2602.
[52] M. Hakkarainen, *Degradable aliphatic polyesters* **2002**, 113.
[53] L. Lu, S. J. Peter, M. D. Lyman, H.-L. Lai, S. M. Leite, J. A. Tamada, S. Uyama, J. P. Vacanti, L. Robert, A. G. Mikos, *Biomaterials* **2000**, *21*, 1837.
[54] K. A. Athanasiou, J. Schmitz, C. Agrawal, *Tissue engineering* **1998**, *4*, 53.
[55] A. Gleadall, J. Pan, M.-A. Kruft, M. Kellomäki, *Acta biomaterialia* **2014**, *10*, 2233.
[56] K. Kim, M. Yu, X. Zong, J. Chiu, D. Fang, Y.-S. Seo, B. S. Hsiao, B. Chu, M. Hadjiargyrou, *Biomaterials* **2003**, *24*, 4977.
[57] X. Xu, X. Chen, A. Liu, Z. Hong, X. Jing, *European polymer journal* **2007**, *43*, 3187.
[58] C. X. F. Lam, D. W. Hutmacher, J.-T. Schantz, M. A. Woodruff, S. H. Teoh, *Journal of biomedical materials research part a* **2009**, *90A*, 906.
[59] M. L. Zhao, G. Sui, X. L. Deng, J. G. Lu, S. K. Ryu, X. P. Yang, *Advanced materials research* **2006**, p. 11/243.
[60] S. J. Hollister, *Nature materials* **2005**, *4*, 518.
[61] W. L. Murphy, R. G. Dennis, J. L. Kileny, D. J. Mooney, *Tissue engineering* **2002**, *8*, 43.
[62] P. Aramwit, J. Ratanavaraporn, S. Ekgasit, D. Tongsakul, N. Bang, *Journal of biomedical materials research part b: applied biomaterials* **2015**, *103*, 915.
[63] M. J. Moore, E. Jabbari, E. L. Ritman, L. Lu, B. L. Currier, A. J. Windebank, M. J. Yaszemski, *Journal of biomedical materials research part a* **2004**, *71A*, 258.
[64] N. Ashammakhi, A. Ndreu, L. Nikkola, I. Wimpenny, Y. Yang, *Regenerative medicine* **2008**, *3*, 547.
[65] T. G. Kim, H. Shin, D. W. Lim, *Advanced functional materials* **2012**, *22*, 2446.
[66] D. W. Hutmacher, M. Sittinger, M. V. Risbud, *Trends in biotechnology* **2004**, *22*, 354.
[67] M. I. Santos, R. L. Reis, *Macromolecular bioscience* **2010**, *10*, 12.
[68] X. Meng, P. Leslie, Y. Zhang, J. Dong, *Springerplus* **2014**, *3*, 80.
[69] H. Zhou, M. D. Weir, H. H. Xu, *Tissue engineering part a* **2011**, *17*, 2603.
[70] H. Mizuno, M. Tobita, A. C. Uysal, *Stem cells* **2012**, *30*, 804.
[71] M. V. Dodson, G. J. Hausman, L. Guan, M. Du, T. P. Rasmussen, S. P. Poulos, P. Mir, W. G. Bergen, M. E. Fernyhough, D. C. McFarland, R. P. Rhoads, B. Soret, J. M. Reecy, S. G. Velleman, Z. Jiang, *International journal of biological sciences* **2010**, *6*, 465.
[72] M. Miura, S. Gronthos, M. Zhao, B. Lu, L. W. Fisher, P. G. Robey, S. Shi, *Proceedings of the national academy of sciences of the united states of america* **2003**, *100*, 5807.
[73] D. Marot, M. Knezevic, G. V. Novakovic, *Stem cell research & therapy* **2010**, *1*, 10.

[74] S. C. Mendes, J. M. Tibbe, M. Veenhof, K. Bakker, S. Both, P. P. Platenburg, F. C. Oner, J. D. de Bruijn, C. A. van Blitterswijk, *Tissue engineering* **2002**, *8*, 911.
[75] M. F. Pittenger, A. M. Mackay, S. C. Beck, R. K. Jaiswal, R. Douglas, J. D. Mosca, M. A. Moorman, D. W. Simonetti, S. Craig, D. R. Marshak, *Science* **1999**, *284*, 143.
[76] A. Trounson, N. D. DeWitt, *Nature reviews molecular cell biology* **2016**, *17*, 194.
[77] Y. Ikada, *Journal of the royal society interface* **2006**, *3*, 589.
[78] S. L. Chen, W. W. Fang, F. Ye, Y. H. Liu, J. Qian, S. J. Shan, J. J. Zhang, R. Z. Chunhua, L. M. Liao, S. Lin, J. P. Sun, *The American journal of cardiology* **2004**, *94*, 92.
[79] J. Kim, J. Kang, J. Park, Y. Choi, K. Choi, K. Park, D. Baek, S. Seong, H.-K. Min, H. Kim, *Archives of pharmacal research.* **2009**, *32*, 117.
[80] P. T. Brown, A. M. Handorf, W. B. Jeon, W.-J. Li, *Current pharmaceutical design* **2013**, *19*, 3429.
[81] W. Chen, Y. Shao, X. Li, G. Zhao, J. Fu, *Nano today* **2014**, *9*, 759.
[82] L. G. Chase, U. Lakshmipathy, L. A. Solchaga, M. S. Rao, M. C. Vemuri, *Stem cell research & therapy* **2010**, *1*, 1.
[83] E. M. Bueno, G. Laevsky, G. A. Barabino, *Journal of biotechnology* **2007**, *129*, 516.
[84] K. Kim, D. Dean, A. G. Mikos, J. P. Fisher, *Biomacromolecules* **2009**, *10*, 1810.
[85] L. E. Freed, A. P. Hollander, I. Martin, J. R. Barry, R. Langer, G. Vunjak-Novakovic, *Experimental cell research* **1998**, *240*, 58.
[86] C. J. Galban, B. R. Locke, *Biotechnology and bioengineering* **1999**, *65*, 121.
[87] F. Zhao, T. Ma, *Biotechnology and bioengineering* **2005**, *91*, 482.
[88] A. L. Olivares, D. Lacroix, *Tissue engineering. part c, methods* **2012**, *18*, 624.
[89] W. Janvikul, P. Uppanan, B. Thavornyutikarn, W. Kosorn, P. Kaewkong, *Procedia engineering* **2013**, *59*, 158.
[90] F. P. Melchels, B. Tonnarelli, A. L. Olivares, I. Martin, D. Lacroix, J. Feijen, D. J. Wendt, D. W. Grijpma, *Biomaterials* **2011**, *32*, 2878.
[91] M. Bitar, R. A. Brown, V. Salih, A. G. Kidane, J. C. Knowles, S. N. Nazhat, *Biomacromolecules* **2008**, *9*, 129.
[92] R. Mauck, S. Seyhan, G. Ateshian, C. Hung, *Annals of biomedical engineering* **2002**, *30*, 1046.
[93] M. Kruyt, J. De Bruijn, J. Rouwkema, C. Van Bliterswijk, C. Oner, A. Verbout, W. Dhert, *Tissue enginnering part a* **2008**, *14*, 1081.
[94] A. S. Goldstein, *Tissue engineering* **2001**, *7*, 817.
[95] A. J. Almarza, K. A. Athanasiou, *Annals of biomedical engineering* **2005**, *33*, 943.
[96] L. Wang, K. Seshareddy, M. L. Weiss, M. S. Detamore, *Tissue engineering part a* **2009**, *15*, 1009.
[97] J. W. Vehof, A. E. de Ruijter, P. H. Spauwen, J. A. Jansen, *Tissue engineering* **2001**, *7*, 373.
[98] C. E. Holy, M. S. Shoichet, J. E. Davies, *Journal of biomedical materials research* **2000**, *51*, 376.
[99] S. Saini, T. M. Wick, *Biotechnology progress* **2003**, *19*, 510.
[100] J. Ma, S. K. Both, F. Yang, F. Z. Cui, J. Pan, G. J. Meijer, J. A. Jansen, J. J. J. P. van den Beucken, *Stem cells translational medicine* **2014**, *3*, 98.
[101] P. Niemeyer, T. S. Schönberger, J. Hahn, P. Kasten, J. Fellenberg, N. Suedkamp, A. T. Mehlhorn, S. Milz, S. Pearce, *Tissue engineering part a* **2009**, *16*, 33.
[102] A. R. Costa-Pinto, V. M. Correlo, P. C. Sol, M. Bhattacharya, S. Srouji, E. Livne, R. L. Reis, N. M. Neves, *Journal of tissue engineering and regenerative medicine* **2012**, *6*, 21.
[103] K. M. Dupont, K. Sharma, H. Y. Stevens, J. D. Boerckel, A. J. García, R. E. Guldberg, *Proceedings of the national academy of sciences* **2010**, *107*, 3305.
[104] B. Rai, J. L. Lin, Z. X. H. Lim, R. E. Guldberg, D. W. Hutmacher, S. M. Cool, *Biomaterials* **2010**, *31*, 7960.
[105] C. M. Cowan, Y.-Y. Shi, O. O. Aalami, Y.-F. Chou, C. Mari, R. Thomas, N. Quarto, C. H. Contag, B. Wu, M. T. Longaker, *Nature biotechnology* **2004**, *22*, 560.
[106] C. Zong, D. Xue, W. Yuan, W. Wang, D. Shen, X. Tong, D. Shi, L. Liu, Q. Zheng, C. Gao, J. Wang, *E uropean cells and materials* **2010**, *20*, 109.
[107] H. Shin, S. Jo, A. G. Mikos, *Biomaterials* **2003**, *24*, 4353.
[108] J. A. Sanz-Herrera, E. Reina-Romo, *International journal of molecular sciences* **2011**, *12*, 8217.
[109] J. M. Anderson, A. Rodriguez, D. T. Chang, *Seminars in immunology* **2008**, *20*, 86.

[110] M. Andersson, F. Suska, A. Johansson, M. Berglin, L. Emanuelsson, H. Elwing, P. Thomsen, *Journal of biomedical materials research part a* **2008**, *84A*, 652.
[111] S. Sakiyama-Elbert, J. Hubbell, *Annual review of materials research* **2001**, *31*, 183.
[112] K. Anselme, *Biomaterials* **2000**, *21*, 667.
[113] A. J. García, *Biomaterials* **2005**, *26*, 7525.
[114] R. O. Hynes, *Cell* **2002**, *110*, 673.
[115] H. Shin, *Biomaterials* **2007**, *28*, 126.
[116] H. Shadpour, N. L. Allbritton, *ACS applied materials & interfaces* **2010**, *2*, 1086.
[117] D. L. Elbert, J. A. Hubbell, *Annual review of materials science* **1996**, *26*, 365.
[118] X. Yao, R. Peng, J. Ding, *Advanced materials* **2013**, *25*, 5257.
[119] E. S. Place, N. D. Evans, M. M. Stevens, *Nature materials* **2009**, *8*, 457.
[120] Z. Ma, Z. Mao, C. Gao, *Colloids and surfaces b: biointerfaces* **2007**, *60*, 137.
[121] E. A. Vogler, *Advances in colloid and interface science* **1998**, *74*, 69.
[122] E. J. P. Jansen, R. E. J. Sladek, H. Bahar, A. Yaffe, M. J. Gijbels, R. Kuijer, S. K. Bulstra, N. A. Guldemond, I. Binderman, L. H. Koole, *Biomaterials* **2005**, *26*, 4423.
[123] S. H. Oh, S. G. Kang, E. S. Kim, S. H. Cho, J. H. Lee, *Biomaterials* **2003**, *24*, 4011.
[124] H. Rashidi, J. Yang, K. M. Shakesheff, *Biomaterials science* **2014**, *2*, 1318.
[125] S. Wu, X. Liu, K. W. K. Yeung, C. Liu, X. Yang, *Materials science and engineering: r: reports* **2014**, *80*, 1.
[126] A. d. Mel, B. G. Cousins, A. M. Seifalian, *International journal of biomaterials* **2012**.
[127] A. G. Mikos, M. D. Lyman, L. E. Freed, R. Langer, *Biomaterials* **1994**, *15*, 55.
[128] Y. Sun, Z. Xing, Y. Xue, K. Mustafa, A. Finne-Wistrand, A.-C. Albertsson, *Biomacromolecules* **2014**, *15*, 1259.
[129] S. Oh, S. Cho, J. Lee, *Molecular crystals and liquid crystals* **2004**, *418*, 229.
[130] Q. Cai, J. Yang, J. Bei, S. Wang, *Biomaterials* **2002**, *23*, 4483.
[131] J. I. Lim, B. Yu, Y. K. Lee, *Biotechnology letters* **2008**, *30*, 2085.
[132] Z. Wang, M. Lin, Q. Xie, H. Sun, Y. Huang, D. Zhang, Z. Yu, X. Bi, J. Chen, J. Wang, W. Shi, P. Gu, X. Fan, *International journal of nanomedicine* **2016**, *11*, 1483.
[133] A. H. Kibbe, "*Handbook of pharmaceutical excipients"*, London, **2000**.
[134] M. M. Malingré, J. H. M. Schellens, O. V. Tellingen, M. Ouwehand, H. A. Bardelmeijer, H. Rosing, F. J. Koopman, M. E. Schot, W. W. T. B. Huinink, J. H. Beijnen, *British journal of cancer* **2001**, *85*, 1472.
[135] H. Zhang, M. Yao, R. A. Morrison, S. Chong, *Archives of pharmacal research* **2003**, *26*, 768.
[136] B. Arechabala, C. Coiffard, P. Rivalland, L. J. M. Coiffard, Y. D. Roeck-Holtzhauer, *Journal of applied toxicology* **1999**, *19*, 163.
[137] C. M. Toutain-Kidd, S. C. Kadivar, C. T. Bramante, S. A. Bobin, M. E. Zegans, *Antimicrobial agents and chemotherapy* **2009**, *53*, 136.
[138] X. Liu, Y. Won, P. X. Ma, *Journal of biomedical materials research part a* **2005**, *74A*, 84.
[139] R. A. Surmenev, M. A. Surmeneva, A. A. Ivanova, *Acta biomaterialia* **2014**, *10*, 557.
[140] M. Bohner, *Biomaterials* **2009**, *30*, 6403.
[141] E. L. W. de Mulder, G. Hannink, M. J. W. Koens, D. W. P. M. Löwik, N. Verdonschot, P. Buma, *Journal of biomedical materials research part a* **2013**, *101A*, 919.
[142] G. Yu, Y. Fan, *Journal of biomaterials science. polymer edition* **2008**, *19*, 87.
[143] A. de Mel, G. Jell, M. M. Stevens, A. M. Seifalian, *Biomacromolecules* **2008**, *9*, 2969.
[144] F. R. Kloss, M. Najam-Ul-Haq, M. Rainer, R. Gassner, G. Lepperdinger, C. W. Huck, G. Bonn, F. Klauser, X. Liu, N. Memmel, E. Bertel, J. A. Garrido, D. Steinmüller-Nethl, *Journal of nanoscience and nanotechnology* **2007**, *7*, 4581.
[145] H. Huang, E. Pierstorff, E. Osawa, D. Ho, *ACS nano* **2008**, *2*, 203.
[146] V. N. Mochalin, O. Shenderova, D. Ho, Y. Gogotsi, *Nature nanotechnology* **2012**, *7*, 11.
[147] Q. Zhang, V. N. Mochalin, I. Neitzel, I. Y. Knoke, J. Han, C. A. Klug, J. G. Zhou, P. I. Lelkes, Y. Gogotsi, *Biomaterials* **2011**, *32*, 87.
[148] S. Suliman, Z. Xing, X. Wu, Y. Xue, T. O. Pedersen, Y. Sun, A. P. Døskeland, J. Nickel, T. Waag, H. Lygre, A. Finne-Wistrand, D. Steinmüller-Nethl, A. Krueger, K. Mustafa, *Journal of controlled release* **2015**, *197*, 148.

[149] Z. Xing, T. O. Pedersen, X. Wu, Y. Xue, Y. Sun, A. Finne-Wistrand, F. R. Kloss, T. Waag, A. Krueger, D. Steinmuller-Nethl, K. Mustafa, *Tissue engineering part a* **2013**, *19*, 1783.
[150] F. Zhang, Q. Song, X. Huang, F. Li, K. Wang, Y. Tang, C. Hou, H. Shen, *ACS applied materials & interfaces* **2016**, *8*, 1087.
[151] M. Okamoto, B. John, *Progress in polymer science* **2013**, *38*, 1487.
[152] C. Choong, S. Yuan, E. S. Thian, A. Oyane, J. Triffitt, *Journal of biomedical materials research part a* **2012**, *100A*, 353.
[153] J. Gao, L. Niklason, R. Langer, *Journal of biomedical materials research* **1998**, *42*, 417.
[154] X. Liu, P. X. Ma, *Annals of biomedical engineering* **2004**, *32*, 477.
[155] P. K. Chu, J. Y. Chen, L. P. Wang, N. Huang, *Materials science and engineering: r: reports* **2002**, *36*, 143.
[156] S. Yoshida, K. Hagiwara, T. Hasebe, A. Hotta, *Surface and coatings technology* **2013**, *233*, 99.
[157] L. Safinia, N. Datan, M. Höhse, A. Mantalaris, A. Bismarck, *Biomaterials* **2005**, *26*, 7537.
[158] R. Quarto, M. Mastrogiacomo, R. Cancedda, S. M. Kutepov, V. Mukhachev, A. Lavroukov, E. Kon, M. Marcacci, *New england journal of medicine* **2001**, *344*, 385.
[159] K. Rezwan, Q. Z. Chen, J. J. Blaker, A. R. Boccaccini, *Biomaterials* **2006**, *27*, 3413.
[160] K. Odelius, P. Plikk, A.-C. Albertsson, *Biomacromolecules* **2005**, *6*, 2718.
[161] S. Kuddannaya, J. Bao, Y. Zhang, *ACS applied materials & interfaces* **2015**, *7*, 25529.
[162] A. Krüger, F. Kataoka, M. Ozawa, T. Fujino, Y. Suzuki, A. E. Aleksenskii, A. Y. Vul', E. Õsawa, *Carbon* **2005**, *43*, 1722.
[163] L. Li, Y. Qian, C. Jiang, Y. Lv, W. Liu, L. Zhong, K. Cai, S. Li, L. Yang, *Biomaterials* **2012**, *33*, 3428.
[164] C. Maniatopoulos, J. Sodek, A. H. Melcher, *Cell and tissue research.* **1988**, *254*, 317.
[165] Z. Xing, Y. Xue, S. Dånmark, K. Schander, S. Østvold, K. Arvidson, S. Hellem, A. Finne-Wistrand, A.-C. Albertsson, K. Mustafa, *Journal of biomedical materials research part a* **2011**, *96A*, 349.
[166] J. M. Sobral, S. G. Caridade, R. A. Sousa, J. F. Mano, R. L. Reis, *Acta biomaterialia* **2011**, *7*, 1009.
[167] Z. Xing, Y. Xue, S. Danmark, A. Finne-Wistrand, K. Arvidson, S. Hellem, Z. Q. Yang, K. Mustafa, *The international journal of artificial organs* **2011**, *34*, 432.
[168] A. B. Yeatts, J. P. Fisher, *Tissue engineering part c: methods* **2011**, *17*, 337.
[169] V. I. Sikavitsas, G. N. Bancroft, A. G. Mikos, *Journal of biomedical materials research* **2002**, *62*, 136.
[170] Z.-Y. Zhang, S. H. Teoh, E. Y. Teo, M. S. Khoon Chong, C. W. Shin, F. T. Tien, M. A. Choolani, J. K. Y. Chan, *Biomaterials* **2010**, *31*, 8684.
[171] M. Stiehler, C. Bünger, A. Baatrup, M. Lind, M. Kassem, T. Mygind, *Journal of biomedical materials research part a* **2009**, *89A*, 96.
[172] P. S. Gomes, M. H. Fernandes, *Laboratory animals* **2011**, *45*, 14.
[173] V. Viateau, D. Logeart-Avramoglou, G. Guillemin, H. Petite, *Sourcebook of models for biomedical research* **2008**, 725.
[174] C. Cheng, V. Alt, L. Pan, U. Thormann, R. Schnettler, L. G. Strauss, M. Schumacher, M. Gelinsky, A. Dimitrakopoulou-Strauss, *Injury* **2014**, *45*, 501.
[175] P. S. Lienemann, S. Metzger, A.-S. Kiveliö, A. Blanc, P. Papageorgiou, A. Astolfo, B. R. Pinzer, P. Cinelli, F. E. Weber, R. Schibli, M. Béhé, M. Ehrbar, *Scientific reports* **2015**, *5*, 10238.
[176] C. K. Hoh, R. A. Hawkins, M. Dahlbom, J. A. Glaspy, L. L. Seeger, Y. Choi, C. W. Schiepers, S. C. Huang, N. Satyamurthy, J. R. Barrio, et al., *Journal of computer assisted tomography* **1993**, *17*, 34.
[177] J. Kim, I. S. Kim, T. H. Cho, H. C. Kim, S. J. Yoon, J. Choi, Y. Park, K. Sun, S. J. Hwang, *Journal of biomedical materials research part a* **2010**, *95A*, 673.
[178] P. Nooeaid, V. Salih, J. P. Beier, A. R. Boccaccini, *Journal of cellular and molecular medicine* **2012**, *16*, 2247.
[179] J. M. Goddard, J. H. Hotchkiss, *Progress in polymer science* **2007**, *32*, 698.
[180] W. Jianhua, I. Toshio, O. Naoto, I. Takayasu, M. Takashi, L. Baolin, Y. Masao, *Biomedical materials* **2009**, *4*, 045002.
[181] Y. Tamada, Y. Ikada, *Journal of colloid and interface science* **1993**, *155*, 334.

[182] F. Wen, C. C. S. Lau, J. Lim, Y. Liao, S. H. Teoh, M. S. K. Chong, *Polymeric Biomaterials for Tissue Regeneration: From Surface/Interface Design to 3D Constructs* **2016**, 123.
[183] A. K. Bassi, J. E. Gough, M. Zakikhani, S. Downes, *Journal of tissue engineering* **2011**, *2011*, 615328.
[184] M. P. Prabhakaran, J. R. Venugopal, S. Ramakrishna, *Biomaterials* **2009**, *30*, 4996.
[185] A. I. Caplan, S. P. Bruder, *Trends in molecular medicine* **2001**, *7*, 259.
[186] D. Kaigler, G. Avila-Ortiz, S. Travan, A. D. Taut, M. Padial-Molina, I. Rudek, F. Wang, A. Lanis, W. V. Giannobile, *Journal of bone and mineral research* **2015**, *30*, 1206.
[187] M. A. Sabatino, R. Santoro, S. Gueven, C. Jaquiery, D. J. Wendt, I. Martin, M. Moretti, A. Barbero, *Journal of tissue engineering and regenerative medicine* **2015**, *9*, 1394.
[188] S. P. Bruder, N. Jaiswal, N. S. Ricalton, J. D. Mosca, K. H. Kraus, S. Kadiyala, *Clinical orthopaedics and related research* **1998**, S247.
[189] S. P. Bruder, A. A. Kurth, M. Shea, W. C. Hayes, N. Jaiswal, S. Kadiyala, *Journal of orthopaedic research* **1998**, *16*, 155.
[190] H. Agata, I. Asahina, N. Watanabe, Y. Ishii, N. Kubo, S. Ohshima, M. Yamazaki, A. Tojo, H. Kagami, *Tissue engineering part a* **2010**, *16*, 663.
[191] H. Castano-Izquierdo, J. Álvarez-Barreto, J. v. d. Dolder, J. A. Jansen, A. G. Mikos, V. I. Sikavitsas, *Journal of biomedical materials research part a* **2007**, *82A*, 129.
[192] J. van den Dolder, J. W. M. Vehof, P. H. M. Spauwen, J. A. Jansen, *Journal of biomedical materials research* **2002**, *62*, 350.
[193] T. B. Prigozhina, S. Khitrin, G. Elkin, O. Eizik, S. Morecki, S. Slavin, *Experimental hematology* **2008**, *36*, 1370.
[194] B. Peterson, J. Zhang, R. Iglesias, M. Kabo, M. Hedrick, P. Benhaim, J. R. Lieberman, *Tissue engineering* **2005**, *11*, 120.
[195] V. Wright, H. Peng, A. Usas, B. Young, B. Gearhart, J. Cummins, J. Huard, *Molecular therapy* **2002**, *6*, 169.
[196] C. Jo, P. Yoon, H. Kim, K. Kang, K. Yoon, *Cell and tissue research.* **2013**, *353*, 41.
[197] S. A. Kuznetsov, M. H. Mankani, P. G. Robey, *Journal of tissue engineering and regenerative medicine* **2013**, *7*, 226.
[198] A. B. Faia-Torres, M. Charnley, T. Goren, S. Guimond-Lischer, M. Rottmar, K. Maniura-Weber, N. D. Spencer, R. L. Reis, M. Textor, N. M. Neves, *Acta biomaterialia* **2015**, *28*, 64.
[199] J. J. Alm, T. J. Heino, T. A. Hentunen, H. K. Vaananen, H. T. Aro, *Tissue engineering part c methods* **2012**, *18*, 658.
[200] F. J. O'Brien, B. A. Harley, I. V. Yannas, L. J. Gibson, *Biomaterials* **2005**, *26*, 433.
[201] K. F. Leong, C. M. Cheah, C. K. Chua, *Biomaterials* **2003**, *24*, 2363.
[202] C. M. Agrawal, R. B. Ray, *Journal of biomedical materials research* **2001**, *55*, 141.
[203] G. R. Beck, *Journal of cellular biochemistry* **2003**, *90*, 234.
[204] G. S. Stein, J. B. Lian, *Endocrine reviews* **1993**, *14*, 424.
[205] J. E. Aubin, *Journal of cellular biochemistry. Supplement* **1998**, *30-31*, 73.
[206] M. Á. Brennan, A. Renaud, J. Amiaud, M. T. Rojewski, H. Schrezenmeier, D. Heymann, V. Trichet, P. Layrolle, *Stem cell research & therapy* **2014**, *5*, 1.
[207] J.-f. Pan, N.-h. Liu, L.-y. Shu, H. Sun, *Journal of nanobiotechnology* **2015**, *13*, 37.
[208] M. Parizek, T. E. L. Douglas, K. Novotna, A. Kromka, M. A. Brady, A. Renzing, E. Voss, M. Jarosova, L. Palatinus, P. Tesarek, P. Ryparova, V. Lisa, A. M. dos Santos, L. Bacakova, *International journal of nanomedicine* **2012**, *7*, 1931.
[209] A. Serafim, S. Cecoltan, A. Lungu, E. Vasile, H. Iovu, I. C. Stancu, *RSC advances* **2015**, *5*, 95467.
[210] A. Krueger, D. Lang, *Advanced functional materials* **2012**, *22*, 890.
[211] D. J. Griffon, J. P. Abulencia, G. R. Ragetly, L. P. Fredericks, S. Chaieb, *Journal of tissue engineering and regenerative medicine* **2011**, *5*, 169.
[212] S. Kuddannaya, Y. J. Chuah, M. H. A. Lee, N. V. Menon, Y. Kang, Y. Zhang, *ACS applied materials & interfaces* **2013**, *5*, 9777.
[213] R. G. Strickley, *Pharmaceutical research* **2004**, *21*, 201.
[214] A. E. Gulyaev, S. E. Gelperina, I. N. Skidan, A. S. Antropov, G. Y. Kivman, J. Kreuter, *Pharmaceutical research* **1999**, *16*, 1564.

[215] K. Prabhakar, S. M. Afzal, G. Surender, V. Kishan, *Acta pharmaceutica sinica b* **2013**, *3*, 345.
[216] T. Komori, *Cell Tissue Res.* **2009**, *339*, 189.
[217] L. Dalle Carbonare, G. Innamorati, M. T. Valenti, *Stem cell reviews and reports* **2011**, *8*, 891.
[218] G. Zhao, Z. Schwartz, M. Wieland, F. Rupp, J. Geis-Gerstorfer, D. L. Cochran, B. D. Boyan, *Journal of biomedical materials research part a* **2005**, *74A*, 49.
[219] D. M. Ornitz, P. J. Marie, *Genes and development* **2002**, *16*, 1446.
[220] E. H. Hartman, J. W. Vehof, P. H. Spauwen, J. A. Jansen, *Biomaterials* **2005**, *26*, 1829.
[221] N. S. Hwang, S. Varghese, H. J. Lee, Z. Zhang, J. Elisseeff, *Tissue engineering part a* **2013**, *19*, 1723.
[222] S.-S. Kim, K.-M. Ahn, M. S. Park, J.-H. Lee, C. Y. Choi, B.-S. Kim, *Journal of biomedical materials research part a* **2007**, *80A*, 206.
[223] T. Sawase, R. Jimbo, K. Baba, Y. Shibata, T. Ikeda, M. Atsuta, *Clinical oral implants research* **2008**, *19*, 491.
[224] H. V. Unadkat, M. Hulsman, K. Cornelissen, B. J. Papenburg, R. K. Truckenmüller, A. E. Carpenter, M. Wessling, G. F. Post, M. Uetz, M. J. T. Reinders, D. Stamatialis, C. A. van Blitterswijk, J. de Boer, *Proceedings of the national academy of sciences of the united states of america* **2011**, *108*, 16565.
[225] R. J. McMurray, N. Gadegaard, P. M. Tsimbouri, K. V. Burgess, L. E. McNamara, R. Tare, K. Murawski, E. Kingham, R. O. C. Oreffo, M. J. Dalby, *Nature materials* **2011**, *10*, 637.
[226] M. J. P. Biggs, R. G. Richards, N. Gadegaard, C. D. W. Wilkinson, R. O. C. Oreffo, M. J. Dalby, *Biomaterials* **2009**, *30*, 5094.
[227] M. M. McCafferty, G. A. Burke, B. J. Meenan, *Journal of tissue engineering* **2014**, *5*, 2041731414537513.
[228] M. Mahmood, Z. Li, D. Casciano, M. V. Khodakovskaya, T. Chen, A. Karmakar, E. Dervishi, Y. Xu, T. Mustafa, F. Watanabe, A. Fejleh, M. Whitlow, M. Al-Adami, A. Ghosh, A. S. Biris, *Journal of cellular and molecular medicine* **2011**, *15*, 2297.
[229] K. K. Wong, M. Piert, *Journal of nuclear medicine* **2013**, *54*, 590.
[230] J. Maciel, M. I. Oliveira, R. M. Gonçalves, M. A. Barbosa, *Acta biomaterialia* **2012**, *8*, 3669.
[231] B. G. Keselowsky, D. M. Collard, A. J. García, *Biomaterials* **2004**, *25*, 5947.
[232] G. C. C. Costa, O. Shenderova, V. Mochalin, Y. Gogotsi, A. Navrotsky, *Carbon* **2014**, *80*, 544.
[233] A. Krueger, *Journal of materials chemistry* **2011**, *21*, 12571.
[234] M.-H. You, M. K. Kwak, D.-H. Kim, K. Kim, A. Levchenko, D.-Y. Kim, K.-Y. Suh, *Biomacromolecules* **2010**, *11*, 1856.
[235] J. Liskova, O. Babchenko, M. Varga, A. Kromka, D. Hadraba, Z. Svindrych, Z. Burdikova, L. Bacakova, *International journal of nanomedicine* **2015**, *10*, 869.
[236] M. I. Santos, I. Pashkuleva, C. M. Alves, M. E. Gomes, S. Fuchs, R. E. Unger, R. L. Reis, C. J. Kirkpatrick, *Journal of materials chemistry* **2009**, *19*, 4091.
[237] H. Liu, T. J. Webster, *Biomaterials* **2007**, *28*, 354.
[238] A. A. Sawyer, K. M. Hennessy, S. L. Bellis, *Biomaterials* **2005**, *26*, 1467.
[239] P. Thevenot, W. Hu, L. Tang, *Current topics in medicinal chemistry* **2008**, *8*, 270.
[240] K. Wang, C. Zhou, Y. Hong, X. Zhang, *Interface focus* **2012**, *2*, 259.
[241] A. Farrugia, *Transfusion medicine reviews* **2010**, *24*, 53.
[242] M.R.R Alves, A.D.G Zuñiga, R.d.C.S Sousa, C.Z Scolforo, *The scientific world journal* **2016**, 2016, 9.
[243] C. F. Wertz, M. M. Santore, *Langmuir* **2001**, *17*, 3006.
[244] E. P. Vieira, S. Rocha, M. Carmo Pereira, H. Mohwald, M. A. Coelho, *Langmuir* **2009**, *25*, 9879.
[245] J. A. Chinn, S. Slack, *The Biomedical Engineering Handbook* **2000**, *200*, 1597.
[246] A. M. Schrand, S. A. C. Hens, O. A. Shenderova, *Critical reviews in solid state and materials sciences* **2009**, *34*, 18.
[247] D. Grafahrend, K. H. Heffels, M. V. Beer, P. Gasteier, M. Moller, G. Boehm, P. D. Dalton, J. Groll, *Nature materials* **2011**, *10*, 67.
[248] M. Kurylowicz, H. Paulin, J. Mogyoros, M. Giuliani, J. R. Dutcher, *Journal of the royal society interface* **2014**, *11*.

[249] E. A. dos Santos, M. Farina, G. A. Soares, K. Anselme, *Journal of materials science: materials in medicine* **2008**, *19*, 2307.
[250] A. Hezi-Yamit, C. Sullivan, J. Wong, L. David, M. Chen, P. Cheng, D. Shumaker, J. N. Wilcox, K. Udipi, *Journal of biomedical materials research part a* **2009**, *90A*, 133.
[251] J. N. Barbosa, M. A. Barbosa, A. P. Águas, *Biomaterials* **2004**, *25*, 2557.
[252] S. Kamath, D. Bhattacharyya, C. Padukudru, R. B. Timmons, L. Tang, *Journal of biomedical materials research part a* **2008**, *86*, 617.

16. Papers I - III

I

Paper I

Mohammed Ahmed Yassin, Knut N. Leknes, Pedersen TO, Zhe Xing, Yang Sun, Stein Atle Lie, Anna Finne-Wistrand, Kamal Mustafa. **Cell seeding density is a critical determinant for copolymer scaffolds-induced bone regeneration**. Journal of Biomedical Materials Research Part A 2015;103(11):3649-3658.

Society For Biomaterials

Cell seeding density is a critical determinant for copolymer scaffolds-induced bone regeneration

Mohammed A. Yassin,[1] Knut N. Leknes,[1] Torbjorn O. Pedersen,[1] Zhe Xing,[1] Yang Sun,[2] Stein A. Lie,[1] Anna Finne-Wistrand,[2] Kamal Mustafa[1]

[1]Faculty of Medicine and Dentistry, Department of Clinical Dentistry, Center for Clinical Dental Research, University of Bergen, Årstadveien 19, N-5009 Bergen, Norway
[2]Department of Fibre and Polymer Technology, School of Chemical Science and Engineering, KTH Royal Institute of Technology, Teknikringen 42, SE-100 44 Stockholm, Sweden

Received 6 March 2015; revised 6 May 2015; accepted 11 May 2015
Published online 4 September 2015 in Wiley Online Library (wileyonlinelibrary.com). DOI: 10.1002/jbm.a.35505

Abstract: Constructs intended for bone tissue engineering (TE) are influenced by the initial cell seeding density. Therefore, the objective of this study was to determine the effect of bone marrow stromal stem cells (BMSCs) density loaded onto copolymer scaffolds on bone regeneration. BMSCs were harvested from rat's bone marrow and cultured in media with or without osteogenic supplements. Cells were seeded onto poly(L-lactide-*co*-ϵ-caprolactone) [poly(LLA-*co*-CL)] scaffolds at two different densities: low density (1×10^6 cells/scaffold) or high density (2×10^6 cells/scaffold) using spinner modified flasks and examined after 1 and 3 weeks. Initial attachment and spread of BMSC onto the scaffolds was recorded by scanning electron microscopy. Cell proliferation was assessed by DNA quantification and cell differentiation by quantitative real-time reverse transcriptase-polymerized chain reaction analysis (qRT-PCR). Five-millimeter rat calvarial defects (24 defects in 12 rats) were implanted with scaffolds seeded with either low or high density expanded with or without osteogenic supplements. Osteogenic supplements significantly increased cell proliferation ($p < 0.001$). Scaffolds seeded at high cell density exhibited higher mRNA expressions of Runx2 $p = 0.001$, Col1 $p = 0.001$, BMP2 $p < 0.001$, BSP $p < 0.001$, and OC $p = 0.013$. More bone was formed in response to high cell seeding density ($p = 0.023$) and high seeding density with osteogenic medium ($p = 0.038$). Poly (LLA-*co*-CL) scaffolds could be appropriate candidates for bone TE. The optimal number of cells to be loaded onto scaffolds is critical for promoting Extracellular matrix synthesis and bone formation. Cell seeding density and osteogenic supplements may have a synergistic effect on the induction of new bone. © 2015 Wiley Periodicals, Inc. J Biomed Mater Res Part A: 103A: 3649–3658, 2015.

Key Words: bone marrow stromal cells, polymer scaffolds, cell seeding density, osteogenic supplements, bone regeneration

How to cite this article: Yassin MA, Leknes KN, Pedersen TO, Xing Z, Sun Y, Lie SA, Finne-Wistrand A, Mustafa K. 2015. Cell seeding density is a critical determinant for copolymer scaffolds-induced bone regeneration. J Biomed Mater Res Part A 2015:103A:3649–3658.

INTRODUCTION

Aliphatic polyesters such as poly(lactide), poly(lactide-*co*-glycolide), and poly(ϵ-caprolactone) and their synthesized copolymers are the most common synthetic biodegradable polymers used as scaffolding in bone tissue engineering (TE). By copolymerization of ϵ-caprolactone with different lactones, the physical and mechanical properties of the polyesters can be tailored, extending the range of applications of scaffolds.[1] Poly(L-lactide-*co*-ϵ-caprolactone) [poly(LLA-*co*-CL)] possesses appropriate mechanical and physical properties. Not only the degradation rate but also the shape of the scaffolds can readily be modified.[2–4] Moreover, animal studies have confirmed that endothelial microvascular networks can be created in porous scaffolds of 3D copolymer and sustained after implantation.[5]

In developing TE constructs which may influence the features and functionality of the engineered tissues, cell seeding density is a critical factor. The optimal seeding density of a scaffold depends on the scaffold biomaterial, the structure of the scaffold, and the seeding technique.[6,7] The influence of cell seeding density on TE constructs has been studied in cardiac tissue, cartilage, and bone.[8–10] In bone TE, cell seeding density influences cell proliferation, distribution, differentiation, extracellular matrix (ECM) synthesis, and tissue formation.[11–16] It has been reported that bone marrow stromal cells (BMSCs), cultured at density of 6.83×10^5 cells/cm^2 in three-dimensional (3D) poly(DL-lactic-*co*-glycolic acid) scaffolds, exhibited rapid proliferation over the first 7 days.[17] Increasing the number of BMSCs from 3.54×10^4 to 3.54×10^5 cells/cm^2 promoted osteogenic

Correspondence to: M. A. Yassin; e-mail: mya058@uib.no
Contract grant sponsor: VascuBone Project, European Union FP7; contract grant number: 242175
Contract grant sponsor: Norwegian State Educational Loan Fund (Quota Programme)

expression in titanium mesh.[18] Similarly, Zhou et al. demonstrated that the total number of cells loaded onto polycaprolactone\tricalciumphosphate scaffolds significantly influenced the production of ALP and osteocalcin.[19] In rabbit segmental bone defect it was shown that a density of 1.5×10^6 cells/scaffold stimulated bone deposition after 2 weeks.[20] However, another study reported that an increase in cell seeding density from 1 to 6×10^6 cells/mL did not enhance bone formation, but promoted more homogenous cell distribution throughout the constructs.[21] Further, *in vivo* studies on cartilage and bone formation have failed to demonstrate any significant effects of high cell seeding density in 3D porous scaffolds.[9,22] The inconclusive results indicate the need for further evaluation of the *in vitro* and *in vivo* effects of cell seeding density.

BMSCs have been widely used and investigated because they can be expanded *in vitro* and differentiated into a variety of cell types such as adipocytes, chondrocytes, myoblasts, and osteoblasts, by supplementing the cell culture medium with specific growth and differentiation factors.[23–25] Osteogenic differentiation of BMSCs can be induced by the introduction of supplements such as ascorbic acid, dexamethasone, and β-glycerophosphate into the culture medium.[26,27] It has been reported that preculture of BMSCs in osteogenic medium for a short period may promote osteogenesis.[28] On the other hand, a published study demonstrated that osteogenetic activity is significantly higher in non-preculture of BMSCs.[29] These contradictory findings indicate that the *in vivo* effect of osteogenic medium needs to be further addressed.

The main objective of this study was to assess the osteogenic potential of a tissue-engineered construct of BMSCs and poly(LLA-*co*-CL) scaffolds *in vitro* and *in vivo*, using the critical size defect model. A further objective was to determine the effect of low and high seeding density of BMSCs, cultured with and without osteogenic supplements, on cell proliferation and differentiation and on bone formation. The synergistic effect of seeding density and osteogenic supplements was also studied.

MATERIALS AND METHODS

Preparation of polymer scaffolds

Copolymer poly(LLA-*co*-CL) material was synthesized as previously described.[30] In brief, monomer, initiator, and catalysts were weighed inside a glove box and bulk polymerized at 110°C for 72 h, then precipitated three times in cold hexane and methanol. Porous scaffolds were produced from the copolymer using a solvent-casting-particulate-leaching method. The pore size was >90 μm and the porosity 90%. After leaching of salt particles, the scaffolds were dried and sterilized in an inert atmosphere using electron beam radiation at a dose of 2.5 Mrad from a pulsed electron accelerator (Mikrotron, Acceleratorteknik, Stockholm, Sweden) at 6.5 MeV.

Cell isolation

Bone marrow stromal cells (BMSCs) were isolated from the femurs of two donor Lewis rats and maintained by a modification of a method previously described.[31] The animals were housed under uniform conditions for at least 1 week before the experiment, then euthanized by an overdose of carbon dioxide (CO_2) inhalation. The femurs were retrieved, cleaned, and washed three times for 5 min in phosphate-buffered saline (PBS) supplemented with 3% penicillin–streptomycin (PS). The metaphyseal ends of the femurs were cut off, and the marrow cavity was flushed with minimum essential medium (αMEM, Invitrogen™, Carlsbad, CA) supplemented with 1% PS and 15% fetal bovine serum (FBS) into a sterile falcon tube. The cells were centrifuged and resuspended in fresh α-MEM medium containing 15% FBS and plated in culture flasks (NUNC A/S, Roskilde, Denmark). The medium was changed the next day, with fresh αMEM medium containing 1% PS and 10% FBS. Cells were cultured in αMEM 1% AB and 10% FBS until they reached 80% confluence, after which they were passaged. Passages 3–5 were used for the *in vitro* studies and passages 3 and 4 for the *in vivo* studies. Half of the cells were cultured in αMEM only, supplemented with 1% PS and 10% FBS. For the other half, the culture medium was supplemented with osteogenic factors [100 n*M* dexamethasone (dex), 10 mMb glycerophosphate, and 0.05 m*M* ascorbic acid][11,32] 7 days before the experiments.

The study was approved by the Norwegian Animal Research Authority and conducted according to the European Convention for the Protection of Vertebrates Used for Scientific Purposes (local approval number 20124903).

Scanning electron microscopy

The poly(LLA-*co*-CL) scaffolds with BMSCs seeded at different densities were examined under scanning electron microscopy (SEM) to determine cell adhesion and spreading. After 7 and 21 days of culture, samples were prepared for SEM as follows; first, the medium was replaced with 2.5% glutaraldehyde in α-MEM without serum and fixed for 30 min at room temperature. Second, samples were fixed in 2.5% glutaraldehyde in 0.1*M* sodium cacodylate pH 7.2 with 0.1*M* sucrose for 30 min at room temperature. The samples were then treated with 1% osmium tetroxide in distilled water for 1 h, followed by dehydration through a graded series of ethanol solutions (70, 80, 95, and 100%), critical-point-dried (using CO_2 as transitional fluid and the specimens mounted on aluminum holders), and sputter-coated with a 10 nm conducting layer of gold platinum. Finally, the samples were examined by SEM (Jeol JSM 7400F, Tokyo, Japan) using a voltage of 10 kV.

DNA quantification of cell proliferation

DNA quantification was carried out as described previously, with some modifications,[33] using reagents from the MasterPure™ Complete DNA and RNA Purification Kit (Epicentre® Biotechnologies, Madison, WI). The amount and purity of DNA per scaffold ($n = 4$ scaffolds for each group and time point) were measured by optical densitometry at 260 and 280 nm, using a Nanodrop ND 1000 spectrophotometer (NanoDrop Technologies, Wilmington, DE).

Real-time reverse transcription-polymerase chain reaction analysis

RNA isolation and RT-PCR were performed as described previously.[32] Briefly, total RNA was collected from cells grown onto the scaffolds ($n = 4$ scaffolds for each group and time point) using an isolation kit (E.Z.N.A^{VR}, Omega Bio-Tek, Norcross, GA) according to the manufacturer's protocol. RNA purity and quantification were determined by spectrophotometry (NanoDrop Spectrophotometer, NanoDrop Technologies). Real-time reverse transcription-polymerase (RT-PCR) was conducted under standard enzyme and cycling conditions on a StepOne^{TM} real-time PCR system, using TaqMan^{VR} gene expression assays (Applied Biosystems^{TM}, Carlsbad, CA): runt-related transcription factor 2 (Runx2), collagen type I (Col I), alkaline phosphatase (ALP), bone morphogenetic protein 2 (BMP2), bone sialoprotein (BSP), osteocalcin (OC), and glyceraldehyde-3-phosphate dehydrogenase (GAPDH). The data were analyzed using a comparative Ct method by StepOne. Expression levels of the genes were normalized to the Housekeeper index with GAPDH serving as the endogenous control.

Graft preparation

Poly (LLA-*co*-CL) scaffolds were placed at the bottom of wells in 96-well plates, prewet with the culture media, and incubated at 37°C and 5% CO_2 overnight. The following morning, BMSCs were trypsinized from the culture flasks and seeded on the top of each scaffold, at low density (1×10^6 cells/scaffold) or high density (2×10^6 cells/scaffold). An orbital shaker (Eppendorf^{VR}, Hamburg, Germany) was applied to facilitate the distribution of the cells from the surface of the scaffold into the pores.[6] The cell/scaffold grafts were incubated for 3 h for cell attachment and then transferred either to rat calvarial bone defects ($n = 12$ rats) for 8 weeks or to four separate spinner flasks (Wheaton Science, Millville, NJ).[32] The spinner flasks were placed on a magnetic stirrer (Stem Stirrer, UK) and the side arm caps kept loose. The grafts were separated by spacers made of silicone tubes and cultured in a CO_2 incubator for 3 weeks.

Surgical procedure and implantation

Twelve male Lewis rats (2.5 months old, weight: 300–350 g) were kept in the animal facility for 1 week to acclimatize to diet, water, and housing, under a 12 h/12 h light/dark cycle. The rats were anesthetized with isofluorane (Isoba vet^{VR}, Schering Plough, Kenilworth, NJ) in combination with NO_2 and O_2, using a custom-made mask. The surgical site was shaved and scrubbed with 70% alcohol. Using sterile instruments and an aseptic technique, a 2-cm anteroposterior cranial skin incision was made along the midline. The subcutaneous tissue, musculature, and periosteum were dissected and reflected to expose the calvaria. A full-thickness defect (5 mm in diameter) was created in the central area of each parietal bone, using a saline-cooled trephine drill to prevent overheating of the bone margins and to remove the bone debris. The dura mater was left undisturbed. Twenty-four defects were implanted with disc-shaped scaffolds of poly(LLA-*co*-CL), 5 mm in diameter × 1.5 mm height, seeded with high or low cell density using two cell culture environment: in medium with or without osteogenic supplements. Accordingly, the scaffolds were classified into four different groups:

i. Six defects implanted with scaffolds seeded with cells in low density without osteogenic supplements (LD-OM).
ii. Six defects implanted with scaffolds seeded with cells in high density without osteogenic supplements (HD-OM).
iii. Six defects implanted with scaffolds seeded with cells in low density with osteogenic supplements (LD + OM).
iv. Six defects implanted with scaffolds seeded with cells in high density with osteogenic supplements (HD + OM).

The periosteum and skin were repositioned and stabilized with sutures (Vicryl Plus 4-0). Topical antibiotic Bacimycine (Bacitracin ointment) was applied to the wound to prevent postoperative infection. All animals were given an intramuscular dose of Buprenorphine (Temgesic® 0.3 mg\kg) as an analgesic and allowed to recover. The status of the surgical wound, food intake, activity, and signs of infection were monitored daily. After 8 weeks, the animals were sacrificed by inhalation of CO_2 and the calvarial defects with surrounding bone and soft tissue were harvested for subsequent evaluation.

X-ray micro-computed tomography

For quantitative evaluation of new bone formation in the rat calvarial defects at 8 weeks, micro-computed tomography (μCT) scans were taken using the SkyScan1172^{VR} microfocus X-ray system (SkyScan^{VR}, Kontich, Belgium) with the CTAn 1.8^{VR} and NRECON RECONSTRUCTION^{VR} CT software (SkyScan^{VR}), as previously described.[34] A 0.5-mm aluminum filter was used to optimize the images. Source voltage and current were set at 50 kV and 200 μA, respectively. After operating CTAn 1.8^{VR} to each reconstructed BMP files, bone volume (BV), tissue volume (TV), and bone volume/tissue volume (BV/TV) values were obtained.

Histology

Specimens for histological examination were fixed with 4% paraformaldehyde (Merck, White House Station, NJ) and decalcified for 4 weeks, using 10% ethylenediaminetetraacetic acid (EDTA) in 0.1*M* Tris buffer and 7.5% polyvinylpyrrolidone (PVP) (Merck). The specimens were then washed in PBS, embedded in paraffin, and serially sectioned using a microtome (HM 325, Thermo Scientific). The sections, 4–6 μm thick, were mounted on glass slides, deparaffinized, hydrated by the application of xylene and alcohol in series, and stained with Masson's Trichrome (MT).

Statistical analysis

Sixteen scaffolds were available for the statistical analyses. From each scaffold four measures were taken: two at day 7 and 2 at day 21. Twelve rats were included in the *in vivo* analysis. To provide more accurate data of the hierarchical structure of the outcome variables a multilevel modeling analysis was applied. For the PCR statistical analyses,

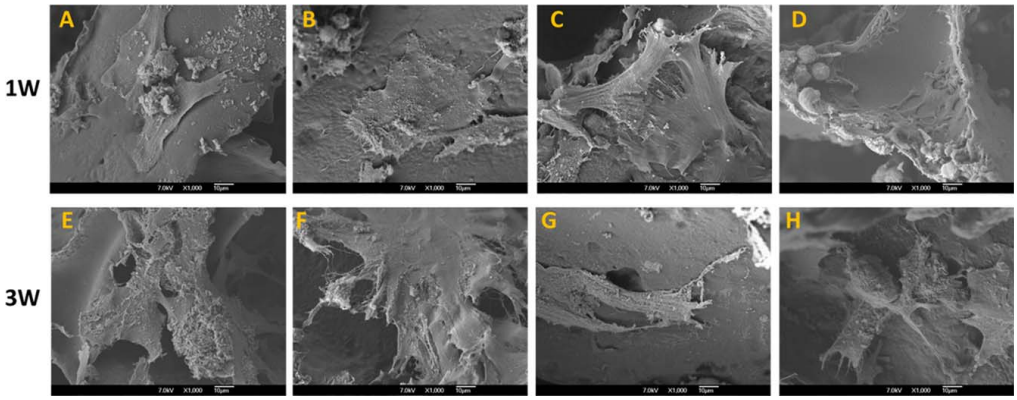

FIGURE 1. SEM images of scaffolds 1 week (1W) (A–D) and 3 weeks (3W) (E–H) after seeding with cultured BMSCs. A and E: Low cell seeding density with cells preincubated with osteogenic medium. B and F: High cell seeding density with cells preincubated with osteogenic medium. C and G: Low cell seeding density with cells preincubated without osteogenic medium. D and H: High cell seeding density with cells preincubated without osteogenic medium. Although seeded at different densities and preincubated with and without osteogenic medium, all cells appear to be flattened and well spread on the scaffolds. [Color figure can be viewed in the online issue, which is available at wileyonlinelibrary.com.]

reference values were first calculated for the low seeding densities without osteogenic medium, for day 7 and day 21, respectively. This was done for all the expression measures. A random effect model with each particular gene as the random factor (to control for the two repeated measures for each gene) was applied. The reference value was defined as the predicted mean from these models. ΔCt values for each gene were thereafter calculated as the difference between the gene measures and the reference values. The ΔΔCt values for all the expressions were then analyzed in linear models using robust variance estimates to control for the repeated measures for each particular gene. Mean values, standard deviations, and 95% confidence intervals were estimated from these models. For low seeding densities without osteogenic medium the mean values are by definition "0." For DNA and the μCT the measured values were used directly in the analyses.

The effects were tested hierarchically. First the main effects of seeding density, osteogenic medium, and days were tested. Thereafter, a model including the first-order interaction was performed (densities*medium, medium*days, density*days), and then a model including the second-order interaction (densities*medium*days). The μCT observations were measured at only one time point. This analytic approach will correspond to performing repeated measures analyses of variance. The statistical package StataIC version 13 was used to analyze the data. The *p*-values less than 0.05 were considered statistically significant.

RESULTS

SEM analysis

Scaffolds with low and high cell seeding densities preincubated in different media demonstrated good cellular attachment at day 7 and day 21. The cells appeared to be flattened and well spread, covering the surface of the scaffolds and migrating into the inner pores of the scaffolds (Fig. 1).

Cell proliferation

Osteogenic medium and incubation time showed a significant overall positive effect on the quantity of DNA ($p = 0.001$), whereas cell seeding density showed no overall effect ($p = 0.32$). There was a significant relationship between osteogenic medium and incubation time ($p = 0.001$). The pairwise comparison at day 7 showed a significant stimulating effect of high cell seeding density with osteogenic medium on the amount of DNA compared with low cell seeding density with osteogenic medium ($p = 0.039$). Similarly, high cell seeding density with osteogenic medium significantly stimulated the amount of DNA compared with high cell seeding density without osteogenic medium ($p < 0.001$). For the pairwise comparison at day 21, significantly higher amounts of DNA were detected for high cell seeding density with osteogenic medium than for high cell seeding density without osteogenic medium ($p < 0.001$) (Fig. 2).

RT-PCR

Runx2 expression exhibited significant overall upregulation in relation to high cell seeding density ($p = 0.001$) and significant overall downregulation in relation to osteogenic medium ($p = 0.005$). There were significant interactions between high cell seeding density and incubation time ($p = 0.042$) and between high cell seeding density and osteogenic medium ($p = 0.046$). The pairwise comparison at day 7 revealed a significantly higher expression of Runx2 for scaffolds with high cell seeding density with osteogenic medium compared with low cell seeding density with osteogenic medium ($p = 0.042$). By day 21, Runx2 expression had increased significantly for high cell seeding density without

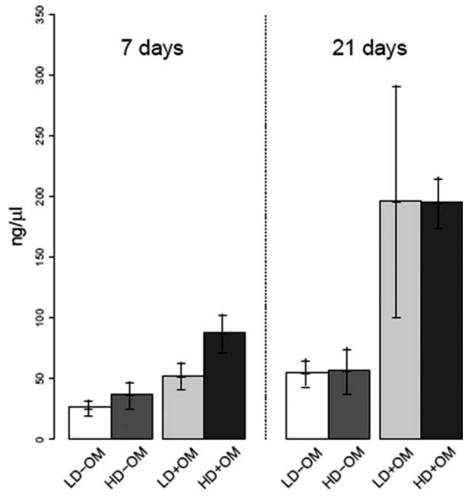

FIGURE 2. Total DNA quantification of cultured cell/scaffold constructs ($n = 4$ for each group and time point). The data are presented as means ± 95% confidence intervals. The results indicate continued proliferation of BMSCs for up to 3 weeks ($p = 0.001$) and a positive effect of osteogenic supplements on cell proliferation ($p < 0.001$).

osteogenic medium compared with low cell seeding density without osteogenic medium ($p = 0.032$). Moreover, from day 7 to day 21, Runx2 expression was significantly upregulated in scaffolds with high cell seeding density without osteogenic medium ($p = 0.029$) [Fig. 3(A)].

Col1 expression disclosed a significant overall upregulation effect of high cell seeding density ($p = 0.009$). There were also significant interactions between high cell density and incubation time ($p = 0.009$) and osteogenic medium and incubation time ($p = 0.019$). Pairwise comparison at day 21 showed significantly higher expression of Col1 for scaffolds with high cell seeding density without osteogenic medium than for low cell seeding density without osteogenic medium ($p = 0.011$) [Fig. 3(B)].

ALP expression was not overall significantly affected by high cell seeding density ($p = 0.38$) or osteogenic medium ($p = 0.69$). Significant relationships were disclosed between osteogenic medium and incubation time ($p < 0.001$) and among high cell seeding density, osteogenic medium, and incubation time ($p = 0.026$). The pairwise comparison at day 7 showed significant upregulation of ALP associated with high cell seeding density with osteogenic medium compared with low cell seeding density with osteogenic medium ($p = 0.020$). Similarly, high cell seeding density with osteogenic medium showed significant upregulation of ALP

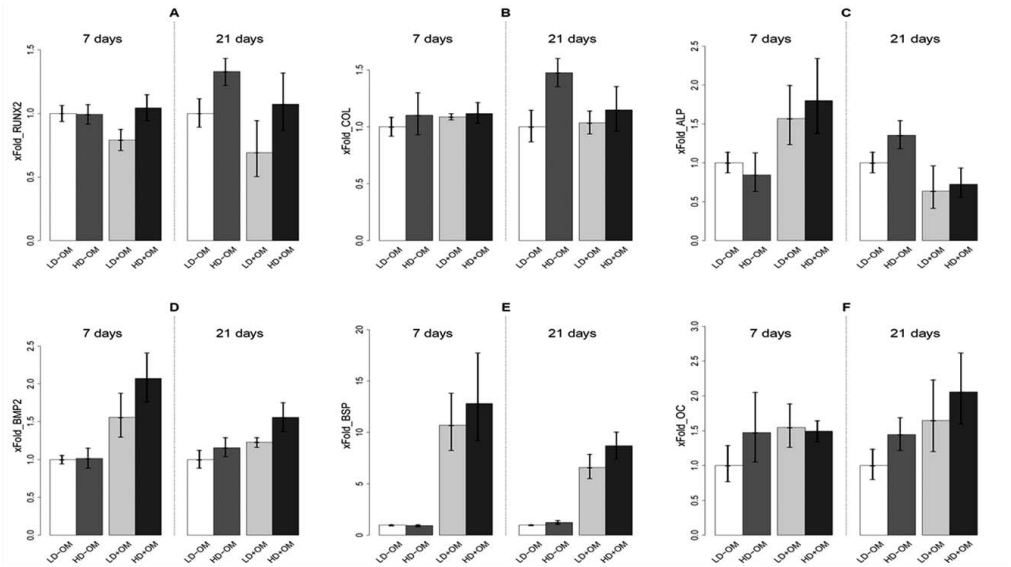

FIGURE 3. mRNA expression of (A) Runx2, (B) Col 1, (C) ALP, (D) BMP2, (E) BSP, and (F) OC by qRT-PCR, presented as *x*-fold changes relative to the expression of the mean of the calibrator sample LD-OM. A: Runx2 expression is downregulated by osteogenic medium ($p = 0.005$) and upregulated by high cell seeding density ($p = 0.001$). B: Col1 expression is upregulated by high cell seeding density ($p = 0.001$). C: ALP expression, disclosing a significant relationship between high cell density, osteogenic medium, and number of days ($p = 0.026$). D: BMP2 expression is upregulated by osteogenic medium ($p < 0.001$) and high cell seeding density ($p = 0.003$). E: BSP expression is upregulated by osteogenic medium ($p < 0.001$) and high cell seeding density ($p = 0.033$). F: OC expression is upregulated by osteogenic medium ($p = 0.002$) and high cell seeding density ($p = 0.013$). The data are presented as means ± 95% confidence intervals.

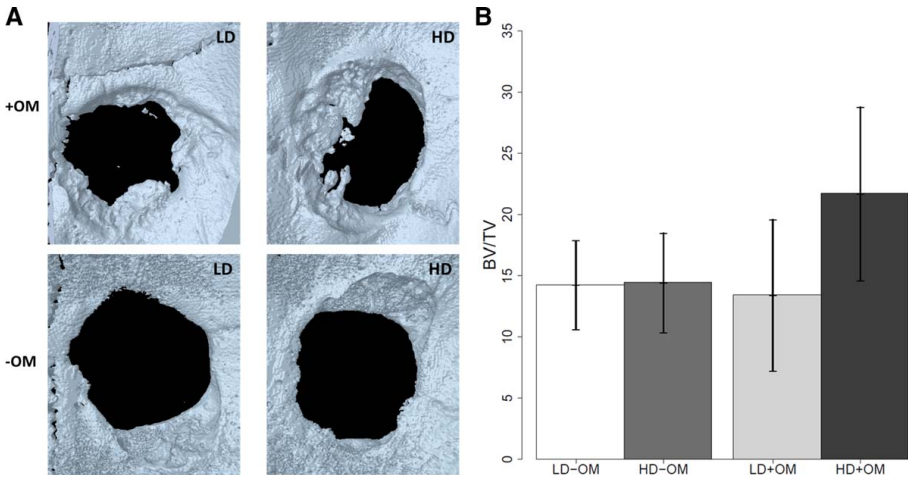

FIGURE 4. Bone formation in critical-size rat calvarial defects. A: Three-dimensionally reconstructed high-resolution μCT image of defects implanted with cells/scaffolds after 8 weeks of healing. Note the new bone formed in the four groups; with osteogenic medium (+OM) or without osteogenic medium (−OM) with different densities of cell seeding (low density (LD) or high density (HD)). B: Quantification of percentage of area and volume of bone regeneration in calvarial defects after 8 weeks of healing. Implantation of scaffolds containing cells seeded at high density and cultured with osteogenic medium exhibit a significant percentage of bone volume ($p = 0.038$). [Color figure can be viewed in the online issue, which is available at wileyonlinelibrary.com.]

compared with high cell seeding density without osteogenic medium ($p = 0.05$). By day 21, ALP levels from scaffolds with high cell seeding density without osteogenic medium showed significant upregulation compared with scaffolds with high cell seeding density and osteogenic medium ($p = 0.021$) [Fig. 3(C)].

BMP-2 expression was significantly overall upregulated in scaffolds with high cell seeding density ($p = 0.003$) and osteogenic medium ($p < 0.001$). Significant relationships were disclosed between high cell seeding density and osteogenic medium ($p = 0.047$) and between osteogenic medium and incubation time ($p = 0.001$). The pairwise comparison at day 7 showed significant upregulation of BMP-2 in low cell seeding density with osteogenic medium compared with low cell seeding density without osteogenic medium ($p = 0.013$). In addition, expression of BMP-2 in high cell seeding density with osteogenic medium was significantly upregulated compared with high cell seeding density without osteogenic medium ($p < 0.001$) [Fig. 3(D)].

BSP expression showed significant overall upregulation in scaffolds with high cell seeding density ($p = 0.033$) and osteogenic medium ($p < 0.001$). In addition, the interaction between osteogenic medium and incubation time was significant ($p < 0.001$). Pairwise comparison at day 7 and day 21 showed significant upregulation of BSP in low cell seeding density with osteogenic medium compared with low cell seeding density without osteogenic medium ($p < 0.001$) and significant upregulation of BSP in high cell seeding density with osteogenic medium compared with high cell seeding density without osteogenic medium ($p < 0.001$) [Fig. 3(E)].

OC expression exhibited a significant overall upregulation effect of high cell seeding density ($p = 0.013$) and osteogenic medium ($p = 0.002$) [Fig. 3(F)].

μCT

Bone formation in the calvarial defects was evaluated at 8 weeks. In defects implanted with constructs seeded with cells cultured at low density in nonosteogenic medium, healing was 14.27% (95% CI: 10.66, 17.88); the corresponding rate for cells cultured at high density in nonosteogenic medium was 14.46% (95% CI: 10.40, 18.51) ($p = 0.99$). Healing of defects treated with cells preincubated in osteogenic medium was 13.43% (95% CI: 7.26, 19.61) for cells cultured at low density and 21.71% (95% CI: 14.63, 28.79) for those cultured at high density ($p = 0.023$). There was a significant interaction effect between high cell density and osteogenic medium ($p = 0.038$) (Fig. 4).

Histology

Various levels of osteoid-like tissue formation are illustrated in Figure 5. Compared with the other groups, more bone-like tissue formed in the group implanted with constructs containing cells cultured in osteogenic medium at high cell seeding density.

DISCUSSION

The objectives of this study were to determine the initial biological responses, the osteogenic potential, and the induction of new bone in response to implanted poly(LLA-*co*-CL) scaffolds seeded with two different densities of

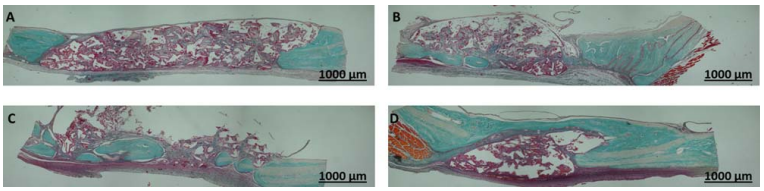

FIGURE 5. Representative sections of Masson's trichrome staining through calvarial defects at 8 weeks (×10). A: Section of a defect implanted with a scaffold containing cells cultured without osteogenic medium and seeded at low density, showing fibrous connective tissue and collagen. B: Defect implanted with a scaffold containing cells cultured without osteogenic medium and seeded at high density, showing osteoid-like tissue (green areas). C: Defect implanted with a scaffold containing cells cultured with osteogenic medium and seeded at low density, showing osteoid-like tissue. D: Defect implanted with a scaffold containing cells cultured with osteogenic medium and seeded at high density, showing formation of a bridge of bone-like tissue. Scale bar = 1000 μm. [Color figure can be viewed in the online issue, which is available at wileyonlinelibrary.com.]

BMSCs. The effects of cell seeding density and pretreatment of BMSCs with osteogenic supplements on cell proliferation, differentiation, and bone formation were also assessed. Moreover, a potential synergistic effect of these factors was evaluated.

In the *in vitro* experiments, the cells were cultured under dynamic cell culture conditions, using spinner-modified flasks. Previous studies show that the shear stress induced by spinner flasks regulates cellular physiological activity through stimulation of mechano-transduction pathways and promotes *in vitro* cell proliferation and differentiation.[33,35,36] Further, the critical size cranial defect model is well established for evaluating orthotopic implantation. However, calvarial bone has a relatively poor blood supply and relative lack of bone marrow, that is, conditions less than ideal for bone formation.[37]

Interactions of BMSCs with their microenvironment play an important role in their morphogenesis and differentiation. An important component of the cell microenvironment is the surrounding matrix, which includes several biophysical and chemical signals. These signals are recognized, integrated, and processed by the cells to determine the behavior and function of the engineered tissues. It has been shown that fibronectin, the extracellular protein present in serum and plasma, is a major mediator of BMSC adhesion to polymeric scaffolds.[38] Thus, by controlling physical and chemical characteristics of poly(LLA-*co*-CL) scaffolds, such as solubility, degradation behavior, chemical composition, crystallinity, and hydrophilicity, it is possible to regulate cell survival, migration, proliferation, and differentiation during the regeneration process.[2,4,30,39]

The number of cells capable of attaching to scaffolds depends on the porosity, mean pore size, and surface area. The porosity of poly(LLA-*co*-CL) scaffolds used in the current experiments is about 85%, providing a large surface area for cellular attachment and proliferation, conducive to uniform cell distribution.[40–42] In a previous study, co-culturing BMSCs with endothelial cells at a density of 5×10^5 cells/scaffold resulted in low bone induction.[32] Hence, the number of cells was increased in this work. We hypothesized that a large scaffold surface area containing more attached cells would further stimulate bone formation.

Cell signaling can result either from direct cell−cell communication or from secreted signaling molecules. With high cell density, cell–cell communication and paracrine signaling increase. Direct cell–cell communication via gap junctions [i.e., gap junction intercellular communication (GJIC)] is an important element promoting growth and differentiation in various tissues.[43] GJIC is mediated by connexins. In particular, connexin 43 (Cx43) plays an important role in regulating signal transmission among different bone cells. Increased cell proliferation has been observed as a result of connexin 43 stimulation.[44] In this study, the *in vitro* data generated at day 7 showed that high density seeding of the copolymer scaffolds led to increased cell proliferation. This stimulation is probably caused by GJIC activity. At day 21, however, there was no correlation between cell proliferation and cell seeding density, suggesting that maturation level had been reached. A logarithmic relationship has been demonstrated before between cell density and bone formation.[13] The optimal cell density above which bone in-growth did not change was identified, that is, increasing the cell numbers above this level did not stimulate more bone formation. This indicates that the direct cell–cell communication through optimal cell seeding density and soluble osteogenic factors might act as synergistic modulators in promoting bone formation.

In animal studies, mesenchymal stem cells (MSCs) have been reported to induce osteogenesis and have been used extensively for regeneration of bone defects.[29,45,46] The optimal protocol for expanding MSCs in medium containing osteogenic supplements may depend on the tissues from which the MSCs were isolated; cells of different origin may have inherited different degrees of osteogenicity.[29,47,48] Osteoprogenitor cells can differentiate in the presence or absence of osteogenic supplements.[49] At least two classes of osteoblast progenitor cells could be defined: those differentiating in the absence of osteogenic supplements and those requiring the supplements to differentiate. In the absence, few cells differentiate and these are only detectable after cell numbers are increased.[49] This hypothesis is supported by the *in vitro* data of the present work which demonstrate that after 21 days in the absence of osteogenic supplements, an increase in cell density upregulates the expression of

osteogenic markers Runx 2, COL1, and ALP. Accordingly, the osteogenic differentiation of BMSCs might depend on the cell density, culture condition, and time. However, when MSCs are fully differentiated, their pluripotency and immunosuppressibility may also decrease and this may impair osteogenicity and bone formation.[50]

Osteogenic differentiation of BMSCs proceeds in three stages: early or commitment to osteogenic differentiation, matrix synthesis, and then the final stage, mineralization.[51] In the osteoblastic differentiation model, cells proliferate rapidly from 7 to 14 days and then start to secrete ECM proteins and produce early differentiation markers such as ALP, which is produced from day 7.[52] Thereafter, as the cells mature, proliferation decreases over time. In *in vitro* data of this study, continued proliferation of BMSCs indicates that the cells were still at the early maturation stage when the experiments were conducted. mRNA expression of ALP was first upregulated at day 7 and then downregulated at day 21. ALP expression is controlled by BMP2 through the Wnt/LRP5 signaling cascade.[53] BMP2 is known to participate in the regulation of cell growth and differentiation, along with the induction of osteogenic progenitor cells in bone defect sites during the healing process. In the group with high cell seeding density and osteogenic supplements, there was a general decline of BMP2 expression at day 21, suggesting that the BMSCs had entered a maturation stage of differentiation.

In this work, cells cultured at high density with osteogenic supplements demonstrated an increase and upregulation of osteocalcin mRNA expression during the experimental period. Osteocalcin is a late, specific marker of osteoblast maturation.[54] This is in agreement with a previous report showing that an increase in cell numbers in the presence of osteogenic supplements upregulated osteocalcin expression and maturation of osteoblasts.[12] A correlation may exist between increased extracellular protein secretion and an increased number of mature osteoblasts, leading to promotion of bone formation. Our *in vivo* data confirmed his observation demonstrating more bone formation in response to an increase in the number of expanded and differentiated cells. Accordingly, the present results indicate that the number of mature osteoblast determined the rate of bone formation.

The *in vivo* findings demonstrate synergistic stimulation of cell seeding density and osteogenic supplements on bone formation. Dex is a synthetic glucocorticoid reported to be an essential requirement for osteoprogenitor cell differentiation of MSCs *in vitro*. The mechanism of action of dex on BMSCs can be through induced transcription of BSP by binding on a glucocorticoid response element in the promoter region of the BSP gene, which is associated with osteoblast differentiation.[55] This was verified *in vitro* by BSP mRNA expression. BSP is an indicator of cellular maturation. On the other hand, osteogenic differentiation of BMSCs was clearly influenced by the initial seeding densities via cell–cell communication. Thus, both factors may accelerate osteoblastic differentiation, leading primarily to more mature osteoblasts and secondarily to more bone formation.

Although the *in vivo* data clearly confirm new bone formation, the μCT images and histology at 8 weeks did not show complete healing and bone regeneration. In bone TE, the transplanted scaffold should act as a temporary ECM substitute, stimulating cell attachment, proliferation, and differentiation, with subsequent bone in-growth until finally being completely degraded and replaced by regenerated bone. Scaffold degradation should be adjusted appropriately to the rate of neobone formation,[56] thus allowing the mechanical load on the scaffold to be transferred gradually to the regenerated tissue. Finally, when total tissue regeneration has been achieved, the scaffold should be completely degraded.

A previous *in vivo* study using similar scaffolds showed slow, gradual degradation of the poly(LLA-*co*-Cl) scaffolds within 91 days of the experimental period.[4] The delayed degradation of the scaffolds might suggest a longer healing process in this experimental model.

CONCLUSIONS

The induction of new bone in a critical size defect indicates that poly(LLA-*co*-CL) scaffolds are appropriate candidates for constructs in bone TE. Bone regeneration might depend on cell–cell communication, which is an important element promoting growth and differentiation in various tissues. The appropriate number of cells to be loaded onto a specific scaffold is a critical, vital factor for promoting ECM synthesis and bone formation. This study demonstrates that increasing cell numbers seeded onto poly(LLA-*co*-Cl) scaffolds promote BMSCs differentiation and bone formation. Osteogenic supplements are key determinants of the ability of MSCs to induce new bone tissue formation. Thus, the synergistic effect of cell density and osteogenic supplements appears to be of major importance in bone formation.

ACKNOWLEDGMENT

The authors thank Dr. Joan Bevenius for language revision of the manuscript.

REFERENCES

1. Fernández J, Etxeberria A, Sarasua J-R. Synthesis, structure and properties of poly(L-lactide-co-caprolactone) statistical copolymers. J Mech Behav Biomed Mater 2012;9:100–112.
2. Idris SB, Arvidson K, Plikk P, Ibrahim S, Finne-Wistrand A, Albertsson AC, Bolstad AI, Mustafa K. Polyester copolymer scaffolds enhance expression of bone markers in osteoblast-like cells. J Biomed Mater Res A 2010;94:631–639.
3. Xue Y, Danmark S, Xing Z, Arvidson K, Albertsson AC, Hellem S, Finne-Wistrand A, Mustafa K. Growth and differentiation of bone marrow stromal cells on biodegradable polymer scaffolds: An in vitro study. J Biomed Mater Res A 2010;95:1244–1251.
4. Danmark S, Finne-Wistrand A, Schander K, Hakkarainen M, Arvidson K, Mustafa K, Albertsson AC. In vitro and in vivo degradation profile of aliphatic polyesters subjected to electron beam sterilization. Acta Biomater 2011;7:2035–2046.
5. Pedersen TO, Xing Z, Finne-Wistrand A, Hellem S, Mustafa K. Hyperbaric oxygen stimulates vascularization and bone formation in rat calvarial defects. Int J Oral Maxillofac Surg 2013;42:907–914.
6. Xing Z, Xue Y, Danmark S, Finne-Wistrand A, Arvidson K, Hellem S, Yang ZQ, Mustafa K. Comparison of short-run cell seeding methods for poly(L-lactide-co-1,5-dioxepan-2-one) scaffold intended for bone tissue engineering. Int J Artif Org 2011;34:432–441.
7. Chen Y, Bloemen V, Impens S, Moesen M, Luyten FP, Schrooten J. Characterization and optimization of cell seeding in scaffolds

by factorial design: Quality by design approach for skeletal tissue engineering. Tissue Eng Part C Methods 2011;17:1211–1221.
8. Dar A, Shachar M, Leor J, Cohen S. Optimization of cardiac cell seeding and distribution in 3D porous alginate scaffolds. Biotechnol Bioeng 2002;80:305–312.
9. Hansen O, Foldager C, Christensen B, Everland H, Lind M. Increased chondrocyte seeding density has no positive effect on cartilage repair in an MPEG-PLGA scaffold. Knee Surg Sports Traumatol Arthrosc 2013;21:485–493.
10. Grayson WL, Bhumiratana S, Cannizzaro C, Chao PH, Lennon DP, Caplan AI, Vunjak-Novakovic G. Effects of initial seeding density and fluid perfusion rate on formation of tissue-engineered bone. Tissue Eng Part A 2008;14:1809–1820.
11. Zhou H, Weir MD, Xu HH. Effect of cell seeding density on proliferation and osteodifferentiation of umbilical cord stem cells on calcium phosphate cement-fiber scaffold. Tissue Eng Part A 2011; 17(21–22):2603–2613.
12. Kim K, Dean D, Mikos AG, Fisher JP. Effect of initial cell seeding density on early osteogenic signal expression of rat bone marrow stromal cells cultured on cross-linked poly(propylene fumarate) disks. Biomacromolecules 2009;10:1810–1817.
13. Kruyt M, De Bruijn J, Rouwkema J, Van Bliterswijk C, Oner C, Verbout A, Dhert W. Analysis of the dynamics of bone formation, effect of cell seeding density, and potential of allogeneic cells in cell-based bone tissue engineering in goats. Tissue Eng Part A 2008;14:1081–1088.
14. Bitar M, Brown RA, Salih V, Kidane AG, Knowles JC, Nazhat SN. Effect of cell density on osteoblastic differentiation and matrix degradation of biomimetic dense collagen scaffolds. Biomacromolecules 2008;9:129–135.
15. Goldstein AS. Effect of seeding osteoprogenitor cells as dense clusters on cell growth and differentiation. Tissue Eng 2001;7: 817–827.
16. Almarza AJ, Athanasiou KA. Effects of initial cell seeding density for the tissue engineering of the temporomandibular joint disc. Ann Biomed Eng 2005;33:943–950.
17. Ishaug SL, Crane GM, Miller MJ, Yasko AW, Yaszemski MJ, Mikos AG. Bone formation by three-dimensional stromal osteoblast culture in biodegradable polymer scaffolds. J Biomed Mater Res 1997;36:17–28.
18. Vehof JW, de Ruijter AE, Spauwen PH, Jansen JA. Influence of rhBMP-2 on rat bone marrow stromal cells cultured on titanium fiber mesh. Tissue Eng 2001;7:373–383.
19. Zhou YF, Sae-Lim V, Chou AM, Hutmacher DW, Lim TM. Does seeding density affect in vitro mineral nodules formation in novel composite scaffolds? J Biomed Mater Res A 2006;78:183–193.
20. Rathbone CR, Guda T, Singleton BM, Oh DS, Appleford MR, Ong JL, Wenke JC. Effect of cell-seeded hydroxyapatite scaffolds on rabbit radius bone regeneration. J Biomed Mater Res A 2014;102: 1458–1466.
21. Holy CE, Shoichet MS, Davies JE. Engineering three-dimensional bone tissue in vitro using biodegradable scaffolds: Investigating initial cell-seeding density and culture period. J Biomed Mater Res 2000;51:376–382.
22. van Gaalen SM, de Bruijn JD, Wilson CE, van Blitterswijk CA, Verbout AJ, Alblas J, Dhert WJ. Relating cell proliferation to in vivo bone formation in porous ca/P scaffolds. J Biomed Mater Res A 2010;92:303–310.
23. Pittenger MF, Mackay AM, Beck SC, Jaiswal RK, Douglas R, Mosca JD, Moorman MA, Simonetti DW, Craig S, Marshak DR. Multilineage potential of adult human mesenchymal stem cells. Science 1999;284:143–147.
24. Zuk PA, Zhu M, Mizuno H, Huang J, Futrell JW, Katz AJ, Benhaim P, Lorenz HP, Hedrick MH. Multilineage cells from human adipose tissue: Implications for cell-based therapies. Tissue Eng 2001;7: 211–228.
25. Majumdar MK, Thiede MA, Mosca JD, Moorman M, Gerson SL. Phenotypic and functional comparison of cultures of marrow-derived mesenchymal stem cells (MSCs) and stromal cells. J Cell Physiol 1998;176:57–66.
26. Ohgushi H, Dohi Y, Katuda T, Tamai S, Tabata S, Suwa Y. In vitro bone formation by rat marrow cell culture. J Biomed Mater Res 1996;32:333–340.
27. Coelho MJ, Fernandes MH. Human bone cell cultures in biocompatibility testing. Part II: Effect of ascorbic acid, β-glycerophosphate and dexamethasone on osteoblastic differentiation. Biomaterials 2000;21:1095–1102.
28. Castano-Izquierdo H, Álvarez-Barreto J, van den Dolder J, Jansen JA, Mikos AG, Sikavitsas VI. Pre-culture period of mesenchymal stem cells in osteogenic media influences their in vivo bone forming potential. J Biomed Mater Res Part A 2007;82:129–138.
29. Jo C, Yoon P, Kim H, Kang K, Yoon K. Comparative evaluation of in vivo osteogenic differentiation of fetal and adult mesenchymal stem cell in rat critical-sized femoral defect model. Cell Tissue Res 2013;353:1–12.
30. Dånmark S, Finne-Wistrand A, Wendel M, Arvidson K, Albertsson A-C, Mustafa K. Osteogenic differentiation by rat bone marrow stromal cells on customized biodegradable polymer scaffolds. J Bioactive Compatible Polym 2010;25:207–223.
31. Maniatopoulos C, Sodek J, Melcher AH. Bone formation in vitro by stromal cells obtained from bone marrow of young adult rats. Cell Tissue Res 1988;254:317–330.
32. Xing Z, Xue Y, Dånmark S, Schander K, Østvold S, Arvidson K, Hellem S, Finne-Wistrand A, Albertsson A–C, Mustafa K. Effect of endothelial cells on bone regeneration using poly(L-lactide-co-1,5-dioxepan-2-one) scaffolds. J Biomed Mater Res A 2011;96: 349–357.
33. Stiehler M, Bünger C, Baatrup A, Lind M, Kassem M, Mygind T. Effect of dynamic 3-D culture on proliferation, distribution, and osteogenic differentiation of human mesenchymal stem cells. J Biomed Mater Res A 2009;89:96–107.
34. Kim J, Kim IS, Cho TH, Kim HC, Yoon SJ, Choi J, Park Y, Sun K, Hwang SJ. In vivo evaluation of MMP sensitive high-molecular weight HA-based hydrogels for bone tissue engineering. J Biomed Mater Res A 2010;95:673–681.
35. Wang Y, Tang L, Wang J, Cai S. [The mechanotransduction mechanism of how osteoblasts respond to mechanical stimulation]. Sheng Wu Yi Xue Gong Cheng Xue Za Zhi 2005;22: 400–402.
36. Meinel L, Karageorgiou V, Fajardo R, Snyder B, Shinde-Patil V, Zichner L, Kaplan D, Langer R, Vunjak-Novakovic G. Bone tissue engineering using human mesenchymal stem cells: Effects of scaffold material and medium flow. Ann Biomed Eng 2004;32: 112–122.
37. Viateau V, Guillemin G, Quarto R, Petite H. Animal Models for Bone Tissue Engineering Purposes. In: Conn PM, editor. Sourcebook of Models for Biomedical Research: Humana Press; 2008; 725–736.
38. Dånmark S, Finne-Wistrand A, Albertsson A-C, Patarroyo M, Mustafa K. Integrin-mediated adhesion of human mesenchymal stem cells to extracellular matrix proteins adsorbed to polymer surfaces. Biomed Mater 2012;7:035011.
39. Xing Z, Pedersen TO, Wu X, Xue Y, Sun Y, Finne-Wistrand A, Kloss FR, Waag T, Krueger A, Steinmuller-Nethl D and others. Biological effects of functionalizing copolymer scaffolds with nanodiamond particles. Tissue Eng Part A 2013;19:1783–1791.
40. O'Brien FJ, Harley BA, Yannas IV, Gibson LJ. The effect of pore size on cell adhesion in collagen-GAG scaffolds. Biomaterials 2005;26:433–441.
41. Leong KF, Cheah CM, Chua CK. Solid freeform fabrication of three-dimensional scaffolds for engineering replacement tissues and organs. Biomaterials 2003;24:2363–2378.
42. Agrawal CM, Ray RB. Biodegradable polymeric scaffolds for musculoskeletal tissue engineering. J Biomed Mater Res 2001;55: 141–150.
43. Chang J-C, Fujita S, Tonami H, Kato K, Iwata H, Hsu S-h. Cell orientation and regulation of cell–cell communication in human mesenchymal stem cells on different patterns of electrospun fibers. Biomed Mater 2013;8:055002.
44. Gramsch B, Gabriel HD, Wiemann M, Grümmer R, Winterhager E, Bingmann D, Schirrmacher K. Enhancement of connexin 43 expression increases proliferation and differentiation of an osteoblast-like cell line. Exp Cell Res 2001;264:397–407.
45. Levi B, James AW, Nelson ER, Vistnes D, Wu B, Lee M, Gupta A, Longaker MT. Human adipose derived stromal cells heal critical size mouse calvarial defects. PLoS One 2010;5:e11177.

46. Bruder SP, Kurth AA, Shea M, Hayes WC, Jaiswal N, Kadiyala S. Bone regeneration by implantation of purified, culture-expanded human mesenchymal stem cells. J Orthopaed Res 1998;16: 155–162.
47. Peterson B, Zhang J, Iglesias R, Kabo M, Hedrick M, Benhaim P, Lieberman JR. Healing of critically sized femoral defects, using genetically modified mesenchymal stem cells from human adipose tissue. Tissue Eng 2005;11:120–129.
48. Wright V, Peng H, Usas A, Young B, Gearhart B, Cummins J, Huard J. BMP4-expressing muscle-derived stem cells differentiate into osteogenic lineage and improve bone healing in immunocompetent mice. Mol Ther 2002;6:169–178.
49. Aubin JE. Osteoprogenitor cell frequency in rat bone marrow stromal populations: Role for heterotypic cell-cell interactions in osteoblast differentiation. J Cell Biochem 1999;72:396–410.
50. Prigozhina TB, Khitrin S, Elkin G, Eizik O, Morecki S, Slavin S. Mesenchymal stromal cells lose their immunosuppressive potential after allotransplantation. Exp Hematol 2008;36:1370–1376.
51. Beck GR. Inorganic phosphate as a signaling molecule in osteoblast differentiation. J Cell Biochem 2003;90:234–243.
52. Stein GS, Lian JB. Molecular mechanisms mediating proliferation/differentiation interrelationships during progressive development of the osteoblast phenotype. Endocr Rev 1993;14:424–442.
53. Rawadi G, Vayssière B, Dunn F, Baron R, Roman-Roman S. BMP-2 controls alkaline phosphatase expression and osteoblast mineralization by a wnt autocrine loop. J Bone Miner Res 2003;18: 1842–1853.
54. Aubin JE. Bone stem cells. J Cell Biochem Suppl 1998;30-31: 73–82.
55. Ogata Y, Yamauchi M, Kim RH, Li JJ, Freedman LP, Sodek J. Glucocorticoid regulation of bone sialoprotein (BSP) gene expression. Identification of a glucocorticoid response element in the bone sialoprotein gene promoter. Eur J Biochem 1995;230: 183–192.
56. Hutmacher DW. Scaffolds in tissue engineering bone and cartilage. Biomaterials 2000;21:2529–2543.

Paper II

Mohammed Ahmed Yassin, Knut N. Leknes, Yang Sun, Stein Atle Lie, Anna Finne-Wistrand, Kamal Mustafa. **Surfactant tuning of hydrophilicity of porous degradable copolymer scaffolds promotes cellular proliferation and enhances bone formation**. Journal of Biomedical Materials Research Part A 2016;104(8):2049-2059.

II

Society For Biomaterials

Surfactant tuning of hydrophilicity of porous degradable copolymer scaffolds promotes cellular proliferation and enhances bone formation

Mohammed A. Yassin,[1] Knut N. Leknes,[1] Yang Sun,[1,2] Stein A. Lie,[1] Anna Finne-Wistrand,[2] Kamal Mustafa[1]

[1]Department of Clinical Dentistry, Faculty of Medicine and Dentistry, University of Bergen, Bergen, Norway
[2]Department of Fibre and Polymer Technology, Royal Institute of Technology (KTH), Stockholm, Sweden

Received 26 January 2016; revised 9 March 2016; accepted 6 April 2016
Published online 19 April 2016 in Wiley Online Library (wileyonlinelibrary.com). DOI: 10.1002/jbm.a.35741

Abstract: Poly(L-lactide-*co*-ε-caprolactone) (poly(LLA-*co*-CL)) has been blended with Tween 80 to tune the material properties and optimize cell–material interactions. Accordingly, the aims of this study were fourfold: to evaluate the effect of low concentrations of Tween 80 on the surface microstructure of 3D poly(LLA-*co*-CL) porous scaffolds: to determine the effect of different concentrations of Tween 80 on proliferation of bone marrow stromal cells (BMSCs) *in vitro* under dynamic cell culture at 7 and 21 days; to assess the influence of Tween 80 on the degradation rate of poly(LLA-*co*-CL) at 7 and 21 days; and in a subcutaneous rat model, to evaluate the effect on bone formation of porous scaffolds modified with 3% Tween 80 at 2 and 8 weeks. Blending 3% (w/w) Tween 80 with poly(LLA-*co*-CL) improves the surface wettability ($p < 0.001$). Poly(LLA-*co*-CL)/3% Tween 80 shows significantly increased cellular proliferation at days 7 and 21 ($p < 0.001$). Moreover, the presence of Tween 80 facilitates the degradation of poly(LLA-*co*-CL). Two weeks post-implantation, the poly(LLA-*co*-CL)/3% Tween 80 scaffolds exhibit significant mRNA expression of Runx2 ($p = 0.004$). After 8 weeks, poly(LLA-*co*-CL)/3% Tween 80 scaffolds show significantly increased *de novo* bone formation, demonstrated by μ-CT ($p = 0.0133$) and confirmed histologically. It can be concluded that blending 3% (w/w) Tween 80 with poly (LLA-*co*-CL) improves the hydrophilicity and osteogenic potential of the scaffolds. © 2016 Wiley Periodicals, Inc. J Biomed Mater Res Part A: 104A: 2049–2059, 2016.

Key Words: hydrophilicity, copolymer scaffolds, Tween 80, bone formation, BMSCs

How to cite this article: Yassin MA, Leknes KN, Sun Y, Lie SA, Finne-Wistrand A, Mustafa K. 2016. Surfactant tuning of hydrophilicity of porous degradable copolymer scaffolds promotes cellular proliferation and enhances bone formation. J Biomed Mater Res Part A 2016:104A:2049–2059.

INTRODUCTION

Porous scaffolding is used in tissue engineering (TE) as a temporary substitute for extracellular matrix (ECM): to promote cell attachment, proliferation, and differentiation in the regeneration of damaged or injured tissues or organs.[1,2] A critical challenge is to optimize scaffold material and design. Both natural and synthetic polymer materials have been used as scaffolds.[3,4] The major advantage of synthetic polymers is that their chemical and physical properties can be modified to provide an optimum scaffold.[5,6] Synthetic aliphatic polyesters such as poly (L-lactide) (PLLA), poly (ε-caprolactone) (PCL), poly glycolide (PGA), and their copolymers, have documented potential as scaffolding in bone defects.[4] PLLA is brittle with a low degradation rate and good tensile strength, whereas PCL is flexible with a low degradation rate and high toughness.[7] Poly(L-lactide-*co*-ε-caprolactone) (poly(LLA-*co*-CL) shows great potential as a scaffold biomaterial for TE, with important inherent properties such as biodegradability, biocompatibility, nontoxicity, and thermoplasticity.[5,6,8,9] Given the significant relationship between surface hydrophilicity and increased cell growth and differentiation, the hydrophobic properties of synthetic degradable polymers were found to inhibit cellular attachment and growth, by limiting absorption/diffusion of cell culture medium into the scaffold.[10–12] Other critical issues are seeding a sufficient number of cells and achieving homogenous distribution throughout the entire structure of the scaffold.[13] Hydrophilic scaffolds can provide an optimal microenvironment for cell behavior, vital to the formation of well-organized engineered tissues.[14–17] Several modifications have been proposed to improve hydrophilicity of degradable polymer scaffolds such as ethanol prewetting,[18] blending two polymers or adjusting the monomer ratio within the copolymer,[14,19,20] alkaline hydrolysis,[21] and plasma treatment of polymeric scaffolds.[22] A recent study has shown that blending copolymers with a surfactant is also an effective means of adjusting hydrophilicity.[23] Tween 80 is a nonionic surfactant, widely used in pharmaceutical formulations and generally regarded as nontoxic and nonirritant.[24] It has three short hydrophilic polyethylene glycol (PEG) chains and a relatively long hydrophobic alkyl chain.

Correspondence to: M. A. Yassin; e-mail: mya058@uib.no
Contract grant sponsor: European Union's Seventh Framework Programme; contract grant number: 242175-VascuBone
Contract grant sponsor: Helse Vest; contract grant number: 502027

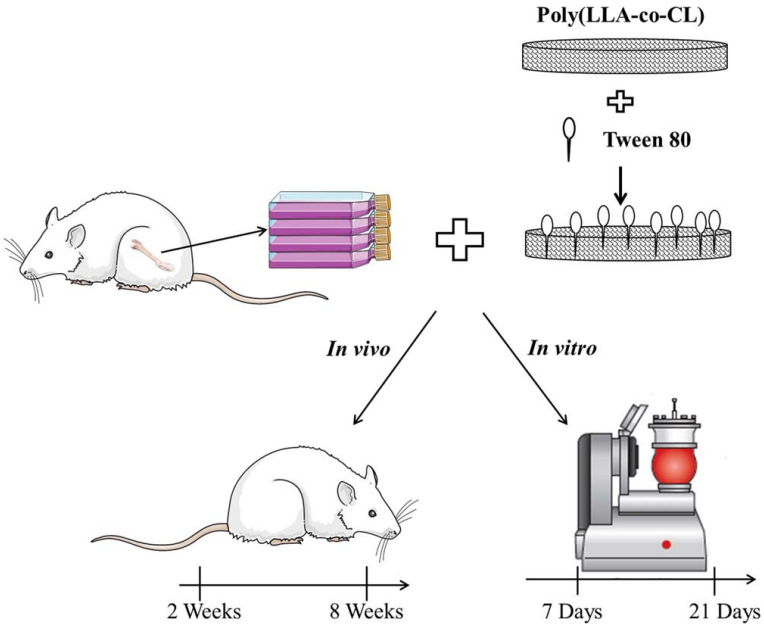

FIGURE 1. Study design.

Tween 80 is amphiphilic: the balance between the hydrophilic and hydrophobic fractions can determine its application. Modification of poly(LLA-*co*-CL) with Tween 80 produces a highly hydrophilic scaffold, with the potential for increased differentiation of human osteoblast-like cells.[23] However, high concentration of Tween 80 had a toxic effect on the cells.[23] In the present study, poly(LLA-*co*-CL) has been blended with low concentrations of Tween 80 to tune the material properties and optimize cell-material interactions *in vitro* and *in vivo*. Thus, the aims were fourfold: to evaluate the effect of low concentrations of Tween 80 on the surface microstructure of 3D poly(LLA-*co*-CL) porous scaffolds; to determine the effect of different concentrations of Tween 80 on proliferation of bone marrow stromal cells (BMSCs) under dynamic culture conditions; to assess the influence of different concentrations of Tween 80 on the degradation rate of poly(LLA-*co*-CL) porous scaffolds; and in a subcutaneous rat model to evaluate the effect on bone formation of porous scaffolds modified with 3% Tween 80.

EXPERIMENTAL

Figure 1 shows the study design.

Material

Poly(LLA-*co*-CL) was synthesized by ring-opening polymerization at 110°C for 72 h.[25] ε-Caprolactone (CL, Sigma-Aldrich, Germany) was dried with CaH_2 overnight and purified by distillation under reduced pressure at 90°C. L-LA (LLA, Boehringer Ingelheim, Germany) recrystallized three times and dried under vacuum for 3 days before use. Ethylene glycol (Sigma-Aldrich, Germany) was used as the initiator and $Sn(Oct)_2$ (Sigma-Aldrich, Germany) as the catalyst. The monomer to catalyst molar ratio was set at 10,000:1 to ensure a low amount of residual tin. The copolymer product was precipitated in cold hexane/methanol three times and dried under vacuum for >3 days. Molecular weights were recorded by size exclusion chromatography (SEC) on a Verotech PL-GPC 50 (Polymer Laboratories, Varian, USA) system, equipped with a refractive index detector and two Polar-Gel-M organic GPC columns (300 × 7.5 mm) from Varian. The system was calibrated against narrow polystyrene standards (Part No. PL2010-0301, range 162–371, 100 g/mol, Varian). The chemical composition and conversion rates (99%) of the polymerization were determined by proton nuclear magnetic resonance (^{1}H NMR) spectrometry (Bruker AC 400, Bruker, Switzerland).

Scaffold preparation

Poly(LLA-*co*-CL) and poly(LLA-*co*-CL)/Tween80 (Polysorbate 80 HX2™, NOF Corporation, Ultra-Pure grade, Japan) were fabricated using different Tween 80 concentrations [up to 3% (w/w)] by a previously described salt-leaching method.[8] Accurate Tween 80 composition was determined by ^{1}H NMR according to a previously published method.[23] Briefly, A 4% (w/v) polymer solution was prepared in chloroform and poured into silanized glass molds containing an NaCl (a controlled particle size between 90 and 500 μm) to polymer ratio of 10:1 by weight. Tween 80 was added and mixed

overnight with the dissolved polymer solution at ratios of 0.5, 1, and 3% (w/w) in chloroform. After removing the solvent, scaffolds were leached out with deionized water for 5 days, covered with aluminum foil and then dried under vacuum. Copolymer without Tween 80 served as a control. The scaffolds were then punched into cylinder shape of 5 mm diameter (Ø) × 1.2 mm thickness (δ) for *in vitro* and *in vivo* application. The scaffolds were sterilized by electron beam radiation (25 kGy dose) using a pulsed electron accelerator (Mikrotron, Acceleratorteknik, Stockholm) in an inert environment at 6.5 MeV.

Characterization of the scaffold

The surface topography of unmodified poly(LLA-*co*-CL) scaffolds and poly(LLA-*co*-CL) scaffolds modified with Tween 80 was evaluated by scanning electron microscopy (SEM) using Jeol JSM 7400F (Tokyo, Japan). All samples were dried and sputter-coated with gold before analysis at an accelerating voltage of 10 kV and magnifications up to 40,000×.

Microcomputed tomography (μ-CT) was used to measure the three-dimensional (3D) porosity, porous interconnectivity and fractal dimension of the scaffolds. Three 5 mm × 1.2 mm cylindrical samples from each scaffold type were scanned with a SkyScan 1172 μ-CT imaging system (SkyScan^{VR} v.1.5.23, Kontich, Belgium) at 10 μm resolution using a voltage of 40 kV, and a current of 250 mA. No filters were used in the μ-CT scanning of the scaffolds. Image reconstruction (NRecon Reconstruction^{VR} v. 1.6.10) and analysis (CTAn 1.15^{VR}) were conducted using the software package provided by SkyScan. The raw images of scaffolds were first reconstructed to serial coronal-oriented tomograms, using a 3D cone beam reconstruction algorithm. A global thresholding procedure was then performed at a threshold level of 40/255.

CAM 200 contact angle goniometry (KSV Instruments, Finland) was used to measure the contact angles of a 5 μL Milli-Q water drop on the surface of homogenous films, prepared by dissolving porous scaffolds in chloroform. The samples were prepared by spin coating corresponding polymer solutions on glass slides, using a Chemat KW-4A spin coater (PI-KEM, UK) at 2500 rpm for 15 s and then at 5000 rpm for 30 s. An average value was calculated from five repeated measurements.

Source and preparation of stem cells

BMSCs were isolated from the femurs of Lewis rats and maintained by a modification of a previously described method.[26] BMSCs were washed, centrifuged and plated into flasks containing minimum essential medium (αMEM, Invitrogen™, Carlsbad, CA) supplemented with 1% penicillin–streptomycin (PS) and 10% fetal bovine serum (FBS). Cells were harvested from passages three to five. Osteogenic supplements (100 nM dexamethasone, 10 mMb-glycerophosphate, and 0.05 mM ascorbic acid) were added 4 days before seeding the cells onto scaffolds. The study was approved by the Norwegian Animal Research Authority and conducted according to the European Convention for the Protection of Vertebrates Used for Scientific Purposes (local approval number 20142029).

***In vitro* cell culture**

Pristine poly(LLA-*co*-CL) scaffolds and scaffolds modified with different concentrations of Tween 80 were prewet with the culture medium and kept in an incubator at 37°C and 5% CO_2 overnight. The BMSCs were then seeded on to the various scaffolds placed at the bottom of wells in 96-well plates, at a density of 2×10^6 cells/scaffold. An orbital shaker (Eppendorf^{VR}, Hamburg, Germany) was used for 5 min at 1000 rpm to facilitate cell distribution within each scaffold.[27] The cell/scaffold grafts were incubated for 3 h to allow cell attachment and then transferred to a TisXell Regeneration System (BXR) (QuinXell International GmbH, Minden, Germany) and cultured for 7 and 21 days. The scaffolds were classified according to the percentage of Tween 80: poly(LLA-*co*-CL)/0.5% Tween 80, poly(LLA-*co*-CL)/1% Tween 80, poly(LLA-*co*-CL)/3% Tween 80, and poly(LLA-*co*-CL) ($n = 8$ per group). The BXR was loaded with a total of 500 mL of osteogenic inductive medium, filling the vessel and the reservoir. The entire bioreactor was placed in an incubator in a humidified atmosphere at 37°C and 5% CO_2. Gaseous exchange was enabled through a special membrane incorporated into the spherical vessel. The spherical vessel was programmed to rotate on two perpendicular axes (X and Z), with both axial rotations set to five rpm as previously described.[28]

Molecular weight measurement and Tween 80 composition

The number average molecular weight (M_n) and The Tween 80 composition of samples harvested after 7 and 21 days were recorded by SEC and ^{1}H NMR, respectively.

Cell proliferation assay

A MTT (3-[4, 5-dimethylthiazol-2-yl]-2, 5-diphenyltetrazolium bromide) assay measuring mitochondrial succinate dehydrogenase activity was used as previously described.[29] This colorimetric assay is based on the ability of living cells to reduce yellow MTT reagent (Sigma, St Louis, MO) to a purple formazan product. Briefly, after 7 and 21 days, scaffolds were transferred into 96-well plates and washed with phosphate buffer solution (PBS). Aliquots containing tetrazolium salt 3-(4,5-dimethylthiazolyle)-2,5-diphenyltetrazolium bromide (1 mg/mL cell culture medium) were added to each sample and incubated in the dark for 4 h at 37°C, under a CO_2 (5%) atmosphere. The MTT was aspirated and the formazan product was solubilized in 0.2 mL DMSO containing 6.25% (v/v) 0.1*M* NaOH. Absorbance was measured at 570 nm, using a microplate reader (BMG LABTECH, GmbH, Germany).

Subcutaneous implantation

Based on the *in vitro* results, poly(LLA-*co*-CL)/3% Tween scaffolds were preselected for further investigation, with poly(LLA-*co*-CL) scaffolds serving as controls. For *in vivo* evaluation, 14 healthy, skeletally mature male Lewis rats (2.5 months old, weight: 300–350 g) were selected (7 rats for each time point). The BMSCs were seeded onto the above preselected scaffold types at a density of 2×10^6 cells/scaffold.[13] One scaffold from each experimental group was implanted into each animal, that is, one poly(LLA-*co*-CL) and one poly(LLA-*co*-CL)/3% Tween 80 scaffold per animal giving a total of 28 implanted scaffolds.

The animals were anesthetized with SevoFlo (sevoflurane, Abbott Laboratories, UK) and oxygen mixture which was then reduced to 2% during the surgical procedure. The animals were placed in a ventral position, the backs shaved and disinfected. A small incision was made along the vertebral column. Using blunt dissection, a pocket was created on both sides of the incision and one scaffold/cell construct was inserted into each pocket. The incisions were closed with Vicryl 4-0 sutures. All animals were given a dose of buprenorphine (Temgesic® 0.3 mg/kg) intramuscularly as an analgesic and allowed to recover. The status of the surgical wound, food intake, activity, and signs of infection were monitored daily. The animals were euthanized after 2 and 8 weeks and the implanted scaffolds were harvested for further analysis.

Total RNA extraction and real-time polymerized chain reaction (RT-PCR) analysis

RNA isolation and RT-PCR were undertaken as previously described.[30] Briefly, total RNA was isolated using an isolation kit (E.Z.N.AVR) and purity and quantification were determined by spectrophotometry (Nanodrop Spectrophotometer). For PCR, cDNA was synthesized from the total RNA, using a High-Capacity cDNA Archive kit (Applied Biosystems, Foster City, CA) following the supplier's instructions. RT-PCR was conducted under standard enzyme and cycling conditions on a StepOne™ real-time PCR system, using TaqMan^{VR} gene expression assays (Applied Biosystems™). Vascular endothelial growth factor (VEGF), Platelet endothelial cell adhesion molecule (CD31), bone related transcription factor (Runx2), alkaline phosphatase (ALP) and osteocalcin (OC) were assessed. The data were analyzed using a comparative Ct method by StepOne. The relative level of expression for each target gene was normalized by the Ct value of TaqMan® Rodent housekeeping gene GAPDH, using an identical procedure ($^{2\Delta}$Ct formula, Perkin Elmer User Bulletin #2). On analysis, undetected levels were scored as 0. Each sample was analyzed in duplicate.

Quantification of ectopic bone

The harvested samples were fixed in 10% formalin for 2 days. Radiographic analysis was undertaken using a μ-CT scanner (Skyscan 1172^{VR}, Kontich, Belgium) with X-ray Source 50 kV/200 μA and a 0.5 mm aluminum filter (Al) for 10 μm resolution. A global thresholding procedure was then performed with a threshold level at 90/255. All samples were placed vertically onto the sample holder. Tomographic acquired images were transformed into sliced volumetric reconstruction using NRecon Reconstruction^{VR} (v. 1.6.10). Bone volume/tissue volume (BV/TV) quantification was measured using the CT-Analyzer program (v.1.15, Skyscan, Belgium) with upper and lower grey value thresholds of 255 and100 respectively. The imaging programs CTVox^{VR} (v.3.1) and CTVol^{VR} (v.2.3) were used to acquire 3D volume and surface rendering images respectively.

Histology

Following scanning, all specimens were prepared for histological evaluation. Harvested samples from each group were decalcified in 10% EDTA at pH 7.4 for 14 days with a biweekly change of solution and subsequently embedded in paraffin. Sections near the central area of the implants were selected for haematoxylin and eosin (H&E) and Masson's Trichrome (MT) staining.

Statistical analysis

Fourteen scaffolds from each group were available for the statistical analysis *in vitro* and 14 rats were included in the *in vivo* analysis. To provide accurate data of the hierarchical structure of the outcome variables, a multilevel modelling analysis was applied. For proliferation assays, four scaffold replicates were repeated in triplicate for all experiments. One-way analysis of variance (ANOVA) was used to test the effect of the different Tween 80 concentrations on cell proliferation. For PCR, reference values for different gene expressions for each rat were calculated using mixed effects models. Delta Ct (ΔCt) values were calculated as the gene expression minus the calculated reference values. Next, a general linear model, with robust variance estimators adjusted for data clustering within rats, were applied. The results expressed mean differences for the $^{2\Delta}$Ct values and were presented as xFold values. For quantitative analysis of bone formation (mean ± standard errors), Student's *t test* was used to compare pristine and modified scaffolds. Stata version 13 (TX) was applied. p values less than 0.05 (5%) were considered statistically significant.

RESULTS

Characterization of scaffolds

Blends of Tween 80 and copolymers were used to prepare well-dispersed Tween 80 porous scaffold samples. M_n was around 120,000 Da and the dispersity (Đ) was around 1.5 for all the materials. The copolymer contained 75 mol % LLA and 25 mol % CL as verified by ^{1}H NMR.

SEM images of the surfaces of poly(LLA-*co*-CL) and poly (LLA-*co*-CL)/Tween80 scaffolds are illustrated in Figure 2. The images show the surface pattern and topography of various scaffolds. (scale bar 100 nm).

The data generated by μ-CT disclosed the surface area of the various scaffolds (SA mm^2), total porosity (P %), closed porosity (%), and fractal dimension. All parameters are described in Table I. Similar morphology was observed in the pristine and copolymer/Tween scaffolds.

The modified scaffolds exhibited no change in porosity. The mean pore size of the scaffolds was about 200 μm, regardless of variation in chemical composition, with almost 100% interconnectivity (Figure 3). Adding low concentrations of Tween 80 to the copolymer did not change the microstructure of the scaffolds.

The hydrophilicity of the scaffolds was evaluated in terms of water contact angles. The contact angle of the pristine poly(LLA-*co*-CL) was 86.6° ± 0.8°. Incorporating low concentrations of Tween 80 (0.5 and 1%) into the copolymer scaffolds did not influence the surface contact angle (87.2° ± 0.6° and 83.7° ± 0.8°, respectively). However, as shown in Figure 4(A), there was a pronounced response to the blend of 3% Tween 80 and poly(LLA-*co*-CL) [55.3° ± 5.3°($p < 0.0001$)]; the

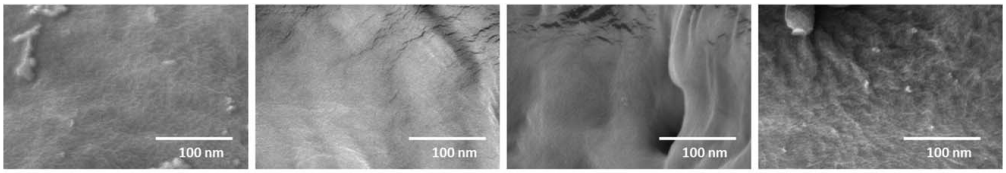

FIGURE 2. SEM images of poly(LLA-*co*-CL) and poly(LLA-*co*-CL)/Tween 80 scaffolds. The images demonstrate surface pattern and topography of various scaffolds (scale bar 100 nm).

contact angles decreased significantly and water droplets were rapidly absorbed [Figure 4(B)].

BMSCs were cultured on to the various scaffolds and incubated in a BXR bioreactor for periods of 7 and 21 days. At each time point *Mn* of poly(LLA-*co*-CL) was determined by SEC (Figure 5). The scaffolds in all groups showed a decrease in *Mn* throughout the entire incubation period.

The concentrations of Tween 80 in the various scaffolds loaded with BMSCs and cultured in a dynamic environment were measured by ^{1}H MNR (Figure 6). The amount of Tween 80 in the scaffolds modified by 0.5 and 1% Tween 80 remained unchanged, with no release of the surfactant. However, almost 50% of the surfactant was released at day 7 from the scaffolds modified with 3% Tween 80.

Effect of hydrophilicity on BMSC proliferation

Cellular proliferation and metabolic activity in pristine and modified copolymer scaffolds were monitored by MTT assay for up to day 21 of culture. Figure 7 presents the metabolic activity of BMSCs cultured onto the various scaffolds (pristine, 0.5%, 1% and 3% Tween 80), at day 7 and day 21. Regardless of the chemical composition of the scaffold, BMSC proliferation increased during the culture period, with a statistically significant increase for 3% Tween 80 at day 7 ($p = 0.0004$). Moreover, compared with pristine scaffolds, cell proliferation on the scaffolds modified with Tween 80 increased significantly at day 21 (0.5% $p = 0.025$. 1% $p = 0.0002$, and 3% $p = 0.0003$).

Effect of Tween 80 on bone formation

A rat subcutaneous model was used to study ectopic bone formation in response to poly(LLA-*co*-CL)/Tween80 blend scaffolds. During the experiment, all the rats remained in good health and there were no wound healing complications or any signs of infection. Local expression of selected genes involved in osteogenesis and angiogenesis were evaluated by real-time PCR from the samples harvested 2 weeks post-implantation (Figure 8). Compared with pristine scaffolds, mRNA expression of Runx2 was significantly upregulated in poly(LLA-*co*-CL)/3% Tween 80 scaffolds ($p = 0.004$). Expression of CD31, ALP, and OC was also increased, but not significantly ($p = 0.57$, $p = 0.367$, $p = 0.758$, respectively). The mRNA expression of VGEF was similar for both types of scaffold ($p = 0.95$).

Formation of mineralized tissues was evaluated by μ-CT (Figure 9) and histology (Figure 10) after 8 weeks. The μ-CT analysis showed that the pristine scaffolds did not exhibit much mineralized tissue formation: the percentage of bone volume/tissue volume was 0.22% ± 0.24%. In contrast, the poly(-LLA-*co*-CL)/Tween 80 scaffolds exhibited significantly increased mineralized tissue formation of about 2.8% ± 1.73% ($p = 0.013$).

Histological analysis revealed similar tissue morphology in and around the scaffold in both groups. The scaffolds were composed of fibrous tissue with a fibrous tissue encapsulation. In both groups, the scaffolds were infiltrated with foreign body giant cells. Blood vessel formation was also observed. Poly(LLA-*co*-CL)/3% Tween 80 scaffolds had large mineralized islands (Figure 10) and newly formed tissues consisting of viable osteocytes within lacunae embedded in osteoid-like matrix. Osteoblast-like cells lined the surface of newly formed bone, most likely producing the bone-like matrix.

DISCUSSION

Tween 80 was selected as the hydrophilic additive because it does not readily leach out into water or cell culture medium. In agreement with previous findings it was found that Tween 80 blends readily in to polymer: hydrophobic interaction between the hydrophobic tail of Tween 80 and the polymer main chain provides homogenous distribution and stability of Tween 80 within the copolymer.[23,31] Moreover, a low concentration of Tween 80 increases the hydrophilicity of poly(LLA-*co*-CL)

TABLE I. Selected Structural Parameters of the Pristine PLCL and Modified PLCL Scaffolds analyzed by μ-CT: Mean Values ± Standard Deviation

	Scaffold Surface Area (mm2)	Porosity (Po %)	Closed Porosity Po (cl) %	Fractal Dimension (FD)
Poly(LLA-*co*-CL)/0.5% Tween 80	25.37 ± 0.67	84.99 ± 0.36	0.0017 ± 0.00096	2.63 ± 0.075
Poly(LLA-*co*-CL)/1% Tween 80	25.43 ± 1.31	85.03 ± 0.4	0.0015 ± 0.00036	2.62 ± 0.067
Poly(LLA-*co*-CL)/3% Tween 80	25.90 ± 0.3	85.93 ± 0.76	0.0015 ± 0.00042	2.56 ± 0.058
Poly(LLA-*co*-CL)	26.73 ± 0.67	88.57 ± 0.45	0.0016 ± 0.0036	2.59 ± 0.047

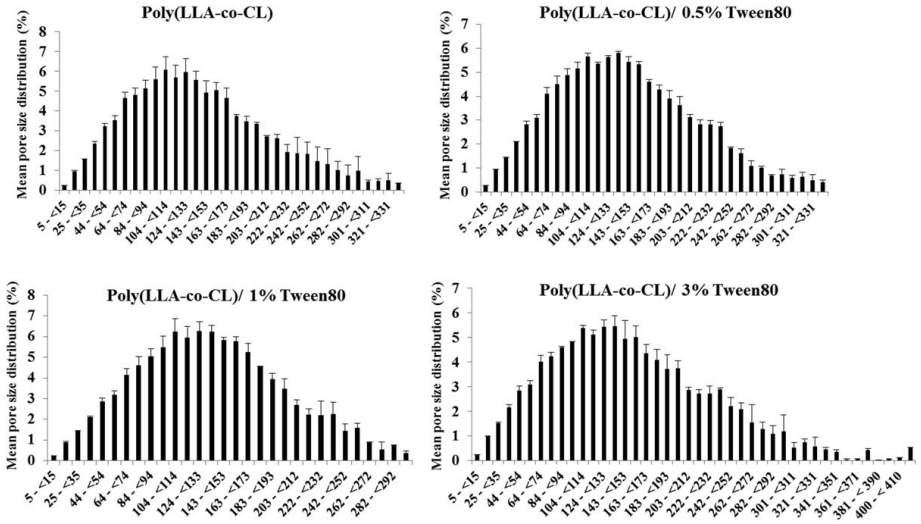

FIGURE 3. Pore size distributions and pore size range determined by μ-CT. No differences in pore size distribution were found.

scaffolds without any changes in surface topography and thermal properties.[23] Poly(LLA-*co*-CL) and poly(LLA-*co*-CL)/Tween 80 scaffolding materials were synthesized by ring opening polymerization. These copolymers were further processed into 3D porous scaffolds with interconnected pores which allow ingrowth of tissue following *in vivo* implantation.

Microstructure analysis revealed an adequate scaffold porosity range for bone tissue engineering applications and

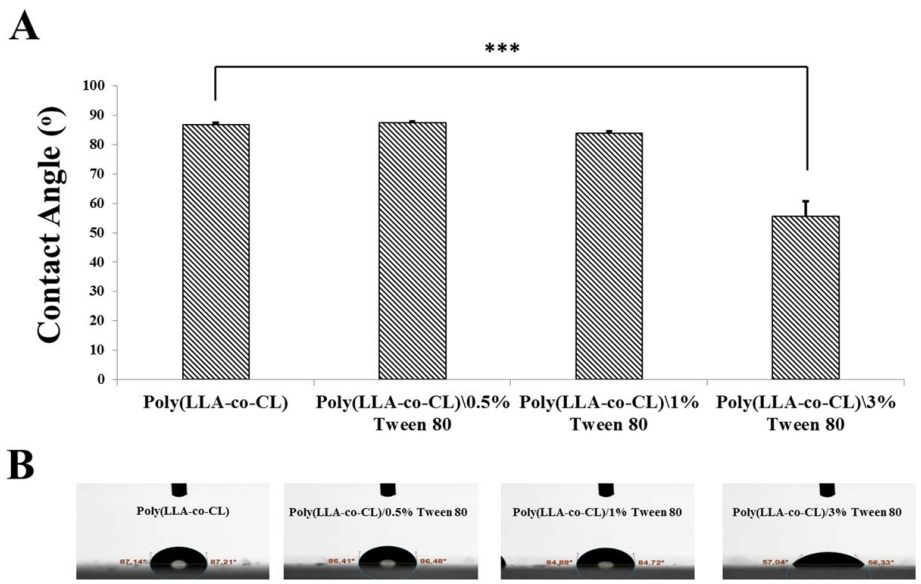

FIGURE 4. Water contact angle of poly(LLA-*co*-CL) and Tween 80 modified scaffolds (A) contact angle values and (B) the corresponding images of contact angles. Compared with pristine poly(LLA-*co*-CL), poly(LLA-*co*-CL)/3% Tween 80 showed a significant reduction in the contact angle ($p < 0.001$) (*$p \leq 0.05$, **$p \leq 0.01$, ***$p \leq 0.001$).

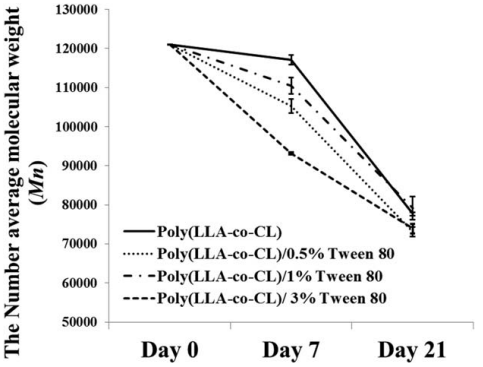

FIGURE 5. *In vitro* mean changes in the average number molecular weight (M_n) of pristine poly(LLA-*co*- CL) porous scaffolds following modification with 0.5, 1, and 3% Tween 80. The scaffolds were seeded with BMSCs and cultured in a BXR bioreactor for up to 21 days.

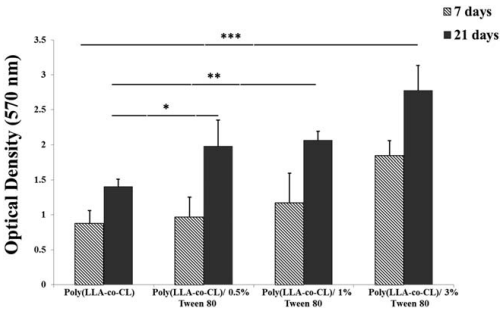

FIGURE 7. Quantitative analysis of metabolic activity of BMSCs seeded on pristine poly(LLA-*co*-CL) and modified Tween 80 scaffolds under dynamic cell culture. The columns present "absorbency at 570 nm". There is a significant increase in cell proliferation in response to 3% Tween 80 at days 7 and 21 ($p = 0.0004$ and $p = 0.0003$, respectively). At day 21 significantly increased cell proliferation was observed on Tween 80 modified scaffolds (0.5% Tween 80 ($p = 0.025$) and 1% Tween 80 ($p = 0.0002$) (*$p \leq 0.05$, **$p \leq 0.01$, ***$p \leq 0.001$).

a pore size within acceptable range for supporting bone ingrowth.[32] 3D analysis of the scaffolds showed similar internal structures for poly(LLA-*co*-CL) and poly(LLA-*co*-CL)/Tween 80 formulations with highly interconnected pores. Furthermore, no differences in fractal dimension were detected among the scaffolds. Fractal dimension expresses the roughness or complexity of the microstructure, which is the repetitive pattern of gray scale configurations, as previously described[33] and is related to the microstructure properties of polymer scaffolds or trabecular bone. Tween 80 concentrations might potentially affect the mechanical properties of the copolymers.[23,31] The plasticizing effect of Tween 80 probably depends on the concentration in the polymer matrix; the higher the Tween 80 concentration, the softer the polymer. However, μ-CT characterization was conducted on dry scaffolds. Under physiological conditions a change in pore size depending on the surface properties, for example, wettability, would be likely due to swelling and uptake of water.

A reduction in molecular weight is an essential change to porous scaffolds during degradation, which might lead to changes in the scaffold properties.[34] In general, the degradation of poly(LLA-*co*-CL) via hydrolysis is caused by random cleavage of main chain ester bonds, which leads to a reduction in the polymer molecular weight.[35–37] In addition, enzymatic degradation can occur in scaffolds seeded with cells.[38] The hydrolytic degradation rate of aliphatic polyesters is affected by water absorption and material crystallinity.[9] Usually a significant change of molecular weight of polymer scaffolds is observed at a late stage of degradation when the degraded compounds, which are usually oligomers, become water soluble and are flushed away. The fastest degradation occurred with poly(LLA-*co*-CL)/3% Tween 80, indicating accelerated reduction in the molecular weight of poly(LLA-*co*-CL) in the hydrophilicity adjustment process. In addition, the rapid degradation rate observed *in vitro* is most likely due to cellular and enzymatic activities on poly(LLA-*co*-CL) and poly(LLA-*co*-CL)/Tween 80 scaffold surfaces. A third factor in this acceleration might be

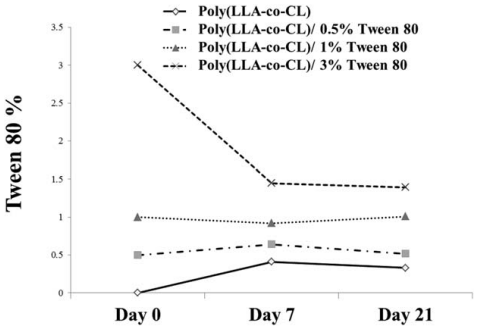

FIGURE 6. Tween 80 concentrations in scaffolds seeded with BMSCs and cultured for 7 and 21 days. The percentages of Tween 80 were evaluated by 1H NMR spectra.

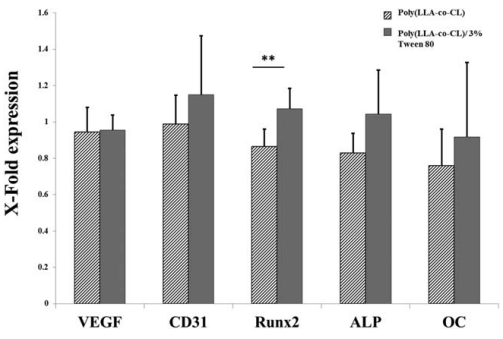

FIGURE 8. mRNA expression profiles of VEGF, CD31, Runx2, ALP, and OC by qRT-PCR, presented as *x*-fold changes after 2 weeks of subcutaneous implantation of poly(LLA-*co*-CL) and poly(LLA-*co*-CL)/3% Tween 80 in Lewis rats. A significant upregulation of Runx2 ($p = 0.004$) was detected in 3% Tween 80 scaffolds. (*$p \leq 0.05$, **$p \leq 0.01$).

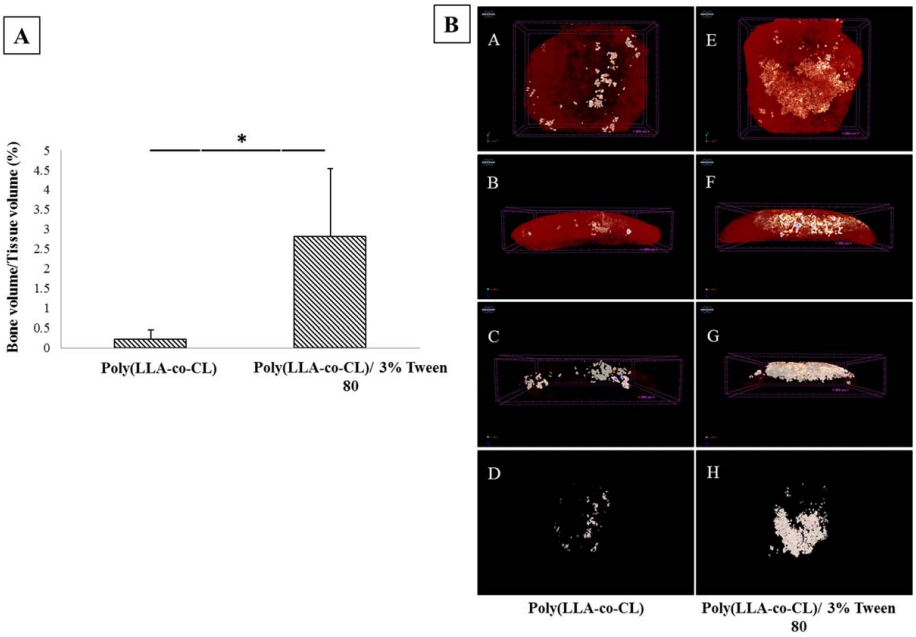

FIGURE 9. μ-CT of copolymer scaffolds loaded with BMSCs: 8 weeks post-implantation in a subcutaneous Lewis rat model. A: The histogram illustrates the statistical difference in bone/tissue formation between pristine poly(LLA-*co*-CL) and poly(LLA-*co*-CL)/3% Tween 80 modified scaffolds ($p = 0.013$). B: μ-CT images of subcutaneously implanted polymer scaffold loaded with BMSCs after 8 weeks showing *de novo* bone formation. 3D reconstructed images; A–F using CTVox software, while D and H using CTVol software. A–D pristine poly(LLA-*co*-CL) scaffolds. E–H poly(LLA-*co*-CL)/3% Tween 80 (*$p \leq 0.05$).

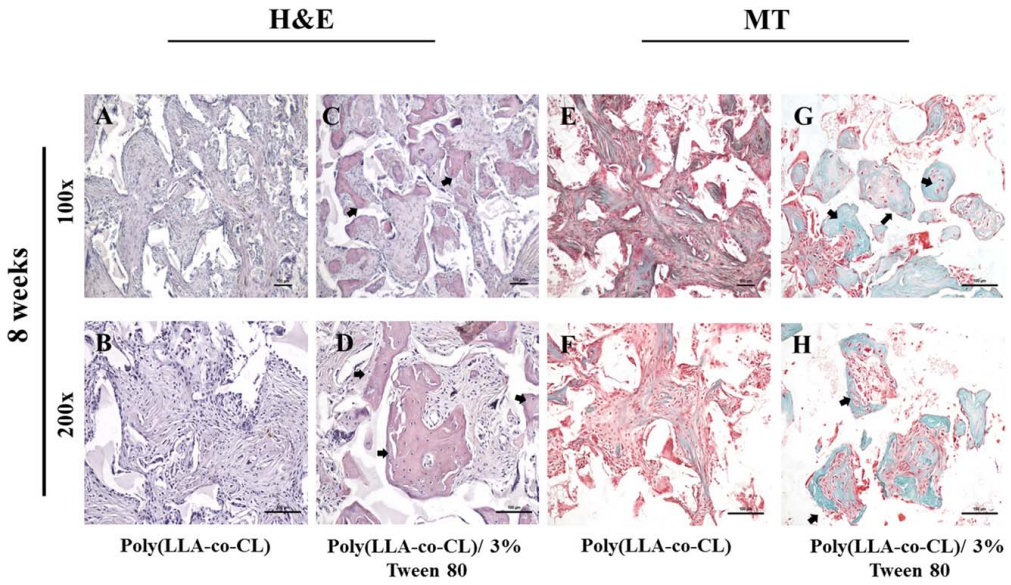

FIGURE 10. Haematoxylin and eosin (H&E) (A–D) and Masson's trichrome (MT) (E–H) staining of the polymer scaffold 8 weeks post-implantation in Lewis rats. Arrows indicate mineralized tissue (scale bar 100 μm).

high perfusion of medium into the scaffold matrix, in a dynamic flowing environment to remove the degradation compounds rapidly by an increased diffusion rate. Taken together, the weight loss of poly(LLA-*co*-CL)/Tween 80 scaffolds, in combination with dynamic cell culture, implies a release of Tween 80 from the scaffolds. These results are in accordance with previous reports indicating that release of Tween 80 from copolymer films[31] and loss of Tween 80 are most likely attributable to rapid degradation of polymer material from the surface, leading to further exposure and release of Tween 80.

The potential for water uptake is intrinsically related to the affinity of the copolymer for water and it can be affected by surface tension, which is partially responsible for and directly related to the degree of cell adhesion to the scaffold surface.[39] In addition, the surface chemistry of biomaterials may influence which serum proteins adhere to their surface, directly impacting biological responses, such as cell adhesion.[40] When a material is exposed to a body fluid or culture medium, one of the first cell–material interactions to occur at the solid/liquid interface is protein adsorption. Cellular adhesion to most TE scaffolds involves a two-step process: ECM proteins present in serum and/or tissues adsorb onto the scaffold surface and the cells then adhere to these proteins.[41] Therefore, both the structure and composition of this protein layer are crucial determinants of cell adhesion and further cell proliferation.[42] Over time, BMSCs grew in all scaffolds, but the poly(LLA-*co*-CL)/3% Tween 80 scaffolds exhibited enhanced cell proliferation. Therefore, increased hydrophilicity of the scaffolds can allow uniform cell seeding at the initial stage, through the homogeneous absorption of culture medium containing cells, providing an optimal microenvironment for physiological cellular activity.[43] Better cell proliferation is probably attributable to preferential adsorption of some serum proteins such as fibronectin and vitronectin from the culture medium onto the moderately hydrophilic surfaces. However, cell–material interactions are determined not only by the hydrophilic character of material surfaces or surface charge: the culture condition and surface roughness may also contribute to the observed behavior of the BMSCs.[28] In the present study, SEM images revealed that surface topography of poly(LLA-*co*-CL)/3% Tween80 scaffolds was different from the topography of the control scaffolds. Both *in vitro* and *in vivo*, the roughness of the material surface influences cellular morphology, proliferation, and phenotype expression. For instance, rat osteoblasts exhibit higher proliferation and expression of ALP and OC on rough surfaces than on smooth.[44]

An advantage of the subcutaneous implantation model is that under physiological conditions, natural bone-forming cells do not occur in the intradermal environment. Thus in theory, the newly formed bone is predominantly of exogenous origin. Osteogenic differentiation of BMSC is a key process for bone regeneration. It is a complex process in which serial steps are tightly regulated by a number of factors in a time-dependent fashion.[45] The upregulation of osteogenic genes in poly(LLA-*co*-CL)/3%Tween 80 indicates that improved hydrophilicity of copolymer scaffolds favors more rapid osteogenic induction of cells.[23] It is suggested that the increased hydrophilicity of the surface might allow formation of a filamentous F-actin cytoskeletal network in the cells initiating osteogenic differentiation of MSCs.[46] Runx 2 is thought to play a central role in regulating the stem cells into an osteoblastic biotype, by directly stimulating the expression of downstream osteogenic genes such as alkaline phosphatase, bone sialoprotein, and osteocalcin.[47] Previously published reports have demonstrated that improved wettability of materials can promote osteogenic differentiation of BMSCs *in vitro*.[48] Moreover, studies on titanium dental implants have reported that chemical modulation to increase hydrophilicity of the surface may lead to more successful osseointegration through bone morphogenetic protein signaling.[49] The BMSCs gene expression profiles indicate that tuning the hydrophilicity of poly(LLA-*co*-CL) scaffolds might increase the osteoconductive potential and allowing rapid *in vivo* fluid infiltration and consequently stable blood clot formation, which is known to initiate the healing cascade, eventually leading to bone ingrowth.[50] The physical and chemical properties of the carrier are critical factors for bone formation.[32,51] The mineralized tissues observed on scaffolds modified with 3% Tween 80 contributed to altered surface properties. Studies on titanium dental implants show that chemically modified surfaces retain the topography of the original surface, but increasing hydrophilicity induces greater bone to implant contact, osteoblast differentiation, growth factor production, and osteogenic gene expression.[52] Similarly, it has been demonstrated that surface treatment of PCL scaffolds with tricalcium phosphate increases the wettability and initial bone ingrowth.[53]

Vascularization is another essential factor for BTE constructs as it determines the extent of blood supply, oxygen, nutrients, and exchange of waste products within the host tissue infiltrating the scaffold. Angiogenesis/neo-vascularization associated with implanted biomaterials is dependent on a number of factors, including the bioactive nature of the scaffold, the porosity, pore interconnectivity, and the metabolic activity of the infiltrating host tissue.[54] The scaffolds used in this study comprised a highly porous structure (porosity about 85%), with well-defined interconnectivity (100%). It was observed that the internal porous structure of both scaffolds was preserved during 8 weeks of implantation; this in turn allowed infiltration of host cells and formation of mineralized tissues in the scaffolds. Importantly, after 8 weeks of implantation, more tissue formation was observed in poly(LLA-*co*-CL)/3% Tween 80 scaffolds than in poly(LLA-*co*-CL) scaffolds indicating more rapid integration of poly(LLA-*co*-CL)/3% Tween 80 scaffolds, due to favorable surface properties. The tissue response to the implanted scaffold depends on the scaffold's surface; hence this is the most vital site of acute immune host response following implantation. The hydrophilic surfaces may reduce the adhesion of monocytes and increase the number of adherent apoptotic macrophages, thereby reducing the risk of implant failure.[55,56] In BTE, the preferred scaffolding material should exert a positive modulating influence on the immune system and subsequently enhance bone repair and regeneration.[57]

CONCLUSION

Based on the results of these *in vitro* and *in vivo* studies it is concluded that blending of 3% (*w/w*) of Tween 80 with

poly(LLA-*co*-CL) scaffolding material significantly improves the hydrophilicity and osteogenic potential of the scaffolds. Tuning surface wettability has a positive influence on the surface characteristics of the scaffolds without adversely affecting the microstructural properties. The 3% Tween 80 porous degradable scaffolds absorb water quickly, significantly increase BMSC proliferation *in vitro* up to 21 days, promote osteogenic differentiation of BMSCs, and significantly increase *de novo* bone formation.

ACKNOWLEDGMENTS

The authors acknowledge Torbjorn O. Pedersen for the support in animal surgery and Randi Sundfjord for technical assistance. The authors thank Dr. Joan Bevenius-Carrick for English revision and constructive criticism of the manuscript.

REFERENCES

1. Hutmacher DW, Sittinger M, Risbud MV. Scaffold-based tissue engineering: rationale for computer-aided design and solid free-form fabrication systems. Trends Biotechnol 2004;22:354–362.
2. Chan BP, Leong KW. Scaffolding in tissue engineering: general approaches and tissue-specific considerations. Eur Spine J 2008; 17:467–479.
3. Middleton JC, Tipton AJ. Synthetic biodegradable polymers as orthopedic devices. Biomaterials 2000;21:2335–2346.
4. Hutmacher DW. Scaffolds in tissue engineering bone and cartilage. Biomaterials 2000;21:2529–2543.
5. Mo XM, Xu CY, Kotaki M, Ramakrishna S. Electrospun P(LLA-CL) nanofiber: a biomimetic extracellular matrix for smooth muscle cell and endothelial cell proliferation. Biomaterials 2004;25:1883–1890.
6. Idris SB, Arvidson K, Plikk P, Ibrahim S, Finne-Wistrand A, Albertsson AC, Bolstad AI, Mustafa K. Polyester copolymer scaffolds enhance expression of bone markers in osteoblast-like cells. J Biomed Mater Res A 2010;94:631–639.
7. Wu D, Zhang Y, Zhang M, Yu W. Selective localization of multiwalled carbon nanotubes in poly(ε-caprolactone)/polylactide blend. Biomacromolecules 2009;10:417–424.
8. Dånmark S, Finne-Wistrand A, Wendel M, Arvidson K, Albertsson A-C, Mustafa K. Osteogenic differentiation by rat bone marrow stromal cells on customized biodegradable polymer scaffolds. J Bioactive Comp Polym 2010;25:207–223.
9. Danmark S, Finne-Wistrand A, Schander K, Hakkarainen M, Arvidson K, Mustafa K, Albertsson AC. *In vitro* and *in vivo* degradation profile of aliphatic polyesters subjected to electron beam sterilization. Acta Biomater 2011;7:2035–2046.
10. Oliveira SM, Alves NM, Mano JF. Cell interactions with superhydrophilic and superhydrophobic surfaces. J Adhes Sci Technol 2012;28:843–863.
11. Yang J, Wan Y, Tu C, Cai Q, Bei J, Wang S. Enhancing the cell affinity of macroporous poly(l-lactide) cell scaffold by a convenient surface modification method. Polym Int 2003;52:1892–1899.
12. Oh SH, Lee JH. Hydrophilization of synthetic biodegradable polymer scaffolds for improved cell/tissue compatibility. Biomed Mater 2013;8:014101.
13. Yassin MA, Leknes KN, Pedersen TO, Xing Z, Sun Y, Lie SA, Finne-Wistrand A, Mustafa K. Cell seeding density is a critical determinant for copolymer scaffolds-induced bone regeneration. J Biomed Mater Res A 2015;103:3649–3658.
14. Oh SH, Kang SG, Kim ES, Cho SH, Lee JH. Fabrication and characterization of hydrophilic poly(lactic-*co*-glycolic acid)/poly(vinyl alcohol) blend cell scaffolds by melt-molding particulate-leaching method. Biomaterials 2003;24:4011–4021.
15. Jiao Y-P, Cui F-Z. Surface modification of polyester biomaterials for tissue engineering. Biomed Mater 2007;2:R24.
16. Yang X, Chen X, Wang H. Acceleration of osteogenic differentiation of preosteoblastic cells by chitosan containing nanofibrous scaffolds. Biomacromolecules 2009;10:2772–2778.
17. Groth T, Altankov G. Studies on cell–biomaterial interaction: Role of tyrosine phosphorylation during fibroblast spreading on surfaces varying in wettability. Biomaterials 1996;17:1227–1234.
18. Mikos AG, Lyman MD, Freed LE, Langer R. Wetting of poly(l-lactic acid) and poly(dl-lactic-*co*-glycolic acid) foams for tissue culture. Biomaterials 1994;15:55–58.
19. Sarasam A, Madihally SV. Characterization of chitosan–polycaprolactone blends for tissue engineering applications. Biomaterials 2005;26:5500–5508.
20. Ivirico JLE, Salmerón-Sánchez M, Ribelles JLG, Pradas MM, Soria JM, Gomes ME, Reis RL, Mano JF. Proliferation and differentiation of goat bone marrow stromal cells in 3D scaffolds with tunable hydrophilicity. J Biomed Mater Res A B Appl Biomater 2009; 91B:277–286.
21. Park GE, Pattison MA, Park K, Webster TJ. Accelerated chondrocyte functions on NaOH-treated PLGA scaffolds. Biomaterials 2005;26:3075–3082.
22. Wan Y, Tu C, Yang J, Bei J, Wang S. Influences of ammonia plasma treatment on modifying depth and degradation of poly(l-lactide) scaffolds. Biomaterials 2006;27:2699–2704.
23. Sun Y, Xing Z, Xue Y, Mustafa K, Finne-Wistrand A, Albertsson A-C. Surfactant as a critical factor when tuning the hydrophilicity in three-dimensional polyester-based scaffolds: impact of hydrophilicity on their mechanical properties and the cellular response of human osteoblast-like cells. Biomacromolecules 2014;15:1259–1268.
24. Kibbe AH. Handbook of Pharmaceutical Excipients. London: Pharmaceutical Press; 2000.
25. Odelius K, Plikk P, Albertsson A-C. Elastomeric hydrolyzable porous scaffolds: Copolymers of aliphatic polyesters and a polyetherester. Biomacromolecules 2005;6:2718–2725.
26. Maniatopoulos C, Sodek J, Melcher AH. Bone formation *in vitro* by stromal cells obtained from bone marrow of young adult rats. Cell Tissue Res 1988;254:317–330.
27. Xing Z, Xue Y, Danmark S, Finne-Wistrand A, Arvidson K, Hellem S, Yang ZQ, Mustafa K. Comparison of short-run cell seeding methods for poly(l-lactide-*co*−1,5-dioxepan-2-one) scaffold intended for bone tissue engineering. Int J Artif Org 2011;34:432–441.
28. Zhang Z-Y, Teoh SH, Teo EY, Khoon Chong MS, Shin CW, Tien FT, Choolani MA, Chan JKY. A comparison of bioreactors for culture of fetal mesenchymal stem cells for bone tissue engineering. Biomaterials 2010;31:8684–8695.
29. Seyedjafari E, Soleimani M, Ghaemi N, Shabani I. Nanohydroxyapatite-coated electrospun poly(l-lactide) nanofibers enhance osteogenic differentiation of stem cells and induce ectopic bone formation. Biomacromolecules 2010;11:3118–3125.
30. Xing Z, Xue Y, Dånmark S, Schander K, Østvold S, Arvidson K, Hellem S, Finne-Wistrand A, Albertsson A-C, Mustafa K. Effect of endothelial cells on bone regeneration using poly(l-lactide-*co*−1,5-dioxepan-2-one) scaffolds. J Biomed Mater Res A 2011; 96A:349–357.
31. Oh S, Cho S, Lee J. Preparation and characterization of hydrophilic PLGA/Tween 80 films and porous scaffolds. Mol Cryst Liq Cryst 2004;418:229–241.
32. Karageorgiou V, Kaplan D. Porosity of 3D biomaterial scaffolds and osteogenesis. Biomaterials 2005;26:5474–5491.
33. Alberich-Bayarri A, Moratal D, Ivirico JLE, Hernández JCR, Vallés-Lluch A, Martí-Bonmatí L, Estellés JM, Mano JF, Pradas MM Ribelles JLG, Salmerón-Sánchez M. Microcomputed tomography and microfinite element modeling for evaluating polymer scaffolds architecture and their mechanical properties. Journal of Biomedical Materials Research Part B: Applied Biomaterials 2009; 91B(1):191–202.
34. Lam CXF, Hutmacher DW, Schantz J-T, Woodruff MA, Teoh SH. Evaluation of polycaprolactone scaffold degradation for 6 months *in vitro* and *in vivo*. J Biomed Mater Res A 2009;90A:906–919.
35. Brunius CF, Edlund U, Albertsson A-C. Synthesis and *in vitro* degradation of poly(*N*-vinyl-2-pyrrolidone)-based graft copolymers for biomedical applications. J Polym Sci A Polym Chem 2002;40:3652–3661.
36. Höglund A, Hakkarainen M, Albertsson A-C. Migration and hydrolysis of hydrophobic polylactide plasticizer. Biomacromolecules 2010;11:277–283.
37. Odelius K, Höglund A, Kumar S, Hakkarainen M, Ghosh AK, Bhatnagar N, Albertsson A-C. Porosity and pore size regulate the

degradation product profile of polylactide. Biomacromolecules 2011;12:1250–1258.
38. Lim H-A, Raku T, Tokiwa Y. Hydrolysis of polyesters by serine proteases. Biotechnol Lett 2005;27:459–464.
39. Lampin M, Warocquier-Clérout R, Legris C, Degrange M, Sigot-Luizard MF. Correlation between substratum roughness and wettability, cell adhesion, and cell migration. J Biomed Mater Res A 1997;36:99–108.
40. Olivieri MP, Kittle KH, Tweden KS, Loomis RE. Comparative biophysical study of adsorbed calf serum, fetal bovine serum and mussel adhesive protein films. Biomaterials 1992;13:201–208.
41. Liu H, Webster TJ. Nanomedicine for implants: a review of studies and necessary experimental tools. Biomaterials 2007;28:354–369.
42. Elbert DL, Hubbell JA. Surface treatments of polymers for biocompatibility. Ann Rev Mater Sci 1996;26:365–394.
43. Wei J, Igarashi T, Okumori N, Igarashi T, Maetani T, Liu B, Yoshinari M. Influence of surface wettability on competitive protein adsorption and initial attachment of osteoblasts. Biomed Mater 2009;4:045002.
44. Hatano K, Inoue H, Kojo T, Matsunaga T, Tsujisawa T, Uchiyama C, Uchida Y. Effect of surface roughness on proliferation and alkaline phosphatase expression of rat calvarial cells cultured on polystyrene. Bone 1999;25:439–445.
45. Stein GS, Lian JB. Molecular mechanisms mediating proliferation/differentiation interrelationships during progressive development of the osteoblast phenotype. Endocr Rev 1993;14:424–442.
46. Curran JM, Tang Z, Hunt JA. PLGA doping of PCL affects the plastic potential of human mesenchymal stem cells, both in the presence and absence of biological stimuli. J Biomed Mater Res A 2009;89A:1–12.
47. Huang W, Yang S, Shao J, Li Y-P. Signaling and transcriptional regulation in osteoblast commitment and differentiation. Front Biosci J Virtual Library 2007;12:3068–3092.
48. Wall I, Donos N, Carlqvist K, Jones F, Brett P. Modified titanium surfaces promote accelerated osteogenic differentiation of mesenchymal stromal cells *in vitro*. Bone 2009;45:17–26.
49. Vlacic-Zischke J, Hamlet SM, Friis T, Tonetti MS, Ivanovski S. The influence of surface microroughness and hydrophilicity of titanium on the up-regulation of TGFβ/BMP signalling in osteoblasts. Biomaterials 2011;32:665–671.
50. Claes L, Recknagel S, Ignatius A. Fracture healing under healthy and inflammatory conditions. Nat Rev Rheumatol 2012;8:133–143.
51. Ma PX, Choi JW. Biodegradable polymer scaffolds with well-defined interconnected spherical pore network. Tissue Eng 2001; 7:23–33.
52. Schwarz F, Wieland M, Schwartz Z, Zhao G, Rupp F, Geis-Gerstorfer J, Schedle A, Broggini N, Bornstein MM Buser D, et al. Potential of chemically modified hydrophilic surface characteristics to support tissue integration of titanium dental implants. J Biomed Mater Res A B Appl Biomater 2009;88B:544–557.
53. Yeo A, Wong WJ, Khoo HH, Teoh SH. Surface modification of PCL–TCP scaffolds improve interfacial mechanical interlock and enhance early bone formation: an *in vitro* and *in vivo* characterization. J Biomed Mater Res A 2010;92A:311–321.
54. Burugapalli K, Pandit A. Characterization of tissue response and *in vivo* degradation of cholecyst-derived extracellular matrix. Biomacromolecules 2007;8:3439–3451.
55. Brodbeck WG, Shive MS, Colton E, Nakayama Y, Matsuda T, Anderson JM. Influence of biomaterial surface chemistry on the apoptosis of adherent cells. J Biomed Mater Res A 2001;55:661–668.
56. Brodbeck WG, Patel J, Voskerician G, Christenson E, Shive MS, Nakayama Y, Matsuda T, Ziats NP, Anderson JM. Biomaterial adherent macrophage apoptosis is increased by hydrophilic and anionic substrates *in vivo*. Proc Natl Acad Sci 2002;99:10287–10292.
57. Mountziaris PM, Spicer PP, Kasper FK, Mikos AG. Harnessing and modulating inflammation in strategies for bone regeneration. Tissue Eng B Rev 2011;17:393–402.